Supersymmetric Dualities and Quantum Entanglement in Conformal Field Theory

Jeongseog Lee

A Dissertation
Presented to the Faculty
of Princeton University
in Candidacy for the Degree
of Doctor of Philosophy

Recommended for Acceptance
by the Department of
Physics
Adviser: Igor R. Klebanov

September 2016

Abstract

Conformal field theory (CFT) has been under intensive study for many years. The scale invariance, which arises at the fixed points of renormalization group in relativistic quantum field theory (QFT), is believed to be enhanced to the full conformal group. In this dissertation we use two tools to shed light on the behavior of certain conformal field theories, the supersymmetric localization and the quantum entanglement Renyi entropies.

The first half of the dissertation surveys the infrared (IR) structure of the $\mathcal{N} = 2$ supersymmetric quantum chromodynamics (SQCD) in three dimensions. The recently developed F-maximization principle shows that there are richer structures along conformal fixed points compared to those in $\mathcal{N} = 1$ SQCD in four dimensions. We refer to one of the new phenomena as a "crack in the conformal window". Using the known IR dualities, we investigate it for all types of simple gauge groups. We see different decoupling behaviors of operators depending on the gauge group. We also observe that gauging some flavor symmetries modifies the behavior of the theory in the IR.

The second half of the dissertation uses the Rènyi entropy to understand the CFT from another angle. At the conformal fixed points of even dimensional QFT, the entanglement entropy is known to have the log-divergent universal term depending on the geometric invariants on the entangling surface. We make an observation about the universal term in free four-dimensional CFT Rènyi entropy. In particular, we study the subleading term of three-dimensional Rènyi entropy with circular entangling surface for massive free scalar. Then, we study the importance of boundary terms in computing Rènyi entropy. We also resolve the issue of Rènyi entropy around $q = 1$ in $\mathcal{N} = 4$ Super-Yang-Mills theory.

Acknowledgements

I would first like to thank my advisor, Igor Klebanov, for his support during graduate school. It is an honor to work with a well-known theoretical physicist. In addition to his admirable intuition for physics, he has been kindly guiding me all the way through the graduate program. Without his timely advice, it would not have been possible to reach this stage.

I am very grateful that I was able to work with my collaborators, Aitor Lewkowycz, Lauren McGough, Eric Perlmutter, Benjamin Safdi, Masahito Yamazaki. Their sharp intuitions and firm knowledge of theoretical physics were the key inspirations to my work in Princeton. I also thank professor Piljin Yi and Sangmin Lee for their encouragement and support.

My awesome friends in Princeton made life more fun and enjoyable here. Thank you very much to all you guys, Eunjeong Choi, Steve Choi, Taehee Han, Jungpyo Hong, Injee Jeong, Junehyuk Jung, Andrew Kim, Jaewook Kim, John Jeongho Kim, Hyungwon Kim, Ringi Kim, Dmitri Krotov, Seongwoo Oh, Jihyun Park, Yeje park, Jungeun Yoon, and Juyoung Yoon.

I admit that studying and living abroad for the first time in my life was tough. However, I was very lucky that I had two people who were always there to cheer me up so that I did not lose my way, my sister Dawoon, and my friend Juho. Dawoon was not only my family, but also my mentor, who taught me how to stay healthy while living thousands of miles away from home. Juho and I studied physics together since high school. We shared similar life experiences for a dozen years and during which I learned numerous life lessons that helped me stay strong. I additionally thank him for teaching me the Python to understand and write the basic scientific codes for my numerical studies.

I thank my friend, Tanawat Phaovibul. Tanawat always offered me his help and gave me suggestions on many occasions for the last couple of years. It is wonderful to have such a great friend, and I hope we continue to stay close.

Last but not least, all these years that I have spent in Princeton would not have been possible without the endless love and support of my parents.

To my wonderful family.

Contents

List of Tables

List of Figures

Chapter 1

Introduction

A very important role in physics is played by the concept of the symmetry. By finding the underlying symmetries of a physics problem, we have a much better chance of solving it. The symmetries often encountered are under spatial and time translations, rotations and Lorentz transformations. Together they form the Poincarè symmetry of the Minkowski spacetime. The Lorentz symmetry forms the $\mathrm{SO}(1, d-1)$ subgroup of the Poincarè symmetry.

In some QFTs the Lorentz group is enhanced to $\mathrm{SO}(2, d)$ conformal group. The conformal group has $\frac{(d+1)(d+2)}{2}$ generators : d for the translation, $\frac{d(d-1)}{2}$ for the rotations and boosts of the Lorentz group, one for the dilatation, and d for the special conformal transformation. The dilatation generates a transformation which scales the spacetime coordinates by a constant $x \to \lambda x$, and the special conformal transformation can be identified as a series of transformations which consists of an inversion, followed by a translation, and then followed by another inversion.

Physicists have also discovered a class of QFTs with the supersymmetry. Supersymmetry is a type of spacetime symmetry that relates a particle to the other particle with all the same characteristics but a different spin. If a particle is a boson with an integer spin, supersymmetry matches it with a fermion with a half-integer spin, vice

versa. Sometimes both supersymmetry and conformal symmetry are present at the same time, especially at the conformal fixed point of the relativistic QFT. We will discuss it in the chapter 2.

Supersymmetry solves many problems in theoretical physics. The most famous application of supersymmetry is to solving the hierarchy problem in the standard model : why is gravity so much weaker than the weak force? This has to do with the mass of the Higgs boson being much smaller than the Planck mass. Without supersymmetry, we have a hard time explaining why the Higgs boson mass should be small because there is a quadratic divergence in the Higgs mass renormalization. Supersymmetry solves this by introducing the superpartner which cancels that divergence. Moreover, in cosmology, supersymmetry provides a strong candidate for cosmological dark matter.

It may seem that supersymmetry is only viable in particle physics, but it is also applicable to condensed matter physics and quantum optics. In condensed matter physics, supersymmetry gives simpler solutions to many problems such as the random magnetic field in the Ising-like model, linear polymer, and electron localization [2–4]. Also in quantum optics, supersymmetry helps realize dissipative dynamics. It is also shown that supersymmetry can be realized in a cavity-QED system [5].

Having seen the broad range of usage of supersymmetry in physics, we will use it in the quantum field theory to reveal an interesting feature of supersymmetric quantum chromodynamics in three dimensions : can we find the range of how many flavors in the theory for it to have an interacting fixed point in the infrared for various gauge groups? If so, is there any transition on behavior within that window? The corresponding problem in the four dimensions have been solved by Seiberg [6] (there is an analogous conformal window in the non-supersymmetric case [7, 8]). We study the similar conformal window in the three dimensions [9, 10].

Scaling dimension is the value denoting how an operator behaves under the rescaling of the spacetime $x \to \lambda x$. At a critical point (or in the scale invariant theory, conformal theory), an operator ϕ with a scaling dimension Δ has a two point function

$$\langle \phi(x)\phi(0)\rangle \sim x^{-2\Delta}\,. \tag{1.1}$$

Computing the scaling dimension is of interest due to the fact that it is related to the critical phenomena of the QFT - it measures the critical exponent η in the continuous phase transition, which measures the scaling exponent away from its canonical dimension,

$$\eta = 2\Delta - (d-2)\,. \tag{1.2}$$

In the supersymmetric QFT, the scaling dimensions of chiral and anti-chiral operators are used to observe the dynamics at the conformal fixed point using the fact that they are proportional to the R-charge because of the superconformal algebra. Any operator that is a chiral primary has a bound on its scaling dimension if we impose the theory to be unitary. In four dimensions, the scaling dimension of the meson M_a^b was used as a probe, but we will see in chapter 2 that the scaling dimension of the monopole is useful in three dimensions.

In the second half of the dissertation, we will consider a different but related concept in the QFT, the Rènyi entropy which is a generalization of the quantum entanglement entropy [11, 12]. In quantum physics, it often happens that a group of particles is entangled that the state of each particle cannot be determined independently. We call it as quantum entanglement, and it is one of the features that cannot be explained by classical physics. To quantify this intriguing phenomenon, physicists have built many measures of it and the standard one is the entanglement entropy.

Entanglement and Rènyi entropy has been widely used in quantum information [13] and condensed matter physics [14–18].

In high energy physics, entanglement entropy has drawn great interest rather recently after the work of Ryu and Takayanagi deriving the entanglement entropy of boundary from the surface in dual geometry [19]. It became even more interesting after its behavior under the renormalization group flow was revealed [20, 21].

More interesting physics came out when the entanglement entropy was applied to the conformal field theory (for review see [22–24]). In conformal field theory, it is natural to map the theory to the sphere and compute its free energy on there. It was shown that, in three dimensions, this three-sphere free energy coincides the entanglement entropy with circular entangling surface up to overall sign and proved it is monotonic under the RG flow [25], proving the known F-theorem.

This inspires one to work on what happens to the Rènyi entropy of the conformal field theories. In chapter 3, we present the work on the Rènyi entropy by investigating the structure of its universal terms and confirm its area dependent nature. After that we present the work on the expansion of Rènyi entropy around the order $q = 1$ for conformal field theory to resolve the conflict within the scalar field.

Organization of the dissertation

In the rest of chapter 1, we review the essential background theories that are used in the main chapters. We first review the three-dimensional $\mathcal{N} = 2$ supersymmetric theory, and how it is written on the curved three-sphere where we can write down the exact partition function via localization method. Then, we move to the renormalization group flow of QFT and quantities that parametrize this flow. In three dimensions, $F = -\log Z_{S^3}$ does the job and maximizing it gives the correct R-symmetry at the IR fixed point. Lastly, we briefly review the concept of entanglement entropy and its generalization, the Rènyi entropy.

In chapter 2, we study the IR structure of the $\mathcal{N} = 2$ SQCD in three dimensions. The recently developed F-maximization principle [26] shows that there are richer structures along conformal fixed points compared to that of $N = 1$ SQCD in four dimensions. In the Veneziano limit, where we send the gauge group parameter N_c and number of flavors N_f to infinity while keeping there ratio $x = N_f/N_c$ fixed, we see that the three-sphere partition function starts to diverge at the critical value x_c. Dual theory then has a converging partition function to define F from $x < x_c$.

From $x < x_c$, emergent symmetry arises in the IR and mixes with the R-symmetry. We give insight to this new global symmetry by studying the scaling dimension of the monopoles exploiting the fact that conformal scaling dimension and R-charge have exactly the same value at conformal fixed points. Monopoles have scaling dimension $\Delta > \frac{1}{2}$ for $x = x_c$, but they hit the unitarity bound $\Delta = \frac{1}{2}$ at $x = x_c$ thereby decoupling from the theory for $x \leq x_c$. Emergent symmetry acts on the monopole sector for $x < x_c$, fixing its scaling dimension to $\frac{1}{2}$. We call this transition of theory at $x = x_c$ a "crack in the conformal window". Using the known IR dualities, we investigate the crack in the conformal window for all possible types of simple gauge groups. Surveying these gauge groups, we find that there is a general formula which determines the scaling dimension of the flavor multiplet to the order of $1/N_f^2$.

It turns out that gauging the flavor symmetry drastically changes the behavior at the IR fixed point. We investigate this by looking at several examples including the quiver gauge theory and different types of orthogonal gauge groups.

Chapter 3 explores the Rènyi entropy of the CFT. At the conformal fixed points of even dimensional QFT, the entanglement entropy is known to have the log-divergent universal term depending on the geometric invariants on the entangling surface. We make an observation about the universal term in free four-dimensional CFT Rènyi entropy. In particular, we numerically study subleading term in $\frac{1}{mR}$ order of three-dimensional Rènyi entropy with circular entangling surface for massive free scalar.

Moreover, we check that Rènyi entropy follows the perimeter law just as the entanglement entropy does.

We can also compute the Rènyi entropy via CFT partition function, but there is an ambiguity due to the boundary terms. This actually corresponds to the choice of regularization for singular conical space. Including the boundary term is the same as putting a hard cutoff, while not including it corresponds to regularizing the conical space by smoothing the singularity, which erases the boundary. We show the importance of the boundary terms by computing the second derivative of the Rènyi entropy for a general CFT, and we find perfect agreement except the conformal scalar field. After correctly considering the boundary term, we eliminate the mismatch of Rènyi entropy for the scalar field. We also resolve the issue of Rènyi entropy around $q = 1$ in $\mathcal{N} = 4$ Super-Yang-Mills theory.

1.1 3-d $\mathcal{N} = 2$ supersymmetric theory

Let us briefly review the $\mathcal{N} = 2$ Supersymmetry in 3-d (we will follow the material of [9]). It has four supercharges and its algebra is given by

$$\begin{aligned} \{Q_\alpha, Q_\beta\} &= \{\bar{Q}_\alpha, \bar{Q}_\beta\} = 0 \\ \{Q_\alpha, \bar{Q}_\beta\} &= 2\sigma^\mu_{\alpha\beta} P_\mu + 2i\epsilon_{\alpha\beta} Z \,, \end{aligned} \tag{1.3}$$

which can be obtained from dimensional reduction of 4-d $\mathcal{N} = 1$ supersymmetry. The spinor indices α and β run from 1 to 2, and Z is a real central charge which originated from the reduced fourth momentum component P_3 in the dimensional reduction. There is an abelian symmetry which rotates Q and $\bar{Q}$ in opposite directions, which is called the $\mathrm{U}(1)_R$ symmetry. We take the convention that Q has charge +1 and $\bar{Q}$ has charge -1 under this symmetry.

The Poincarè algebra contains two Casimir operators

$$P^2 = P_\mu P^\mu \quad , \quad W^2 = W_\mu W^\mu \tag{1.4}$$

where $W^\mu = \frac{1}{2}\epsilon^{\mu\nu\rho\sigma} P_\nu M_{\rho\sigma}$ is the Pauli-Lubanski vector. These Casimirs commute with all generators of symmetry group, which lets them determine the quantum numbers of different states in the irreducible representation. In the rest frame, $P^2 = m^2$ and $W^2 = -m^2 s(s+1)$, so different particle states have different masses and spins. However, W^2 is no longer a Casimir in the case of supersymmetry. Therefore, particles of different spin belong to same supermultiplet.

The irreducible representations of 3-d $\mathcal{N} = 2$ supersymmetry contains a chiral multiplet and vector multiplet. A chiral multiplet contains complex scalar ϕ, Dirac fermion ψ, and auxiliary field f. In superspace notation, it can be written as

$$\Phi = \phi + \sqrt{2}\theta\psi - \theta\theta f \,. \tag{1.5}$$

A chiral superfield of charge q is invariant under the gauge transformation

$$\Phi \to e^{-iq\Lambda}\Phi \,. \tag{1.6}$$

Similarly, we can define the anti chiral multiplet $\bar{\Phi}$.

A vector multiplet contains gauge field A, real scalar σ, complex gaugino λ, and auxiliary field D. In Wess-Zumino gauge, a vector multiplet V can be compactly written as

$$V_{\mathrm{WZ}} = \theta\sigma^\mu\bar{\theta}A_\mu + \theta\theta\sigma + i\theta\theta\bar{\theta}\bar{\lambda} - i\bar{\theta}\bar{\theta}\theta\lambda + \frac{1}{2}\theta\theta\bar{\theta}\bar{\theta}D \,. \tag{1.7}$$

It has a chiral and anti-chiral field strength supermultiplets

$$W_\alpha = -\frac{1}{4}\bar{D}\bar{D}e^{-V}D_\alpha e^V\,, \bar{W}_\alpha = -\frac{1}{4}DDe^{-V}\bar{D}_\alpha e^V\,. \tag{1.8}$$

Under general non-abelian gauge transformation, W transforms as

$$W \to e^{-i\Lambda}We^{i\Lambda}\,. \tag{1.9}$$

The lowest component of W is a gaugino, but we can also define a supermultiplet whose lowest component is a scalar, so called linear supermultiplet Σ. It is defined by

$$\Sigma = \bar{D}^\alpha D_\alpha V\,, \tag{1.10}$$

which satisfies

$$D^\alpha D_\alpha \Sigma = \bar{D}^\alpha \bar{D}_\alpha \Sigma = 0\,. \tag{1.11}$$

Its lowest component is now σ. From these supermultiplets, we can write down the classical lagrangian kinetic terms as

$$\mathcal{L}_{\text{kinetic}} = \frac{1}{g^2}\int d^2\theta\ \text{Tr}\ W_\alpha^2 + \text{h.c.} + \sum_f \int d^2\theta d^2\bar{\theta}\ Q_f^\dagger e^V Q_f\,, \tag{1.12}$$

where we denoted chiral multiplet as a set of flavor multiplet Q_f, which is a superquark. The Yang-Mills term of (1.12) can be also written in terms of the linear supermultiplet (1.10)

$$\mathcal{L}_{\text{YM}} = \frac{1}{4g^2}\int d^2\theta d^2\bar{\theta}\ \text{Tr}\ \Sigma_\alpha^2\,. \tag{1.13}$$

For abelian factors of gauge group, we can also add Fayet-Iliopoulos (FI) term by

$$\mathcal{L}_{\mathrm{YM}} = \zeta \int d^2\theta d^2\bar{\theta} V \,. \tag{1.14}$$

where ζ is a FI parameter.

It is important to know how we can parametrize possible sets of supersymmetric vacua, which is the moduli space of vacua. There is a branch, called "Coulomb branch", where the real scalar σ has a non-vanishing vacuum expectation value (VEV) in the Cartan subalgebra of the gauge group. This breaks the gauge group G into $\mathrm{U}(1)^r$ for $r = \mathrm{rank}(G)$. In the Coulomb branch, $\mathrm{U}(1)^r$ gauge fields can be dualized to scalars γ^j. They live on the r-dimensional torus defined by charge quantization rule. σ^j and γ^j can be combined into the chiral supermultiplet Φ^j with scalar component $\sigma^j + i\gamma^j$.

The other branch of the moduli space is the "Higgs branch". In (1.12), it contains a potential term

$$\sum_f |\sigma Q_f^2| \,, \tag{1.15}$$

and Higgs branch is where this Q_f has the non-zero VEV, which requires VEV of σ to vanish. Hence, in general, the Coulomb branch and the Higgs branch do not overlap. However, there can be a mixed branch where both $\langle\sigma\rangle$ and $\langle Q_f\rangle$ are non-zero but (1.15) vanishes for some specific matter contents.

1.2 Supersymmetric partition function on S^3

In this section, we will review how to put $\mathcal{N} = 2$ supersymmetric theory on the round three-sphere, and how to compute its partition function. We will follow [26–28].

1.2.1 $\mathcal{N} = 2$ Supersymmetry on S^3

As mentioned in the previous section, 3-d $\mathcal{N} = 2$ supersymmetry has four real supercharges, equivalent to two complex spinors. We can write down the supersymmetric action on the three-sphere S^3 by adding conformal coupling term to the fields and modifying the action and transformation rules to close the supersymmetry algebra. We will use the component field notation in this section. First, action for the Yang-Mills part on S^3 is [26, 27]

$$S_{\rm YM} = \frac{1}{g^2}\int d^3x\sqrt{g}\,{\rm Tr}\left(\frac{1}{2}F^{\mu\nu}F_{\mu\nu} + D_\mu\sigma D^\mu\sigma + (\sigma+D)^2 + i\lambda^\dagger\gamma^\mu\nabla_\mu\lambda + i[\lambda^\dagger,\sigma]\lambda - \frac{1}{2}\lambda^\dagger\lambda\right). \tag{1.16}$$

Fermionic symmetries are generated by the Killing spinor. The Killing spinor ϵ satisfies the condition

$$\nabla_\mu\epsilon = \gamma_\mu\epsilon' \tag{1.17}$$

for some spinor ϵ'. For the suitable choice of vielbein basis on S^3, we can make $\epsilon' \propto \epsilon$ such that $\nabla_\mu\epsilon = \pm\frac{i}{2}\gamma_\mu\epsilon$. With this choice of Killing spinors, we choose supersymmetry generator to be $\delta = \frac{1}{\sqrt{2}}(Q_1^1 + iQ_1^2)$. Then each component of the vector multiplet obeys transformation

$$\begin{aligned}
\delta A_\mu &= -\frac{i}{2}\lambda^\dagger\gamma_\mu\epsilon \\
\delta\sigma &= -\frac{1}{2}\lambda^\dagger\epsilon \\
\delta D &= -\frac{i}{2}D_\mu\lambda^\dagger\gamma^\mu\epsilon + \frac{1}{4}\lambda^\dagger\epsilon + \frac{i}{2}[\lambda^\dagger,\sigma]\epsilon \\
\delta\lambda &= (-\frac{1}{2}\gamma^{\mu\nu}F_{\mu\nu} - D + i\gamma^\mu\partial_\mu\sigma - \sigma)\epsilon \\
\delta\lambda^\dagger &= 0\,.
\end{aligned} \tag{1.18}$$

We can also write down the action for the matter part on S^3 as

$$S_{\text{matter}} = \frac{1}{g^2}\int d^3x\sqrt{g}\Big(D_\mu\phi^\dagger D^\mu\phi + \Delta(2-\Delta)\phi^\dagger\phi + i\psi^\dagger \not{D}\psi + i\phi^\dagger D\phi + \phi\sigma^2\phi + F^\dagger F \\ - i\psi^\dagger\sigma\psi + i\phi^\dagger\lambda^\dagger\psi - i\psi^\dagger\lambda\phi + (\Delta-\frac{1}{2})\psi^\dagger\psi + 2i(\Delta-\frac{1}{2})\phi^\dagger\sigma\phi\Big)\,. \tag{1.19}$$

We have written down the action for non-trivial R-charge Δ for the lowest component for further purpose. Note that the second term of (1.19) is a conformal coupling term of scalar to the curvature of S^3. Each component of the matter multiplet obeys transformation

$$\begin{aligned}
\delta\phi &= 0 \\
\delta\phi^\dagger &= \psi^\dagger\epsilon \\
\delta\psi &= (-i\gamma^\mu D_\mu\phi - i\sigma\phi + \Delta\phi)\epsilon \\
\delta\psi^\dagger &= \epsilon^T F^\dagger \\
\delta F &= \epsilon^T\left(-i\gamma^\mu D_\mu\psi + i\sigma\psi + \left(\frac{1}{2}-\Delta\right)\psi + i\lambda\phi\right) \\
\delta F^\dagger &= 0\,.
\end{aligned} \tag{1.20}$$

Using (1.18) and (1.20), we can verify that $\delta^2 = 0$. Also, our choice of δ satisfies

$$\{\delta, \delta^\dagger\} = M_{12} + R\,, \tag{1.21}$$

for rotation generator M_{12} and R-symmetry R and also generates the isometry

$$\begin{aligned}
\{\delta,\delta^\dagger\}\phi &= (-iv^\mu D_\mu + \sigma)\phi + \Delta\phi \\
\{\delta,\delta^\dagger\}\psi &= (-iv^\mu D_\mu + \sigma)\psi + (\Delta-1)\psi \\
\{\delta,\delta^\dagger\}F &= (-iv^\mu D_\mu + \sigma)F + (\Delta-2)F\,.
\end{aligned} \tag{1.22}$$

where $v_\mu = \epsilon^\dagger \gamma_\mu \epsilon$ is a Killing vector generated by Killing spinor ϵ. For standard dimension $\Delta = \frac{1}{2}$, all actions, transformations and symmetries reduce to the standard conformal theory on S^3.

1.2.2 Localization of S^3 partition function

With the full $\mathcal{N} = 2$ supersymmetric action on S^3 that we have written down, we can proceed even further to do some exact calculation by the method called "Localization". Let us write down the Q-exact term δV satisfying $\delta^2 V = 0$. Let us sketch the idea of localization of the partition function. Consider a generic partition function

$$Z = \int D\Phi e^{-S[\Phi]} \,. \tag{1.23}$$

Then we can add the positive definite term δV to the lagrangian such that

$$Z_t = \int D\Phi e^{-S[\Phi] - t\delta V} \,, \tag{1.24}$$

and this Z_t satisfies

$$\frac{dZ_t}{dt} = -\int D\Phi \delta V e^{-S[\Phi] - t\delta V} = -\int D\Phi \delta (V e^{-S[\Phi] - t\delta V}) = 0 \,. \tag{1.25}$$

This says that the partition function is the same for any value of t. If we take the large negative value of t, then the path integral will only get contributions from the neighborhood of $\delta V = 0$. By expanding fields around the classical saddle point by $\Phi = \Phi_0 + \frac{1}{\sqrt{t}}\tilde{\Phi}$, the deformed action will have a form of

$$S[\Phi] + t\delta V = S[\Phi_0] + \delta V[\Phi_0]\tilde{\Phi}^2 + O\left(\frac{1}{\sqrt{t}}\right) \tag{1.26}$$

where we have simplified all possible quadratic fluctuations by $\tilde{\Phi}^2$. Now the partition function (1.24) becomes

$$Z = \lim_{t\to\infty} Z_t = \int D\Phi e^{-S[\Phi_0]+\delta V[\Phi_0]\tilde{\Phi}^2} = \int D\Phi_0 e^{-S[\Phi_0]} D\tilde{\Phi} e^{\delta V[\Phi_0]\tilde{\Phi}^2} = \int D\Phi_0 e^{-S[\Phi_0]} Z_1 \tag{1.27}$$

where $Z_1 = \det(\delta V[\Phi_0])$ is a one-loop fluctuation part.

The simplest Q-exact term for $\mathcal{N} = 2$ theory is [26, 27]

$$\begin{aligned} \delta V_{\rm YM} &= \delta(\mathrm{Tr}((\delta\lambda)^\dagger\lambda)) \\ \delta V_{\rm matter} &= \delta((\delta\psi)^\dagger\psi + \psi^\dagger(\delta\psi^\dagger))\,, \end{aligned} \tag{1.28}$$

which turns into

$$\begin{aligned} \delta V_{\rm YM} &= \mathrm{Tr}\left(\frac{1}{2}F^{\mu\nu}F_{\mu\nu} + D_\mu\sigma D^\mu\sigma + (\sigma+D)^2 + i\lambda^\dagger\gamma^\mu\nabla_\mu\lambda + i[\lambda^\dagger,\sigma]\lambda - \frac{1}{2}\lambda^\dagger\lambda\right) \\ \delta V_{\rm matter} &= \partial_\mu\phi\partial^\mu\phi^\dagger + \phi^\dagger\sigma_0^2\phi + 2i(\Delta-\frac{1}{2})\phi^\dagger v^\mu\partial_\mu\phi + \Delta^2\phi^\dagger\phi + F^\dagger F \\ &\quad + \psi^\dagger\left(i\not{\nabla} - i\sigma_0 + \frac{1+2(1-\Delta)\not{v}}{2}\right)\psi\,. \end{aligned} \tag{1.29}$$

One can easily show that these Q-exact terms have zero locus at

$$\begin{aligned} A_\mu = 0 \quad &, \quad \sigma = -D = \mathrm{const} = \sigma_0 \\ F = 0 \quad &, \quad \phi = 0\,. \end{aligned} \tag{1.30}$$

Applying these to (1.27) gives us the final localized partition function S^3 [26]

$$Z = \int \prod_{\sigma:\mathrm{cartan}} e^{i\pi\,\mathrm{Tr}\,\sigma^2} d\sigma \det_{\rm Adj} \sinh(\pi\sigma) \prod_{\text{Chiral rep}\,R_i} \det_{R_i}(e^{l(1-\Delta_i+i\sigma)}) \tag{1.31}$$

where Tr is the Chern-Simons form, Δ_i is the R-charge of the chiral multiplet, and l-function is defined by

$$l(z) = -\frac{i\pi}{12} - z\log(1-e^{2\pi iz}) + \frac{i}{2}\left(\pi z^2 + \frac{1}{\pi}\mathrm{Li}_2(e^{2\pi iz})\right) . \tag{1.32}$$

1.3 F-maximization

1.3.1 Renormalization group flow

Back in the 60s, renormalization was considered as a technique to get rid of ultraviolet divergences in QFT perturbatively, especially in quantum electrodynamics (QED) which successfully explained experimental results of electrodynamics in the very small scale. Renormalization group (RG) by then was used to see the leading divergence from the lower order for renormalizable theories, which can become perfectly converging by introducing finite numbers of parameters.

In the 60's and 70's, a novel point of view emerged that renormalizability is related to the behavior of theory at longer scales [29–33]. The concepts of relevant and irrelevant operators gives a deeper insight on renormalizability which in turn explains what type of interactions survive at the scale we are interested in. Therefore, Wilsonian RG shed light on QFT to show that we can connect physics at different scales.

Knowing that RG flow describes QFT at all scales, scientists started to ask the question : what can be a good parameter which tells us where in the RG flow are we? Zamolodchikov came out with the c-theorem in two dimension [34] by using the stress-energy tensor two-point function. His c-function satisfies the property that $c_{\mathrm{UV}} > c_{\mathrm{IR}}$, thereby serving as a parameter of RG flow. Moreover, at the RG fixed point, c-function exactly matches with the Weyl anomaly c which is defined by the

expectation of trace of the stress-energy tensor

$$\langle T^a_a \rangle = -\frac{c}{12} R \,. \tag{1.33}$$

where R is the curvature scalar. In four dimensions, the trace of the stress-energy tensor again defines

$$\langle T^a_a \rangle = -\frac{c}{16\pi^2} W_{abcd} W^{abcd} - 2aE_4 \tag{1.34}$$

where W_{abcd} is the Weyl tensor and E_4 is the Euler density. Cardy proposed the a-theorem [35] : $a_{\rm UV} > a_{\rm IR}$. This a-theorem passed numerous checks for 20 years until Komargodski and Schwimmer proved it by explicitly constructing a-function along RG flow which matches with a in (1.34) at the fixed point [36].

1.3.2 Superconformal theory and maximization principle

More interesting things happen when we add supersymmetry. In [37, 38], central charges a and c for 4-d $\mathcal{N} = 1$ superconformal theory can be completely determined by $\mathrm{U}(1)_R$ symmetry via t'Hooft anomaly matching such that

$$a = \frac{3}{32}(3\,\mathrm{Tr}\, R^3 - \mathrm{Tr}\, R) \quad , \quad c = \frac{1}{32}(9\,\mathrm{Tr}\, R^3 - 5\,\mathrm{Tr}\, R) \,. \tag{1.35}$$

Then finding the a-anomaly coefficient reduces to finding the R-symmetry of the superconformal theory. If there are abelian flavor symmetries, the R-symmetry is not unique since it can be mixed with those flavor symmetries by

$$R_t = R_0 + \sum_I s_I F_I \,. \tag{1.36}$$

Intriligator and Wecht proposed the idea of a-maximization [39] that at the fixed point correct R-symmetry maximizes a.

Jafferis came up with the corresponding idea in the $\mathcal{N} = 2$ superconformal theory in three dimension [26], arguing that correct R-symmetry at the IR fixed point extremizes F (Z in original paper) which is defined by

$$F = -\log Z_{S^3} \,. \tag{1.37}$$

Using the localization method, he showed in many examples that F-maximization principle correctly reproduces the known R-charges of chiral primary operators. However, there are no a or c in the odd dimension because the trace anomaly vanishes in the odd dimension. Inspired by F-maximization, Klebanov *et al.* [40, 41] proposed F-theorem that (1.37) satisfies $F_{\rm UV} \geq F_{\rm IR}$.

1.3.3 Superconformal algebra

Superconformal algebra tells us that there is a relationship between conformal scaling dimension and R-charge of the operator by

$$D(\mathcal{O}) \geq \frac{d-1}{2} R(\mathcal{O}) \,. \tag{1.38}$$

Moreover, this inequality becomes saturated when $\mathcal{O}$ is a chiral primary operator. In 3-d this implies

$$\Delta_{\mathcal{O}} = R_{\mathcal{O}} \,. \tag{1.39}$$

Any operators in the unitary QFT in 3-d should satisfy the unitarity bound

$$\Delta_{\mathcal{O}} \geq \frac{1}{2} \tag{1.40}$$

where the inequality is saturated if and only if $\mathcal{O}$ is a free field. Therefore, combining the idea of F-maximization, (1.39) and (1.40) enables us to explore the physics of 3-d superconformal field theory at the fixed point, determining when operators decouple from the theory. This will be the key idea of the chapter 2.

1.4 Entanglement and Rènyi entropy in QFT

In chapter 3, we will present the work regarding the Rènyi entropy in QFT, which is a direct generalization of the entanglement entropy. For the convenience of the reader, we introduce the concept of entanglement entropy and Rènyi entropy, then sketch how it is related to the F-theorem mentioned in the previous section for motivation.

Quantum entanglement is one of the most interesting phenomena of quantum theory. In the early days of quantum mechanics, it seemed that this entanglement could introduce the nonlocal spooky action culminated in the paper of Einstein *et al.* [42], famously known as EPR paradox. Many resolutions of this paradox have been suggested, including Bell's theorem, but the common conclusion is that the classical view of physics is not enough to explain the real world.

For the given pure quantum state $|\psi\rangle$, the density matrix is given by $\rho = |\psi\rangle\langle\psi|$. The density matrix can neatly express the expectation value of operator $\mathcal{A}$ by $\langle\psi|\mathcal{A}|\psi\rangle = \mathrm{tr}(\rho\mathcal{A})$. Under the complete basis $|\phi_n\rangle$ of the Hilbert space, if the probability that the given state stays at $|\phi_n\rangle$ is p_n, then the expectation value of

operator can be written as

$$\langle \mathcal{A} \rangle = \sum_n p_n \langle \phi_n | \mathcal{A} | \phi_n \rangle = \mathrm{tr}(\rho \mathcal{A}) \tag{1.41}$$

for $\rho = \sum_n p_n |\phi_n\rangle \langle \phi_n|$ where p_n sums to one. This is the general form of the density matrix for both pure and mixed states. Now we can define the von Neumann entropy of the quantum system by

$$\begin{aligned} S_{\text{von Neumann}} &= -\mathrm{tr}(\rho \log \rho) \\ &- = \sum_n p_n \log p_n \end{aligned} \tag{1.42}$$

In the second line, we have substituted general form of ρ. This form of entropy is called Shannon entropy, which defines the expected value of information contained in the system. The direct generalization of the entanglement entropy is the Rènyi entropy [43, 44]

$$S_q = \frac{1}{1-q} \mathrm{tr}\, \rho^q \tag{1.43}$$

where it approaches to the von Neumann entropy as $q \to 1$.

Von Neumann and Rènyi entropy becomes more interesting when we have a quantum system where its Hilbert space can be divided into separate Hilbert space by $\mathcal{H} = \mathcal{H}_A \bigotimes \mathcal{H}_B$. This time we can define the reduced density matrix in system $A(B)$ as $\rho_{A(B)} = \mathrm{tr}_{B(A)}(\rho)$ where we integrate out all degrees of freedom in system $B(A)$. Then the von Neumann entropy for this reduced matrix is $S_A = -\mathrm{tr}(\rho_A \log \rho_A)$, which is the entanglement entropy measuring the degree of entanglement of system A to the other system B. Similarly, Rényi entanglement entropy for system A is written as $S_q^A = \frac{1}{1-q} \mathrm{tr}\, \rho_A^q$.

Let us discuss generalization of Entanglement entropy to QFT. In this case, the whole system will be the spacetime in d-dimensions, and it is separated into two systems A and B by some specific spacelike entanglement surface Σ of dimension $d-2$. In this dissertation, we will use the density matrix of vacuum only $\rho = |0\rangle\langle 0|$. Then the entanglement entropy or Rènyi entropy with entangling surface Σ will be same as we have defined before.

1.4.1 Relation to the F-theorem

The entanglement entropy we just have introduced is actually directly related to the F-theorem we mentioned in section 1.3.2. At the conformal fixed point, entanglement entropy coincides with F by a minus sign [20, 21]

$$F_{S^3} = -S(R)\,, \tag{1.44}$$

for three-sphere of radius R. However, QFT computation in practice always comes with the lattice spacing (inverse of UV cutoff) ϵ suffering us from the UV divergence. Naively, we can think that there are R/ϵ degrees of freedom per dimension, and the holographic nature of entanglement entropy will give rise to the leading divergence $S \sim (R/\epsilon)^{d-2}$. To remove this divergence, in $d = 3$, we can define renormalized entanglement entropy

$$\mathcal{F}(R) = -S(R) + R\frac{dS(R)}{dR}\,. \tag{1.45}$$

From (1.44), it is evident that renormalized entanglement entropy again coincides with renormalized F at the conformal fixed point. Casini and Huerta have shown that any theory with Lorentz invariance requires entanglement entropy with circular entangling surface that $S''(R) \leq 0$ [25]. Since $\mathcal{F}'(R) = RS''(R)$, and that $\mathcal{F}(R)$

approaches to the value of F at IR fixed point in large R limit [45], proves the F-theorem that $\mathcal{F}_{\rm UV} \geq \mathcal{F}_{\rm IR}$.

Moreover, Rènyi entropy is directly related to the thermal free energy on the hyperbolic cylinder [46]. The reduced density matrix on a disk of radius R in $(2+1)-$dimensions can be mapped to the hyperbolic cylinder by

$$\rho = \frac{e^{-2\pi R\mathcal{H}_t}}{\mathrm{tr}\, e^{-2\pi R\mathcal{H}_t}}\,, \tag{1.46}$$

where $\mathcal{H}_t$ is the Hamiltonian on the hyperbolic cylinder. Putting this (1.43) we get the Rènyi entropy

$$S_q = \frac{q\mathcal{F}_1 - \mathcal{F}_q}{1-q} \quad , \quad S_1 = -\mathcal{F}_1\,, \tag{1.47}$$

where we get $\mathcal{F}_q$ through the relation $Z_q = \mathrm{tr}\, e^{-2\pi Rq\mathcal{H}_t} = e^{-\mathcal{F}_q}$. This Z_q can be thought of as the thermal partition function with the temperature $T = 1/2\pi Rq$. The Euclidean hyperbolic cylinder can be conformally mapped to the q-fold covering of the three-sphere. Note that this and (1.47) mean that the entanglement entropy is the same as the three-sphere partition function that we talked before, especially, giving us a connection between the concepts of chapter 2 and 3.

Chapter 2

$\mathcal{N} = 2$ supersymmetric QCD in three dimension

This chapter contains the edited version of [47], which was written in collaboration with Igor Klebanov and Benjamin Safdi, and [48], which was written in collaboration with Masahito Yamazaki.

2.1 Introduction

Supersymmetry has been one of the most important tools for understanding strongly coupled dynamics in quantum field theory. Since supersymmetric theories are much easier to deal with at strong coupling than their counterpart in non-supersymmetric theories, there has been an enormous effort to understand the supersymmetric quantum field theory. In four dimensions the infrared behavior of $\mathcal{N} = 1$ supersymmetric QCD (SQCD) was surveyed [6, 49–51] in the 1990's, and many similarities were found with the expected behavior of non-supersymmetric QCD. For example, the SQCD theory with $SU(N_c)$ gauge group and N_f non-chiral massless flavors, where each flavor multiplet consists of a fundamental and anti-fundamental chiral superfield, $(Q, \tilde{Q})$, flows to an interacting infrared fixed point in the Seiberg conformal

window $\frac{3N_c}{2} < N_f < 3N_c$ [6]. A similar conformal window is believed to exist for the non-supersymmetric $SU(N_c)$ gauge theory coupled to massless flavors [8]. Its upper boundary, $N_f = 11N_c/2$, is determined by asymptotic freedom, but its lower boundary is not yet known precisely.

The dynamics of gauge theories in three dimensions is of much interest due, in part, to their relation to statistical mechanics and condensed matter physics. For example, it is expected that the $U(N_c)$ gauge theory with N_f massless flavors flows to an interacting infrared fixed point when $N_f > N_{\rm crit}$, where $N_{\rm crit}$ is some critical number of flavors [52,53]. For large N_f the scaling dimensions of composite operators may be calculated using the $1/N_f$ expansion. For $N_f < N_{\rm crit}$ the theory is thought to flow to a gapped phase in the infrared, though this phenomenon is difficult to study due to the strong coupling nature of the transition.

In order to gain more insight into the nature of the conformal window in 3-d gauge theories, it is instructive to study such theories with $\mathcal{N} = 2$ supersymmetry, which are under an improved theoretical control. The $U(N_c)$ gauge theory with N_f non-chiral flavors flows to an IR fixed point for $N_f \geq N_c$, while for $N_f < N_c$ supersymmetry is broken [9]. For $N_f \geq N_c$ the $\mathcal{N} = 2$ superconformal theories possess the Aharony duality [54] mapping them to $U(N_f - N_c)$ theories with N_f non-chiral flavors along with extra neutral matter, in analogy with the Seiberg duality [6] in 4-d $\mathcal{N} = 1$ theories. Also for the $USp(2N_c)$ gauge theory with $2N_f$ non-chiral flavors, for $N_f > N_c + 1$, there is a dual theory with $USp(2N_f - 2N_c - 2)$ gauge group and $2N_f$ non-chiral flavors with additional chiral multiplets [54, 55]. When a Chern-Simons term is added, this is generalized to the Giveon-Kutasov duality [56]. Similarly, theories with SU(N_c) and O(N_c) type of gauge groups also have their IR duals [57–59].

In order to figure out how IR fixed point looks like, we need to know the IR scaling dimensions (same as R-charges due to the superconformal algebra we saw

in section 1.3.3) of matter fields. In the past few years, localization on the three-sphere [26–28] unveiled new features of 3-d $\mathcal{N}=2$ theories. The S^3 partition function is given by (without Chern-Simons terms, FI parameters and real masses)

$$Z = \frac{1}{|W|}\int_{\text{Cartan}} d\sigma \prod_{\alpha:\text{root}} [\sinh \pi\alpha(\sigma)]^2 \prod_{\Phi:\text{ chiral multiplet}} \prod_{\rho:\text{ weight of } R_\Phi} e^{[l(1-\Delta_\Phi + i\rho(\sigma))]} , \quad (2.1)$$

where $|W|$ is the order of the Weyl group, R_Φ (Δ_Φ) is the representation under the gauge group (R-charge) of the chiral multiplet Φ and the function $l(z)$ is defined by

$$l(z) := -z\log(1-e^{2\pi i z}) + \frac{i}{2}\left(\pi z^2 + \frac{1}{\pi}\text{Li}_2(e^{2\pi i z})\right) - \frac{i\pi}{12} . \quad (2.2)$$

What makes 3-d $\mathcal{N}=2$ theories interesting is that its abelian R-symmetry can be mixed with other abelian flavor symmetries in the IR, which seems to open up uncertainty. The correct IR R-symmetry can be calculated using the principle of F-maximization [26,40,60], which states that the correct R-symmetry locally maximizes the Euclidean three-sphere free energy $F = -\log Z$.

In section 2.2.3 we introduce three methods for F-maximization to determine IR scaling dimension Δ. The first method is to numerically compute the distribution of eigenvalues at the saddle point in the large N_c limit using a procedure similar to that of [61]. The second method is to extrapolate small N_c results, by computing integral (2.1) numerically, to the large N_c limit. Lastly, the third method computes Δ analytically in an asymptotic expansion in $1/x$ (expansion in $(x-1)$ when x is close to 1).

However, the three sphere partition functions do not always converge [62]. This causes a problem, since we need S^3 partition function to determine the correct IR scaling dimension. However, as we will see in the following sections, whenever the electric theory has a divergent partition function, the magnetic partition function is convergent. Therefore we can perform F-maximization using one of the dual theories.

We will also show that convergence issue is equivalent to the positivity of the monopole scaling dimension in section 2.2.2.

In the Veneziano limit [63], where N_c is taken to infinity while keeping the ratio $x = \frac{N_f}{N_c}$ fixed, we find that this divergence occurs at certain critical values $x = x_c$. For $x < x_c$ a new "accidental" global symmetry emerges in the infrared and mixes with the IR R-symmetry. A key insight into the nature of this global symmetry is found by studying the scaling dimension of the protected monopole operators, which are local operators in three-dimensions, as functions of x. We find that the monopole operators are above the unitarity bound for $x > x_c$ and reach the unitarity bound $\Delta = 1/2$ at $x = x_c$. When $x < x_c$ the monopole fields become free and *decouple*, so that the accidental global symmetry acts on the monopole sector. In the dual magnetic theories, this global symmetry acts on chiral superfields, dual to the monopole fields in the electric theory. This allows us to fix the dimensions of those chiral superfields to $1/2$ then use F-maximization to fix the IR R-symmetry when $x < x_c$. We refer to the transition in the behavior of the theory at $x = x_c$ as "a crack in the superconformal window." The existence of the "crack" has interesting effects on the properties of observables. For example, as we show in section 2.5, when F is plotted at fixed N_f as a function of N_c, it is peaked at the "crack."

From section 2.2 to 2.5, we consider SQCD with all types of gauge groups, $\mathrm{U}(N_c)$, $\mathrm{SU}(N_c)$, $\mathrm{USp}(2N_c)$ and $\mathrm{SO}(N_c)$. We analyze the unitarity bound of the matter fields and convergence bound of the three-sphere partition function, then carry out F-maximization explicitly to determine the correct IR scaling dimension in the Veneziano limit. In all cases we find critical values $x_c > 1$, generally around 1.45, below which some of the monopole operators decouple. Once some operators decouple we can re-do the F-maximization following the prescription of [64–66]. In section 2.6, we find the formula for the IR scaling dimension Δ to any gauge group in the large N_f limit, up to the order of $1/N_f^2$ (2.110).

We also point out that a gauging of flavor symmetries can drastically modify the IR behavior of the theory. In section 2.3, we see that gauging the $\mathrm{U}(1)_B$ symmetry to obtain the $\mathrm{U}(N_c)$ SQCD from the $\mathrm{SU}(N_c)$ SQCD, which is interesting because magnetic theory works only works below x_c for $\mathrm{U}(N_c)$ SQCD while that of $\mathrm{SU}(N_c)$ SQCD works above x_c as well. Things become more interesting in section 2.5, where we gauge discrete symmetries $\mathbb{Z}_2$ or $\mathbb{Z}_2 \times \mathbb{Z}_2$ in the $\mathrm{SO}(N_c)$ SQCD to obtain $\mathrm{O}(N_c)_+$, $\mathrm{O}(N_c)_-$, $\mathrm{Spin}(N_c)$ or $\mathrm{Pin}(N_c)$ SQCD. In this case gauging changes the monopole operator with the minimal charge. We find some examples where the monopole operator decouples for $\mathrm{SO}(N_c)$ and $\mathrm{O}(N_c)_+$ gauge groups, but not for $\mathrm{O}(N_c)_-$, $\mathrm{Spin}(N_c)$, $\mathrm{Pin}(N_c)$ gauge groups. When we move on to discuss possible generalizations of our procedure to quiver gauge theories in section 2.7, gauging changes not only the IR scaling dimensions, but also changes the convergence bound for the S^3 partition functions.

Lastly, in section 2.8, we turn into chiral $\mathcal{N} = 2$ theory by turning on the Chern-Simons (CS) coupling. The transition at $x = x_c$ we saw before disappears when we add in a CS term at level k to the gauge sector. This is because there are no gauge invariant BPS operators which can be constructed from the monopole operators in the theories with $k \neq 0$. The S^3 partition function is converging everywhere above the supersymmetry bound when the CS level is non-vanishing. It is still instructive in this case to keep track of the scaling dimensions of the protected meson operators as functions of $x = \frac{N_f}{N_c}$ and $\kappa = \frac{|k|}{N_c}$ in the Veneziano limit. We find three different types of behavior at small x depending on whether $\kappa < 1$, $\kappa = 1$, or $\kappa > 1$. The theories with $\kappa < 1$ reach the supersymmetry bound at $x = 1 - \kappa$, and at this point the meson operators have dimension $1/2$ and become free fields. The theories with $\kappa = 1$ are quite special; at small x the scaling dimensions of the meson operators approach $\frac{2}{3}$ due to the cubic superpotential in the magnetic Giveon-Kutasov theory. In the theories with $\kappa > 1$ the meson dimensions approach unity at small x, which is likely due to an enhanced higher spin symmetry in this limit [67–69].

2.2 U(N_c) SQCD

Let us start by discussing non-chiral $\mathcal{N} = 2$ SQCD with U(N_c) gauge group without Chern-Simons coupling and with N_f flavor multiplets. It is known that this theory has a stable supersymmetric vacuum when $N_f \geq N_c$ [9].

2.2.1 Dual Pairs

Electric Theory This theory has a $U(N_f) \times U(N_f)$ global flavor symmetry. However, the diagonal $U(1)_V$, which rotates the Q_a and $\tilde{Q}^a$ by opposite phases, is gauged, and this reduces the global flavor symmetry to $SU(N_f) \times SU(N_f) \times U(1)_A$, where the $U(1)_A$ rotates the two chiral superfields by the same phase. There is also a $U(1)_R$ symmetry. At superconformal fixed points the scaling dimension of an operator is equal to the absolute value of its $U(1)_R$ charge. The UV R-charges of the chiral superfields $(Q_a, \tilde{Q}^a)$ thus take the free value 1/2. The correct R-symmetry at the IR fixed point may be a combination of the UV R-symmetry and the other global $U(1)$ symmetries.

There are also N_c topological currents $j_{\text{top}} = \star \operatorname{tr} F$, where the field strength F is proportional to a Cartan generator of $U(N_c)$. The monopole operators, which are local operators in three-dimensions, are charged under the topological $U(1)$'s. More specifically, in the presence of a monopole operator charged under the topological $U(1)$ with current $j_{\text{top}} = \star \operatorname{tr} F$ inserted at the origin, the field strength takes the form

$$F = \frac{M}{2} \star d\frac{1}{|x|}\,, \tag{2.3}$$

where M is an element of the Cartan subalgebra. The Dirac quantization condition restricts

$$M = \mathrm{diag}(q_1, \ldots, q_{N_c})\,, \tag{2.4}$$

with integer $q_1 \geq q_2 \cdots \geq q_{N_c}$, up to gauge transformations. Semi-classically we may construct BPS field configurations in $\mathcal{N} = 2$ theories by combining the field strength in (2.3) with background configurations for the adjoint scalar σ in the vector multiplet. The monopole can then be thought of as being the spin-0 component of a chiral superfield. These chiral superfields parameterize the classical Coulomb branch of the theory. However, in the quantum theory only two of these monopole operators survive in the chiral ring, and these are the monopole operators with Cartan generators $M = \mathrm{diag}(\pm 1, 0, \ldots, 0)$ [9, 70]. We refer to these special monopole operators which remain in the chiral ring as V_+ and V_-. A summary of the global and gauge symmetries of the theory is given in table 2.5.

	$\mathrm{U}(N_c)$	$\mathrm{SU}(N_f)_L$	$\mathrm{SU}(N_f)_R$	$\mathrm{U}(1)_A$	$\mathrm{U}(1)_J$	$\mathrm{U}(1)_{\mathrm{R-UV}}$
Q	$\boldsymbol{N_c}$	$\boldsymbol{N_f}$	$\mathbf{1}$	1	0	0
$\tilde{Q}$	$\overline{\boldsymbol{N_c}}$	$\mathbf{1}$	$\overline{\boldsymbol{N_f}}$	1	0	0
$V_\pm$	$\mathbf{1}$	$\mathbf{1}$	$\mathbf{1}$	$-N_f$	± 1	$N_f - N_c + 1$

(2.5)

For our purposes the most important property of the monopoles is their IR R-charge. The monopoles acquire an R-charge [71–73], with the result

$$\Delta_{V_\pm} = -N_c + 1 + N_f(1 - \Delta)\,, \tag{2.6}$$

where the first contribution is from the gauginos and the second is from the fermions in the flavor multiplets. Here Δ is the IR R-charge of the flavor supermultiplets which turns out to be same $\mathrm{U}(1)_A$ charge. The monopole operators also acquire a $U(1)_A$ charge of $-N_f$ at one loop.

One might worry that (2.6) is not exact since the topological $U(1)_J$ under which the monopole operators are charged can in principle mix with the R-symmetry. To understand the resolution to this question, it is useful to review the relevant discrete symmetries of the theory. The SYM theory is invariant under charge conjugation symmetry and parity symmetry. Charge conjugation acts by exchanging the fundamental flavors with the anti-fundamental flavors. Parity symmetry acts by exchanging the monopole operators V_+ and V_-. Thus, charge conjugation symmetry implies that the R-charge of the fundamental flavors equals the R-charge of the anti-fundamental flavors, and parity symmetry restrict the R-charges of V_+ and V_- to be the same. The R-symmetry cannot mix with $U(1)_J$ since this would necessarily lead to different R-charges for the two monopole operators.

Magnetic Theory Let us first assume $N_f > N_c$. The magnetic theory has gauge group $\mathrm{U}(\tilde{N}_c)$ (remember the definition $\tilde{N}_c := N_f - N_c$), and has dual quark q, anti-quarks $\tilde{q}$, and the meson $M = Q\tilde{Q}$ and $V_\pm$. The magnetic theory also has two monopole operators $\tilde{V}_\pm$ for the dual photons of magnetic gauge groups. The superpotential is given by

$$W_{\text{magnetic}} = \tilde{q}Mq + V_+\tilde{V}_- + V_-\tilde{V}_+ \ . \tag{2.7}$$

The theory again has the same flavor symmetry as the electric theory, under which the fields transform as follows:

	$\mathrm{U}(\tilde{N}_c)$	$\mathrm{SU}(N_f)_L$	$\mathrm{SU}(N_f)_R$	$\mathrm{U}(1)_A$	$\mathrm{U}(1)_J$	$\mathrm{U}(1)_{\mathrm{R-UV}}$
q	$\boldsymbol{\tilde{N}_c}$	$\overline{\boldsymbol{N_f}}$	$\mathbf{1}$	-1	0	1
$\tilde{q}$	$\overline{\boldsymbol{\tilde{N}_c}}$	$\mathbf{1}$	$\boldsymbol{N_f}$	-1	0	1
M	$\mathbf{1}$	$\boldsymbol{N_f}$	$\overline{\boldsymbol{N_f}}$	2	0	0
$V_\pm$	$\mathbf{1}$	$\mathbf{1}$	$\mathbf{1}$	$-N_f$	± 1	$\tilde{N}_c+1$
$\tilde{V}_\pm$	$\mathbf{1}$	$\mathbf{1}$	$\mathbf{1}$	N_f	± 1	$-\tilde{N}_c+1$

(2.8)

For $N_f = N_c$, the magnetic theory do not have a gauge group, and is described by the chiral superfields $V_\pm, M$, with the superpotential

$$W = V_+ V_- \det(M) \ . \tag{2.9}$$

The charge assignment in this case is

	$\mathrm{SU}(N_f)_L$	$\mathrm{SU}(N_f)_R$	$\mathrm{U}(1)_A$	$\mathrm{U}(1)_J$	$\mathrm{U}(1)_{\mathrm{R-UV}}$
M	$\boldsymbol{N_f}$	$\overline{\boldsymbol{N_f}}$	2	0	0
$V_\pm$	$\mathbf{1}$	$\mathbf{1}$	$-N_f$	± 1	$\tilde{N}_c+1$

(2.10)

2.2.2 IR Analysis

As already mentioned in Introduction, the R-symmetry mentioned above is only one of the many possible R-symmetries in the UV, and the correct IR R-symmetry inside the superconformal algebra is a mixture of the UV R-symmetry with global symmetries. The correct combination is determined by the procedure of F-maximization [26].

Since non-Abelian flavor symmetries do not mix with the U(1) R-symmetry, we can parametrize the R-symmetry as

$$R_{\rm IR} = R_{\rm UV} + aJ_A \ . \tag{2.11}$$

Note that we do not need to consider the mixing with the topological $\mathrm{U}(1)_J$ symmetry, since otherwise the parity is broken.

Unitarity Bound The dimensions of Q, $\tilde{Q}$, $V_\pm$, and M are given by

$$\Delta_{Q,\tilde{Q}} = a \ , \qquad \Delta_{V_\pm} = (N_f - N_c + 1) - N_f a \ , \qquad \Delta_M = 2a \ , \tag{2.12}$$

which leads to the unitarity bound

$$V_\pm : \ a \leq \frac{N_f - N_c + \frac{1}{2}}{N_f} \ , \qquad M : \ a \geq \frac{1}{4} \ , \tag{2.13}$$

which in the Veneziano limit simplifies to

$$\frac{1}{4} \leq a \leq 1 - \frac{1}{x} \ . \tag{2.14}$$

Note this requires $x \geq \frac{4}{3}$, and we will find the crack before this value.

Partition Function As mentioned in the introduction, we need to write down the S^3 partition functions [26–28] of the electric and magnetic theories. The partition function of the electric theory is given by

$$\begin{aligned} Z_{\rm electric} = \frac{1}{N_c!} \int \prod_{i=1}^{N_c} d\sigma_i \overbrace{\prod_{1\leq i<j\leq N_c} \sinh^2[\pi(\sigma_i - \sigma_j)]}^{\text{measure}} \\ \times \overbrace{\prod_{i=1}^{N_c} \exp\left[N_f \, l(1 - \Delta + i\sigma_i) + N_f \, l(1 - \Delta - i\sigma_i)\right]}^{Q,\tilde{Q}} \ , \end{aligned} \tag{2.15}$$

and that of the magnetic theory (for $N_f > N_c$) by

$$Z_{\text{magnetic}} = \frac{1}{\tilde{N}_c!} \exp\left[\overbrace{N_f^2\, l(1-2\Delta)}^{M} + \overbrace{2l\left(1-(\tilde{N}_c+1)+N_f\,\Delta\right)}^{V_\pm}\right] \times \int \prod_{i=1}^{\tilde{N}_c} d\sigma_i \overbrace{\prod_{1\le i<j\le \tilde{N}_c} \sinh^2[\pi(\sigma_i-\sigma_j)]}^{\text{measure}} \overbrace{\prod_{i=1}^{\tilde{N}_c} \exp\left[N_f\, l\left(\Delta+i\sigma_i\right)+N_f\, l\left(\Delta-i\sigma_i\right)\right]}^{q,\,\tilde{q}} \,. \tag{2.16}$$

Convergence We have written down the expressions for the S^3 partition function, however they are in general only formal integral expressions and are actually not convergent.

We can analyze the convergence condition of the partition function by sending one of the σ_i's to infinity. In the limit $\sigma_1 \to \infty$, we can extract the leading behavior of the integrand from asymptotic expansions:

$$\begin{aligned} l(\Delta \mp i\sigma_1) &= \pm\frac{i\pi}{2}\sigma_1^2 - \pi\sigma_1\Delta + \mathcal{O}(\sigma_1^0)\,, \\ \prod_{i<j}^{N_c} \sinh^2[\pi(\sigma_i-\sigma_j)] &= e^{2\pi(N_c-1)\sigma_1+\mathcal{O}(\sigma_1^0)}\,. \end{aligned} \tag{2.17}$$

Then we can derive the convergence bounds of the partition functions as

$$\begin{aligned} &\text{electric:} \quad \Delta < \frac{N_f-N_c+1}{N_f} \approx 1-\frac{1}{x}\,, \\ &\text{magnetic:} \quad \Delta > \frac{N_f-N_c-1}{N_f} \approx 1-\frac{1}{x}\,. \end{aligned} \tag{2.18}$$

It turns out that these conditions are the same as the condition that the dimensions of the monopole operators ($V_\pm$ for the electric theory, $\tilde{V}_\pm$ for the magnetic theory)

are non-negative:

$$\begin{aligned} V_\pm &: \Delta_{V_\pm} = (N_f - N_c + 1) - N_f\Delta \geq 0 \ , \\ \tilde{V}_\pm &: \Delta_{\tilde{V}_\pm} = -(N_f - N_c - 1) + N_f\Delta \geq 0 \ . \end{aligned} \tag{2.19}$$

That we obtain the same conditions from two different considerations is not a coincidence, and we will encounter the same phenomena in later sections. In fact, we can think of this as a convenient way to obtain the R-charge/conformal dimension of monopole operators.

When we analyze the convergence of the partition function, we go to infinity in the Coulomb branch in the direction of the Cartan corresponding to a monopole operator V. Since the Coulomb branch parameter is a dynamical version of the real mass parameter, this has the effect of making the fields massive. We can integrate out these massive modes, except that we then could have induced Chern-Simons term with level k_{eff} and induced FI parameter ζ_{eff}. In the theories discussed in this paper, we have $k_{\text{eft}} = 0$ however $\zeta_{\text{eff}} \neq 0$, leaving to the expression

$$Z \sim \int d\sigma_1 \ e^{-2\pi\zeta_{\text{eff}}\sigma_1} \ , \tag{2.20}$$

and the dimension (or equivalently the $\mathrm{U}(1)_R$-charge) of the monopole operator V, whose real part is $e^{-2\pi\sigma_1}$, can be identified with ζ_{eff}:

$$\zeta_{\text{eff}} = \Delta_V \ . \tag{2.21}$$

In our example, the partition function gives:

$$\begin{aligned} &\text{electric:} \quad \zeta_{\text{eff}} = \overbrace{-(N_c - 1)}^{\text{measure}} + \overbrace{N_f(1-\Delta)}^{Q,\tilde{Q}} = (N_f - N_c + 1) - N_f\,\Delta \ , \\ &\text{magnetic:} \quad \zeta_{\text{eff}} = \overbrace{-(\tilde{N}_c - 1)}^{\text{measure}} + \overbrace{N_f\Delta}^{q,\tilde{q}} = -(N_f - N_c - 1) + N_f\,\Delta \ . \end{aligned} \tag{2.22}$$

and their positivity conditions indeed match with (2.19).

As a side remark, this also explains clearly that the convergence condition is weaker than the unitarity constraint: for a monopole operator V the former requires $\Delta_V \geq 0$, while the latter requires $\Delta_V \geq \frac{1}{2}$.

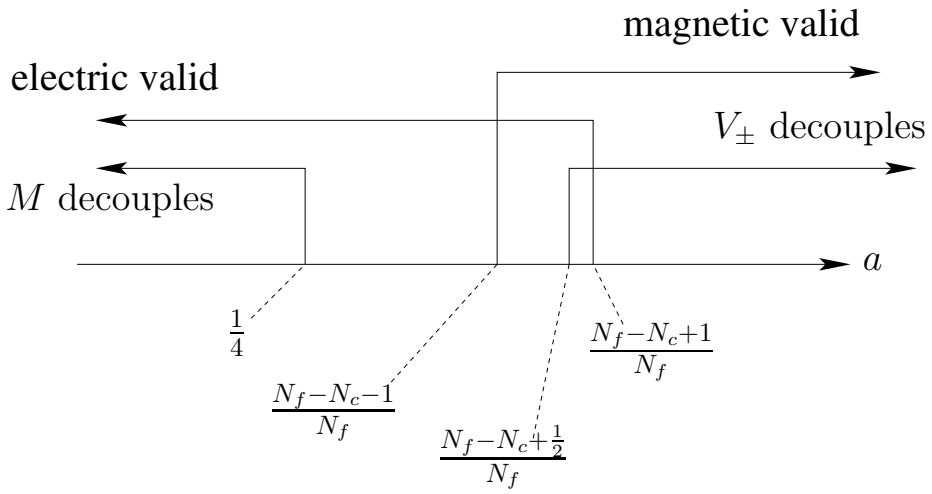

Figure 2.1: The unitarity bound and the convergence bound for the 3d $\mathcal{N}=2$ U(N_c) SQCD with N_f flavors with $N_f > N_c$, plotted in terms of the mixing parameter a (see (2.11)). The correct IR value of a should be determined from F-maximization.

2.2.3 F-maximization methods

To determine the correct R-symmetry in IR, we need to do the F-maximization, by explicitly evaluating the integrals which we are interested in evaluating are given in (2.15) and (2.16). Evaluating these integrals directly in the large N_c limit is difficult when N_f is of order N_c. We take three approaches to approximating these integrals, and more importantly the critical R-charges, and we show that the different approaches give consistent results. We will describe the methods applied for the U(N_c) case and generalizations to the theories with other gauge groups are straightforward.

Method 1: The saddle point approximation

In the large N_c limit we may evaluate the integrals in the saddle point approximation; the integral localizes to the configuration of eigenvalues for which the integrand is an extremum. Our first method numerically solves for this saddle point [61]. Since we only take into account the contribution from the saddle point, our approximation to the function $\Delta(x)$ is off by terms of order $1/N_c$. We take into account finite N_c corrections by repeating the calculation at increasing values of N_c and then extrapolating to $N_c = \infty$.

To begin it is instructive to rewrite the integral in (2.15) in the form

$$Z = \frac{2^{N_c(N_c-1)}}{N_c!} \int \left(\prod_{i=1}^{N_c} \frac{d\lambda_i}{2\pi} \right) e^{-F[\lambda]} \,, \tag{2.23}$$

where

$$\begin{aligned} F[\lambda] = &- \sum_{i<j}^{N_c} \log \left(\sinh^2 \left[\frac{\lambda_i - \lambda_j}{2} \right] \right) \\ &- N_f \sum_{i=1}^{N_c} \left[\ell \left(1 - \Delta + i \frac{\lambda_i}{2\pi} \right) + \ell \left(1 - \Delta - i \frac{\lambda_i}{2\pi} \right) \right] . \end{aligned} \tag{2.24}$$

The saddle point configuration minimizes $F[\lambda]$,

$$\frac{\partial F[\lambda]}{\partial \lambda_i} = 0 \,, \qquad i = 1, \ldots, N_c \,, \tag{2.25}$$

and thus gives the dominant contribution to the partition function in the large N_c limit. The free energy $F = -\log|Z|$ is then approximated by the real part of the functional $F[\lambda]$ evaluated on the saddle point.

We numerically solve the saddle point equations (2.25) following the prescription in [61]. We solve the saddle point equations multiple times for each x, incrementing Δ each time, until we find the configuration which locally maximizes F. Figure 2.2 shows

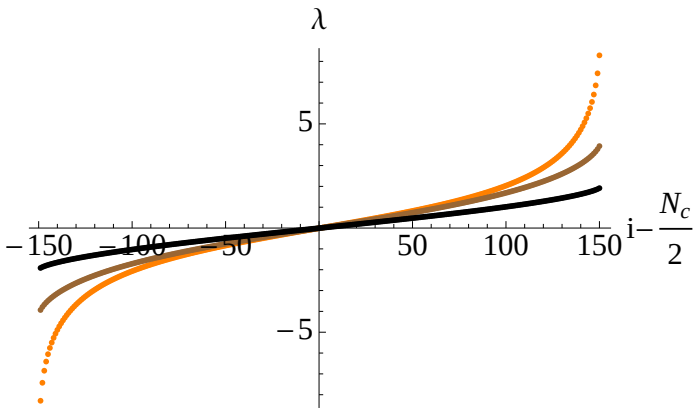

Figure 2.2: Eigenvalue distributions at the saddle point with $x = 1.5$ (orange), 2 (brown), and 5 (black), where $x = \frac{N_f}{N_c}$. We have taken $N_c = 300$ for this example. The eigenvalues are manifestly antisymmetric about $i = \frac{N_c}{2}$, where $i = 1, \ldots, N_c$ labels the Cartan of the $U(N_c)$ gauge group. As x approaches the lower bound $x_c \approx 1.45$ the outer eigenvalues begin to repel each other.

a few eigenvalue distributions, computed at the critical Δ, at increasing values of x with $N_c = 300$. As can be seen directly from (2.24), the eigenvalues are antisymmetric about $i = \frac{N_c}{2}$. The eigenvalues also remain order unity in the large N_c limit, and as a result the free energy scales as N_c^2 at large N_c. As x approaches $x_c \approx 1.45$ the outer eigenvalues begin to repel each other.

For each x we take into account finite N_c corrections by computing Δ for a range of N_c between 100 and 500 and fitting the results to a function of the form

$$\Delta_0 + \frac{\Delta_1}{N_c} + \frac{\Delta_2}{N_c^2} + O(1/N_c^3)\,. \tag{2.26}$$

The quantity Δ_0 is then a good approximation to the function $\Delta(x)$ at $N_c = \infty$. We illustrate this procedure in figure 2.3 for $x = 1.5$. In that example we find $\Delta_0 \approx .319$.

Method 2: Extrapolating from small N_c

Our second method numerically evaluates the partition function for $1 \leq N_c \leq 4$ over a range of N_f. For each N_f we find the Δ which locally maximizes the free energy.

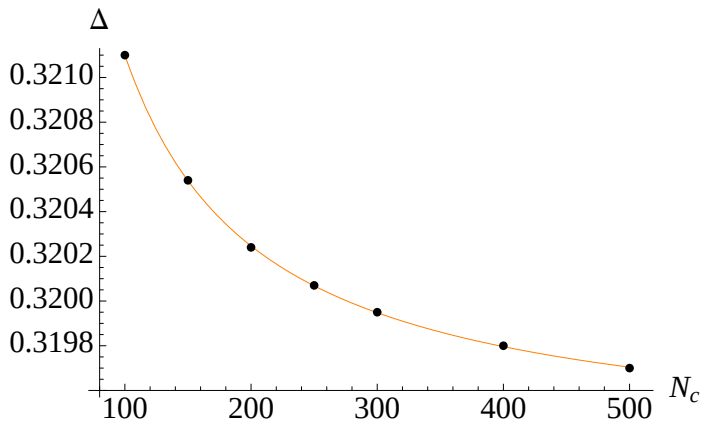

Figure 2.3: A plot of Δ at $x = 1.5$ as a function of N_c in the saddle point approximation, where $x = \frac{N_f}{N_c}$. The black points come from numerically solving the saddle point equations (2.25) and performing F-maximization. The orange curve is a best fit to a function of the form (2.26), with $\Delta_0 \approx .319$, $\Delta_1 \approx .189$, and $\Delta_2 \approx -1.24$.

We can then plot Δ at fixed x as a function of N_c. This is illustrated in figure 2.4, where we also include a fit to a function of the form

$$\Delta(x) = \Delta_0(x) + \frac{\Delta_1(x)}{N_c^2} + \frac{\Delta_2(x)}{N_c^4} + O(1/N_c^6)\,. \tag{2.27}$$

The quantity $\Delta_0(x)$ should be the correct value for $\Delta(x)$ in the Veneziano limit. The reason why the series in (2.27) only includes inverse powers of N_c^2 is explained in the following subsection.

Method 3: The $1/x$ and $(x-1)$ expansions

Our third method gives analytic approximations to Δ in the Veneziano limit at large x and at x slightly above unity. These approximations are computed using the electric and magnetic formulations of the theory, respectively.

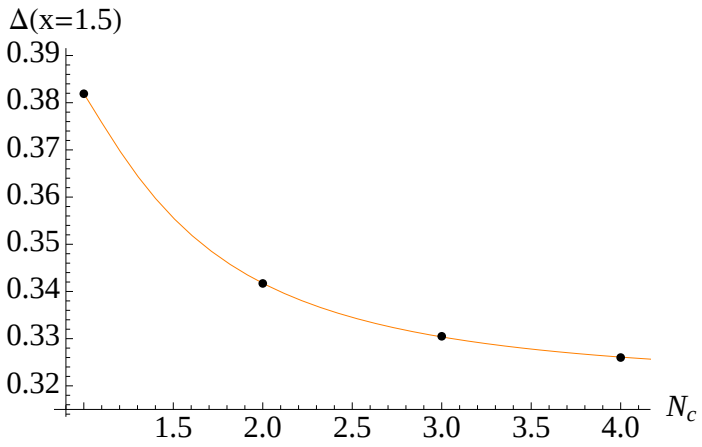

Figure 2.4: A plot of Δ at $x = 1.5$ as a function of N_c. The black points were computed by numerically integrating (2.15) for integer $1 \leq N_c \leq 4$. The smooth orange curve fits these points to the expansion in (2.27); in this example we find $\Delta_0 \approx .320$, $\Delta_1 \approx .0934$, and $\Delta_2 \approx -.0319$.

$1/x$ expansion in the electric theory

In the limit $N_f \gg N_c$, the effects of the gauge field are small and the flavors are almost free; $\Delta \approx \frac{1}{2}$. We perturbatively evaluate corrections to $\Delta = \frac{1}{2}$ in a $1/x$ expansion. This expansion turns out to be a good approximation all the way down to $x \approx x_c$.

We begin by reviewing the theory with $N_c = 1$ and $x = N_f$, since this example, while technically the simplest, still illustrates the main points of the $1/x$ procedure. The $U(1)$ theory was discussed in some detail in [74]. The partition function as a function of Δ is simply given by

$$Z = \int_{-\infty}^{+\infty} \frac{d\lambda}{2\pi} e^{N_f[\ell(1-\Delta+i\frac{\lambda}{2\pi})+\ell(1-\Delta-i\frac{\lambda}{2\pi})]} . \tag{2.28}$$

In the limit of large N_f we may evaluate (2.28) in the saddle point approximation; the partition function localizes around $\lambda = 0$. At $\lambda = 0$ the integrand in (2.28) is minimized at $\Delta = \frac{1}{2}$, which shows that $\Delta = \frac{1}{2} + O(1/N_f)$.

To calculate the higher order terms in the $1/N_f$ expansion we begin by writing

$$\Delta = \Delta_0 + \frac{\Delta_1}{N_f} + \frac{\Delta_2}{N_f^2} + \cdots \tag{2.29}$$

and rescaling the Cartan generator λ to $\tilde{\lambda} = \lambda(2\pi)^{-1}\sqrt{N_f}$. Substituting (2.29) into (2.28), we expand in powers of $1/N_f$ to obtain

$$Z = \frac{1}{2^{N_f}\sqrt{N_f}} \int_{-\infty}^{+\infty} d\tilde{\lambda} e^{-\pi^2\tilde{\lambda}^2/2} \left[1 + \frac{6\pi^2\Delta_1^2 + 24\Delta_1\tilde{\lambda}^2 + \tilde{\lambda}^4}{12N_f} + \dots\right]. \tag{2.30}$$

We may perform the integrals in (2.30) term by term in the $1/N_f$ expansion. Doing so leads to the free energy

$$F_{U(1)}(\Delta) = N_f \log 2 + \frac{1}{2}\log\frac{\pi N_f}{2} - \left(\frac{\pi^2\Delta_1^2}{2} + 2\Delta_1 + \frac{1}{4}\right)\frac{1}{N_f} + \cdots. \tag{2.31}$$

Maximizing (2.31) with respect to Δ_1 leads to $\Delta_1 = -2/\pi^2$. This result can be reproduced by using Feynman diagram techniques [47] , which generalizes into

$$\Delta_1 = -\frac{2\,N_c}{\pi^2} \tag{2.32}$$

for arbitrary N_c.

It is useful to verify explicitly (2.32) for a few small N_c using the F-maximization procedure. Increasing the rank of the gauge group to $N_c = 2$, the partition function is given by the double integral

$$Z = 2\int_{-\infty}^{+\infty} \frac{d\lambda_1 d\lambda_2}{(2\pi)^2}\, \sinh^2\left(\frac{\lambda_1 - \lambda_2}{2}\right) \sum_{i=1}^{2} e^{N_f[\ell(1-\Delta+i\frac{\lambda_i}{2\pi})+\ell(1-\Delta-i\frac{\lambda_i}{2\pi})]}. \tag{2.33}$$

As in the $U(1)$ case, we see here that in the large N_f limit the free energy is locally maximized by $\Delta = 1/2 + O(1/N_f)$. To calculate the subleading terms in Δ, we rescale

the λ_i to $\tilde{\lambda}_i = \lambda_i (2\pi)^{-1}\sqrt{N_f}$ and we calculate the partition function as a function of Δ in the $1/N_f$ expansion:

$$Z = \frac{\pi^2}{2^{N_f-1}N_f}\int_{-\infty}^{+\infty} d\tilde{\lambda}_1 d\tilde{\lambda}_2 e^{-\pi^2(\tilde{\lambda}_1^2+\tilde{\lambda}_2^2)/2}(\tilde{\lambda}_1-\tilde{\lambda}_2)^2\,[1+ \\ + \frac{1}{N_f}\frac{\pi^2}{12}\left(12\Delta_1^2 + 4(\tilde{\lambda}_1-\lambda_2)^2 + 24\Delta_1(\tilde{\lambda}_1^2+\tilde{\lambda}_2^2) + \pi^2(\tilde{\lambda}_1^4+\tilde{\lambda}_2^4)\right) + O(1/N_f^2)\Big]\,, \tag{2.34}$$

which leads to

$$F_{U(2)}(\Delta) = (2N_f)\log 2 + \left[2\log\left(\frac{N_f\pi}{2}\right) - \log 2\pi\right] \\ - \frac{1}{N_f}\left(\frac{7}{2} + \Delta_1(8+\pi^2\Delta_1)\right) + O(1/N_f^2)\,. \tag{2.35}$$

Maximizing (2.35) with respect to Δ_1 yields $\Delta_1 = -4/\pi^2$, consistent with (2.32). Carrying out this procedure for $N_c = 3$ gives

$$F_{U(3)}(\Delta) = (3N_f)\log 2 + \left[\frac{9}{2}\log\left(\frac{N_f\pi}{2}\right) - 3\log(2\pi) - \log 2\right] \\ - \frac{1}{N_f}\left(\frac{51}{4} + \Delta_1\Big(18 + \frac{3}{2}\pi^2\Delta_1\Big)\right) + O(1/N_f^2)\,, \tag{2.36}$$

which is maximized by $\Delta_1 = -6/\pi^2$; again, this is consistent with (2.32).

Iterating the procedure described above, we are able to solve for Δ as a function of N_f and N_c to arbitrary order in $1/N_f$. Below we list the terms through order $1/N_f^4$,

$$\Delta(N_f,N_c) = \frac{1}{2} - N_c\frac{2}{\pi^2 N_f} + \frac{-2\pi^2(5N_c^2-2)+72\,N_c^2}{3\pi^4 N_f^2} \\ - N_c\left[\frac{14\pi^4(N_c^2-1) - 8\pi^2(37N_c^2-18)+1536\,N_c^2}{3\pi^6 N_f^3}\right] \\ + \frac{1}{15\,\pi^8 N_f^4}\Big[-2\pi^6(47N_c^4-65N_c^2+18) + 80\pi^4(49N_c^4-49N_c^2+4) \\ -320\pi^2(156N_c^4-83N_c^2) + 201600\,N_c^4\Big] + O(1/N_f^5)\,. \tag{2.37}$$

The expression for Δ in (2.37) simplifies in the Veneziano limit, with $x = N_f/N_c$ held fixed, and gives the result (2.43). It is also interesting to note that the corrections to $\Delta(x)$ proceed in powers of $1/N_c^2$.

We also find that the N_c dependence of the free energy is given by

$$\begin{aligned} F = {} & N_c N_F \log 2 + \left[\frac{N_c^2}{2} \log(\pi N_f) - \frac{1}{2} N_c (N_c - 1) \log(2\pi) - \log(1!2! \cdots (N_c - 1)!) \right] \\ & + \frac{N_c}{N_f} \left[- \left(\frac{\pi^2 - 4}{2\pi^2} \right) N_c^2 + \frac{1}{4} \right] \\ & + \frac{N_c^2}{N_f^2} \left[- \left(\frac{512 - 112\,\pi^2 + 7\,\pi^4}{24\pi^4} \right) N_c^2 + \left(\frac{7}{24} - \frac{8}{3\,\pi^2} \right) \right] + O(1/N_f^3)\,. \end{aligned} \tag{2.38}$$

These $1/x$ expansions of $\Delta(x)$ and $F(x)$ are not convergent series, but rather asymptotic ones. Keeping the first few terms provides good numerical approximations at large x.

$(x-1)$ expansion in the magnetic theory

Let's now consider the limit where x is slightly above 1. We know that $\Delta = \frac{1}{4}$ at the SUSY bound ($x = 1$), so it is tempting to search for an asymptotic expansion of the form

$$\Delta = \frac{1}{4} + \tilde{\Delta}_1 (x-1) + \tilde{\Delta}_2 (x-1)^2 + \dots\,. \tag{2.39}$$

Indeed, we may find such an expansion by perturbation theory in the Aharony dual

It is convenient to make the choice $N_f = N_c + 1$, so that the partition function of the dual theory is given by

$$Z = \frac{e^{(N_c+1)^2 \ell(1-2\Delta)}}{2} \int \frac{d\lambda}{2\pi} e^{(N_c+1)[\ell(\Delta + i\frac{\lambda}{2\pi}) + \ell(\Delta - i\frac{\lambda}{2\pi})]} \tag{2.40}$$

and so that (2.39) takes the form

$$\Delta = \frac{1}{4} + \frac{\tilde{\Delta}_1}{N_c} + \frac{\tilde{\Delta}_2}{N_c^2} + \dots \,. \tag{2.41}$$

Substituting (2.41) into (2.40) and rescaling $\lambda \to \lambda/\sqrt{N_c}$, we may expand about $N_c = \infty$ to find

$$\begin{aligned} F = -\log|Z| = N_c^2 \frac{\log 2}{2} + N_c \left(\frac{5\,\log 2}{4} + \frac{G}{\pi}\right) + \frac{1}{2}\log N_c \\ + \left(\frac{\pi\,\tilde{\Delta}_1}{2}(1 - 2\,\pi\,\tilde{\Delta}_1) + \frac{3\log 2}{4} + \frac{G}{\pi} + \log(\pi - 2) + \frac{3\log\pi}{2}\right) + O(1/N_c)\,. \end{aligned} \tag{2.42}$$

Performing F-maximization at this order then gives $\tilde{\Delta}_1 = 1/(4\pi)$. Expanding F to one more order in $1/N_c$ and performing F-maximization for $\tilde{\Delta}_2$ gives the result in (2.45). A simple way to check this result is to repeat the analysis with $N_f = N_c + n$ for other small n. In doing so we may also verify that F is approximated by (2.46) in the Veneziano limit for x slightly greater than one.

2.2.4 Results

Using the three methods discussed in previous section, we obtain Δ in the Veneziano limit as

$$\begin{aligned} \Delta(x) = \frac{1}{2} - \frac{2}{\pi^2 x} + \frac{2(36 - 5\,\pi^2)}{3\,\pi^4 x^2} - \frac{2(\pi^2 - 12)(7\,\pi^2 - 64)}{3\pi^6 x^3} \\ - \frac{2(47\,\pi^6 - 1960\,\pi^4 + 24960\,\pi^2 - 100800)}{15\,\pi^8 x^4} \\ - \frac{2(189\,\pi^8 - 12832\,\pi^6 + 289424\,\pi^4 - 2679360\,\pi^2 + 8847360)}{45\,\pi^{10} x^5} + O(1/x^6)\,. \end{aligned} \tag{2.43}$$

In figure 2.5 we plot the results for Δ as a function of x. The electric theory stops to work at some value x_c, which we call as the "crack in the conformal window", and

we determine numerically that $x_c \approx 1.45$. In figure 2.6 we plot F/N_c^2 as a function of

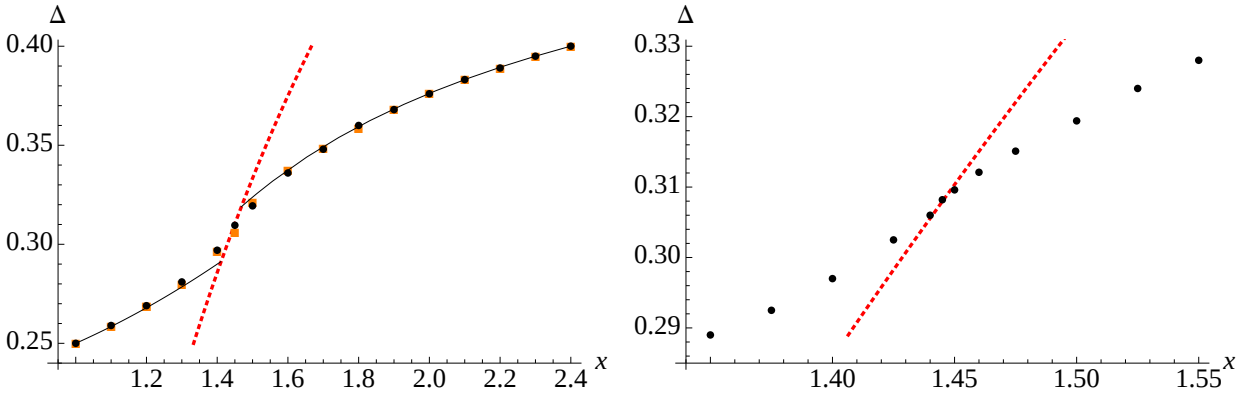

Figure 2.5: Δ as a function of $x = \frac{N_f}{N_c}$ in the Veneziano limit. The black points were computed using the saddle point method (method 1, section 2.2.3) and the orange boxes were computed by extrapolating from the small N_c numerical results (method 2, section 2.2.3). The dotted red curve is the convergence bound $1 - \frac{1}{x}$; we find that Δ meets the convergence bound at the critical value $x_c \approx 1.45$. The smooth black curves at large and small values of x are the analytic approximations (2.43) and (2.45), respectively. In the region right of the red curve we use the electric formulation of the theory, and in the region left of the red curve we use the magnetic formulation modified by decoupling the fields $V_\pm$. The right plot is a zoomed in version of the left one and includes only the numerical results from method 1.

x, and we compare it to the asymptotic expansion

$$\begin{aligned}\frac{F}{N_c^2} &= x\log 2 + \frac{1}{2}\log x + \left(\frac{3}{4} - \log 2\right) - \frac{1}{x}\left(\frac{\pi^2 - 4}{2\pi^2}\right) \\ &\quad - \frac{1}{x^2}\left(\frac{512 - 112\,\pi^2 + 7\,\pi^4}{24\pi^4}\right) + O(1/x^3)\,,\end{aligned} \tag{2.44}$$

which we compute in section 2.2.3. The observation that F/N_c^2 is a monotonically decreasing function of x is consistent with the F-theorem [20,25,40,41], since we may flow to theories with smaller x by giving mass to some of the flavor multiplets. We also compute Δ as a function of x in the dual theory using the methods given in section 2.2.3, and the results are presented in figure 2.5. In the magnetic theory we may calculate analytic approximations to Δ and F/N_c^2 as asymptotic expansions in

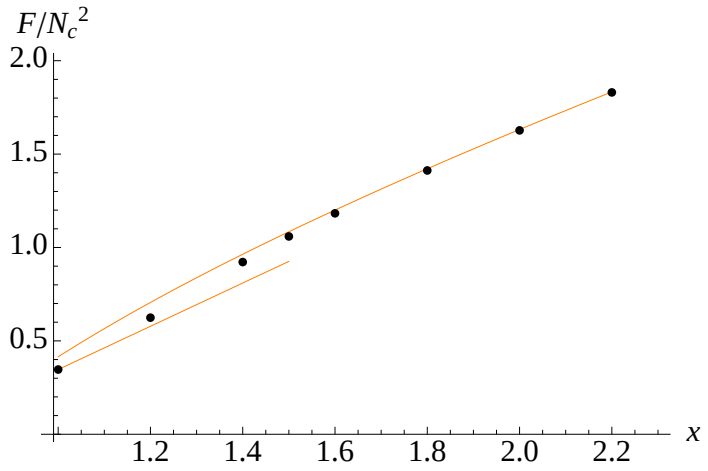

Figure 2.6: F/N_c^2 in the Veneziano limit as a function of $x = \frac{N_f}{N_c}$. The free energy decreases monotonically as a function of x, consistent with the F-theorem. The black points were computed numerically using the saddle point method (method 1, section 2.2.3). The upper orange curve is the analytic approximation (2.44) and the lower orange linear approximation at smaller x is given in (2.46).

powers of $(x-1)$, with the results (see section 2.2.3)

$$\Delta(x) = \frac{1}{4} + \frac{1}{4\pi}(x-1) + \frac{(26-7\,\pi)\pi - 8}{8(\pi-2)\pi^2}(x-1)^2 + O\left((x-1)^3\right) \tag{2.45}$$

and

$$\frac{F}{N_c^2} = \frac{\log 2}{2} + (x-1)\left(\frac{5\log 2}{4} + \frac{G}{\pi}\right) + O(x-1)^2\,, \tag{2.46}$$

where $G \approx 0.916$ is Catalan's constant.

Note that Δ smoothly approaches $1/4$ as $x \to 1$ and also continuously connects with the electric curve at $x = x_c$. It appears that Δ and F might be non-analytic at $x = x_c$, though our limited numerical precision does not allow us to make a precise statement. A general reason to expect a non-analyticity is that the global symmetry of the theory changes at x_c.

	$N_f=1$	$N_f=2$	$N_f=3$	$N_f=4$	$N_f=5$	$N_f=6$	$N_f=7$
$N_c=1$	1/3 (.8724)	.4085 (1.934)	.4370 (2.838)	.4519 (3.679)	.4611 (4.486)	.4674 (5.272)	.4719 (6.044)
$N_c=2$	-	1/4 (2.079)	.3417 (4.722)	.3852 (6.875)	.4101 (8.817)	.4263 (10.64)	.4375 (12.38)
$N_c=3$	-	-	1/4 (3.812)	.3058 (8.188)	.3517 (11.81)	.380 (15.0)	.400 (18.0)
$N_c=4$	-	-	-	1/4 (6.238)	.2809 (12.19)	.3276 (17.51)	.357 (22.2)
$N_c=5$	-	-	-	-	1/4 (9.357)	.2672 (16.62)	.3086 (23.85)
$N_c=6$	-	-	-	-	-	1/4 (13.17)	.2643 (21.67)
$N_c=7$	-	-	-	-	-	-	1/4 (17.68)

Table 2.1: The scaling dimension Δ of the flavor multiplets and the value of F (in parenthesis) at the conformal fixed points for a few small values of N_f and N_c in the $\mathcal{N}=2$ SYM theory at vanishing Chern-Simons level. For N_c and N_f where we have to use the modified magnetic formulation of the theory with $V_\pm$ treated as free fields, the results are enclosed in boxes.

2.2.5 RG flows and the F-theorem

Table 2.1 summarizes our results for some small values of N_c and $N_f \geq N_c$. We note that moving to the left along each row, which corresponds to RG flows associated with making some flavors massive, decreases the value of F in agreement with the F-theorem [20, 25, 40, 41]. This may also be seen in the Veneziano limit in figure 2.6. On the Higgs branch the theory may flow from $U(N_c)$ with N_f massless flavors in the UV to $U(N_c-1)$ with N_f-1 massless flavors in the IR. According to table 2.1, this movement along the diagonals makes F decrease in agreement with the F-theorem.

We note, however, that F is not monotonic along the columns. In moving down each column with $N_f > 2$, F first increases, peaks around the "crack in the conformal window," and then decreases towards the edge of the window, $N_c = N_f$. This effect becomes more pronounced for large N_f. In figure 2.7 we plot F/N_f^2 in the Veneziano

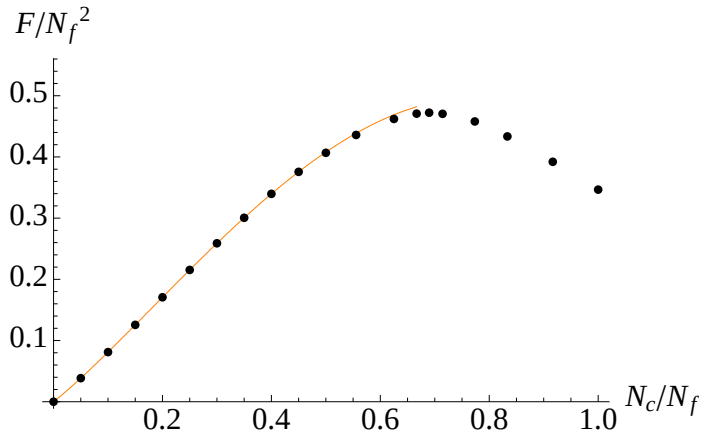

Figure 2.7: F/N_f^2 in the Veneziano limit as a function of N_c/N_f. The quantity is peaked at the "crack in the conformal window", $N_c/N_f \approx 1/1.45$. The black points were computed numerically using the saddle point method (method 1, section 2.2.3). The left orange curve is calculated from the analytic approximation (2.44), and the right orange curve at larger values of N_c/N_f is calculated from (2.46).

limit as a function of N_c/N_f, and we see that this quantity is peaked at the crack, $N_c/N_f \approx 1/1.45$. Using figure 2.7 we estimate that near the crack the value of F is $F_{\text{crack}} \approx 0.47N_f^2$. This is much bigger than the value at the edge $N_c = N_f$, $F_{\text{edge}} = \left(\frac{N_f^2}{2} + 1\right) \log 2 \approx 0.35N_f^2$.

Let us propose a tentative interpretation of the non-monotonic behavior of F at fixed N_f. In the standard electric $U(N_c)$ theory, on the Coulomb branch the gauge group may be broken to $U(N_c - 1) \times U(1)$. The F-theorem then tells us that $F_{U(N_c)} > F_{U(N_c-1)}$ at fixed N_f. We observe this behavior for N_c small enough that the monopole operators $V_\pm$, responsible for the Coulomb branch, are not decoupled; in the Veneziano limit this is the requirement $N_c \lesssim N_f/1.45$. For larger N_c the monopole operators of the electric theory are decoupled, and its Coulomb branch is no longer available. Instead, we can go on the Coulomb branch in the modified magnetic $U(N_f - N_c)$ theory, and this *increases* N_c. In this regime, which in the Veneziano limit corresponds to $N_c \gtrsim N_f/1.45$, the F-theorem implies that F is a decreasing function of N_c, as may be observed in figure 2.7 and in table 2.1.

Let us also note in passing that, in the 4-dimensional Seiberg conformal window, the Weyl anomaly coefficient a is not a monotonic function of N_c at fixed N_f. The exact formula for $SU(N_c)$ gauge group with N_f non-chiral flavors is [37]

$$a = \frac{3}{16}\left(2N_c^2 - 1 - 3\frac{N_c^4}{N_f^2}\right) \ . \tag{2.47}$$

In the Veneziano limit,

$$\frac{a}{N_f^2} = \frac{3}{16}\left(2y - 3y^2\right) \ , \tag{2.48}$$

where $y = (N_c/N_f)^2$. Clearly, a/N_f^2 is maximized at $y = 1/3$. This corresponds to $N_f = N_c\sqrt{3}$, which lies slightly above the strongly coupled edge of the conformal window, $N_f = 3N_c/2$.

2.3 SU(N_c) SQCD

Now consider SU(N_c) SQCD with N_f flavors, and its magnetic dual [57]. Note that in three dimensions even a U(1) gauge group becomes strongly coupled in the IR, and we indeed will find crucial differences from the case of U(N_c) SQCD.

2.3.1 Dual Pairs

Electric Theory The electric theory has a gauge group SU(N_c), as well as quarks Q in the fundamental representation and anti-quarks $\tilde{Q}$ in the anti-fundamental representation (these fields are 3d $\mathcal{N} = 2$ chiral multiplets). We do not have a superpotential term: $W_{\text{electric}} = 0$. The theory has $N_c - 1$ independent monopole operators corresponding to the Cartan of the gauge group, however most of them are lifted by the instanton-generated superpotential, with the exception of a a single unlifted monopole operator which is typically denoted by Y in the literature [9]. This should

be contrasted with the case of a $\mathrm{U}(N_c)$ gauge group, where we have two unlifted monopole operators $V_\pm$ [9, 70].

The theory has $\mathrm{SU}(N_f)_L \times \mathrm{SU}(N_f)_R \times \mathrm{U}(1)_B \times \mathrm{U}(1)_A \times \mathrm{U}(1)_{\mathrm{R-UV}}$ flavor symmetries, under which the fields $Q, \tilde{Q}, Y$ transform as follows:

	$\mathrm{SU}(N_c)$	$\mathrm{SU}(N_f)_L$	$\mathrm{SU}(N_f)_R$	$\mathrm{U}(1)_B$	$\mathrm{U}(1)_A$	$\mathrm{U}(1)_{\mathrm{R-UV}}$
Q	$\boldsymbol{N_c}$	$\boldsymbol{N_f}$	$\mathbf{1}$	1	1	0
$\tilde{Q}$	$\overline{\boldsymbol{N_c}}$	$\mathbf{1}$	$\overline{\boldsymbol{N_f}}$	-1	1	0
Y	$\mathbf{1}$	$\mathbf{1}$	$\mathbf{1}$	0	$-2N_f$	$2(N_f - N_c + 1)$

(2.49)

Here the $\mathrm{U}(1)_R$-charge was denoted $\mathrm{U}(1)_{\mathrm{R-UV}}$, to emphasize that it is one of the many possible U(1) R-symmetries of the UV theory and is not the IR U(1) R-symmetry inside the superconformal algebra. We listed the $\mathrm{U}(1)_{\mathrm{R-UV}}$-charge of the monopole operator Y [71]; we will comment more on this later when we discuss the S^3 partition function.

Note also that the theory has no topological $\mathrm{U}(1)_J$ symmetry: the topological $\mathrm{U}(1)_J$ symmetry is generated by the current $J = *\mathrm{Tr}F$, however this vanishes since the gauge field is traceless.

Magnetic Theory Let us first assume that $N_f > N_c$. The electric theory then has a magnetic dual [57] (see also [59]).

The gauge group is $\mathrm{SU}(N_f - N_c) \times \mathrm{U}(1)_{\mathrm{diag}} \simeq \mathrm{U}(N_f - N_c)$, and not $\mathrm{SU}(N_f - N_c)$ as one might naively expect. For notational simplicity we define $\tilde{N}_c$ by

$$\tilde{N}_c := N_f - N_c \ . \tag{2.50}$$

The theory has dual quark q and anti-quark $\tilde{q}$, and also b and $\tilde{b}$. The meson $M = Q\tilde{Q}$ and the monopole operator Y of the electric theory are now fundamental fields in the magnetic theory. The magnetic theory also has two unlifted monopole operators $\tilde{X}_{\pm}$.

The theory also has a superpotential

$$W_{\text{magnetic}} = Mq\tilde{q} + Yb\tilde{b} + \tilde{X}_{-} + \tilde{X}_{+} \ . \tag{2.51}$$

Note that this superpotential breaks the topological $\mathrm{U}(1)_J$ symmetry, which rotates the fields $\tilde{X}_{\pm}$.

The magnetic theory has the same flavor symmetry as the electric theory, under which the fields transform as follows:

	$\mathrm{SU}(\tilde{N}_c)$	$\mathrm{U}(1)_{\text{diag}}$	$\mathrm{SU}(N_f)_L$	$\mathrm{SU}(N_f)_R$	$\mathrm{U}(1)_B$	$\mathrm{U}(1)_A$	$\mathrm{U}(1)_{\text{R}-\text{UV}}$
q	$\boldsymbol{\tilde{N}_c}$	$\frac{1}{\tilde{N}_c}$	$\overline{\boldsymbol{N_f}}$	$\mathbf{1}$	0	-1	1
$\tilde{q}$	$\overline{\boldsymbol{\tilde{N}_c}}$	$-\frac{1}{\tilde{N}_c}$	$\mathbf{1}$	$\boldsymbol{N_f}$	0	-1	1
b	$\mathbf{1}$	-1	$\mathbf{1}$	$\mathbf{1}$	N_c	N_f	$-\tilde{N}_c$
$\tilde{b}$	$\mathbf{1}$	1	$\mathbf{1}$	$\mathbf{1}$	$-N_c$	N_f	$-\tilde{N}_c$
M	$\mathbf{1}$	0	$\boldsymbol{N_f}$	$\overline{\boldsymbol{N_f}}$	0	2	0
Y	$\mathbf{1}$	0	$\mathbf{1}$	$\mathbf{1}$	0	$-2N_f$	$2(\tilde{N}_c+1)$
$\tilde{X}_{\pm}$	$\mathbf{1}$	0	$\mathbf{1}$	$\mathbf{1}$	0	0	2

(2.52)

Since $\mathrm{U}(1)_{\text{diag}}$ is an Abelian symmetry, there is no canonical normalization of its charges; the charges above, which differ from those in [57] by a factor of $\tilde{N}_c$, are chosen in such a way that it matches with the standard normalization when embedded into the $\mathrm{U}(\tilde{N}_c)$ gauge group.

The case of $N_f = N_c$ requires a separate analysis. In this case the magnetic theory does not have any gauge fields, and is described by chiral multiplets $Y, M, B, \tilde{B}$ with

the superpotential

$$W = Y(B\tilde{B} - \det(M)) \ . \tag{2.53}$$

The fields Y and M are the monopole operator and the meson of the electric theory, as before. The fields B and $\tilde{B}$ are the baryons, which when $N_f > N_c$ are gauge-invariant and related to the $b, \tilde{b}$ of the above-mentioned magnetic theory by the relation

$$B = q^{\tilde{N}_c} b \ , \quad \tilde{B} = \tilde{q}^{\tilde{N}_c} \tilde{b} \ . \tag{2.54}$$

The charge assignment of the fields $M, Y, B, \tilde{B}$ is

	$\mathrm{SU}(N_f)_L$	$\mathrm{SU}(N_f)_R$	$\mathrm{U}(1)_B$	$\mathrm{U}(1)_A$	$\mathrm{U}(1)_{\mathrm{R-UV}}$
M	$\boldsymbol{N_f}$	$\overline{\boldsymbol{N_f}}$	0	2	0
Y	$\mathbf{1}$	$\mathbf{1}$	0	$-2N_c$	2
B	$\mathbf{1}$	$\mathbf{1}$	N_c	N_c	0
$\tilde{B}$	$\mathbf{1}$	$\mathbf{1}$	$-N_c$	N_c	0

(2.55)

The case of $N_f < N_c$ can be derived from the $N_f = N_c$ theory by mass deformation. For $N_f = N_c - 1$ the Coulomb branch smoothly connects with the Higgs branch, giving rise the to constraint $Y\det(M) = 1$ [9]. When we have $N_f < N_c - 1$, the instanton-generated superpotential completely lifts the vacuum moduli space [75]. For this reason we will concentrate on the case $N_f \geq N_c$ in the rest of this section.

2.3.2 IR Analysis

Considering all Abelian symmetries in the theory, we can parametrize the R-symmetry as

$$R_{\rm IR} = R_{\rm UV} + aJ_A + bJ_B \ , \tag{2.56}$$

where $R_{\rm UV}, R_{\rm IR}, J_A, J_B$ are generators of $\mathrm{U}(1)_{\rm R-UV}, \mathrm{U}(1)_{\rm R-IR}, \mathrm{U}(1)_A, \mathrm{U}(1)_B$, respectively.

As we will see momentarily F-maximization gives $b = 0$, and b does not play crucial roles below.

Unitarity Bound The dimensions of the operators Y, M are given by

$$\begin{aligned} Y &: \ \Delta_Y = 2(N_f - N_c + 1) - 2N_f\, a \ , \\ M &: \ \Delta_M = 2a \ . \end{aligned} \tag{2.57}$$

The unitary bound $\Delta_{Y,M} \geq \frac{1}{2}$ is given by

$$\begin{aligned} Y &: \ a \leq \frac{N_f - N_c + \frac{3}{4}}{N_f} \approx 1 - \frac{1}{x} \ , \\ M &: \ a \geq \frac{1}{4} \ , \end{aligned} \tag{2.58}$$

where here and in the following the symbol $\approx$ will denote the Veneziano limit.

Note that there are other gauge singlet operators, such as $\tilde{q}q$ and $\tilde{b}b$ in the magnetic theory, whose dimension could become smaller than the threshold value $\frac{1}{2}$. However these are not chiral primary operators, and hence the constraints from the unitarity bound does not necessarily apply. For example, the operator $\tilde{q}q$ is trivial in the chiral ring thanks to the F-term relation for the field M, and hence is not a chiral primary. The same applies to the operator $\tilde{b}b$.

Partition function The partition function of electric theory is given by

$$Z_{\text{electric}} = \frac{1}{N_c!}\int \prod_{i=1}^{N_c} d\sigma_i\, \delta\left(\sum_{i=1}^{N_c}\sigma_i\right) \overbrace{\prod_{1\le i<j\le N_c} \sinh^2[\pi(\sigma_i-\sigma_j)]}^{\text{measure}} \times \overbrace{\prod_{i=1}^{N_c} \exp\left[N_f\, l(1-a\pm b\pm i\sigma_i)\right]}^{Q,\tilde{Q}} \ . \tag{2.59}$$

Here and in the following we use the shorthanded notation that $\pm$ inside the expression means the sum of the corresponding two expressions. For example,

$$l(1-a\pm b\pm i\sigma_i) := l(1-a+b+i\sigma_i) + l(1-a-b-i\sigma_i)\ . \tag{2.60}$$

For the magnetic theory, let us first consider the case $N_f > N_c$. We then have

$$\begin{aligned} Z_{\text{magnetic}} = \frac{1}{\tilde{N}_c!}\exp\left[\overbrace{N_f^2\, l(1-2a)}^{M} + \overbrace{l\left(1+2N_f\, a - 2(\tilde{N}_c+1)\right)}^{Y}\right] \\ \times \int d\sigma \int \prod_{i=1}^{\tilde{N}_c} d\sigma_i\ \delta\left(\sum_{i=1}^{N_c}\sigma_i\right) \overbrace{\prod_{1\le i<j\le \tilde{N}_c} \sinh^2[\pi(\sigma_i-\sigma_j)]}^{\text{measure}} \\ \times \overbrace{\prod_{i=1}^{\tilde{N}_c} \exp\left[N_f\, l\left(a\pm i\sigma_i \pm i\frac{1}{\tilde{N}_c}\sigma\right)\right]}^{q,\tilde{q}} \times \overbrace{\exp\left[l\left(1+\tilde{N}_c - N_f\, a \pm N_c\, b \mp i\sigma\right)\right]}^{b,\tilde{b}}\ , \end{aligned} \tag{2.61}$$

where σ_i (σ) parametrizes the Cartan of $\mathrm{SU}(\tilde{N}_c)$ ($\mathrm{U}(1)_{\text{diag}}$). The σ-dependence inside the integrand can be eliminated by the shift $\sigma_i \to \sigma_i - \frac{1}{N_c}\sigma$, after which the delta function constraint becomes $\sigma = \sum_{i=1}^{\tilde{N}_c}\sigma_i$, i.e. σ is the diagonal part of the $\mathrm{U}(\tilde{N}_c)$

gauge group. After a trivial delta-function integral over σ we obtain

$$\begin{aligned} Z_{\text{magnetic}} = & \frac{1}{(N_f - N_c)!} \exp\left[N_f^2\, l(1-2a) + l\,(1 + 2N_f\, a - 2(N_f - N_c + 1))\right] \\ & \times \int \prod_{i=1}^{\tilde{N}_c} d\sigma_i \prod_{1 \le i < j \le N_f - N_c} \sinh^2[\pi(\sigma_i - \sigma_j)] \\ & \times \prod_{i=1}^{N_f - N_c} \exp\left[N_f\, l\,(a \pm i\sigma_i)\right] \times \exp\left[l\left(1 + \tilde{N}_c - N_f\, a \pm N_c\, b \mp i \sum_{i=1}^{\tilde{N}_c} \sigma_i\right)\right] . \end{aligned} \tag{2.62}$$

The case of $N_f = N_c$ is much simpler thanks to the absence of the gauge group in the magnetic theory. We have

$$Z^{N_f = N_c}_{\text{magnetic}} = \exp\left[\overbrace{N_f^2\, l(1-2a)}^{M} + \overbrace{l(1 - 2 + 2N_c a)}^{Y} + \overbrace{l(1 - N_c(a \pm b))}^{B,\tilde{B}}\right] . \tag{2.63}$$

Note that this expression can also be obtained by formally setting $N_f = N_c$ in (2.62).

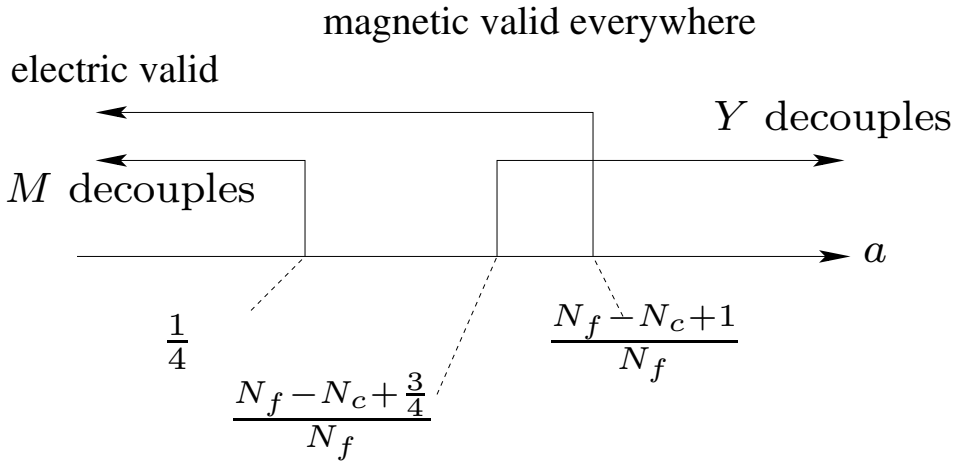

Figure 2.8: The unitarity bound and the convergence bound for 3d $\mathcal{N} = 2$ SU(N_c) SQCD with N_f flavors with $N_f > N_c$, plotted in terms of the mixing parameter a (see (2.56), with $b = 0$). The correct IR value of a should be determined from F-maximization.

Convergence As before in U(N_c) case, we can analyze the convergence condition of the partition function by sending one of the σ_i's to infinity (in this case we need to send one to infinity and another to minus infinity, for the consistency with the traceless constraint $\sum_i \sigma_i = 0$), while keeping other σ_i's finite. Using (2.17), we see that the convergence bounds of the partition functions are

$$\begin{aligned} &\text{electric:} \quad a < \frac{N_f - N_c + 1}{N_f} \approx 1 - \frac{1}{x} \ , \\ &\text{magnetic: converges for any values of } a \ . \end{aligned} \tag{2.64}$$

Note that for numerical computations the practical convergence bound is slightly stronger than this, since as we approach the convergence bound the computational time becomes increasingly large.

Again, we can either derive this from the positivity of the dimension of the monopole operators

$$\begin{aligned} &Y : \Delta_Y = 2(N_f - N_c + 1) - 2N_f\, a \geq 0 \ , \\ &\tilde{X}_\pm : \Delta_{\tilde{X}_\pm} = 2 \geq 0 \ , \end{aligned} \tag{2.65}$$

or from the positivity of the effective FI parameter

$$\text{electric:} \quad \zeta_{\text{eff}} = -\overbrace{(N_c - 1)}^{\text{measure}} + \overbrace{N_f(1-a)}^{Q,\tilde{Q}} = N_f - N_c + 1 - N_f\, a \ , \tag{2.66}$$

$$\text{magnetic:} \quad \zeta_{\text{eff}} = -\overbrace{(\tilde{N}_c - 1)}^{\text{measure}} + \overbrace{N_f a}^{q,\tilde{q}} + \overbrace{1 + \tilde{N}_c - N_f\, a}^{b,\tilde{b}} = 2 \ , \tag{2.67}$$

Duality as Equality In the literature, the duality between two 3d $\mathcal{N} = 2$ theories is often translated to an equivalence of the S^3 partition functions:

$$Z_{\text{electric}} = Z_{\text{magnetic}} \ . \tag{2.68}$$

Such equivalences have been verified in [57, 62, 76–78].

There are subtleties to the identity (2.68), however. In fact, as we have already seen in (2.64), we find that as a function of the parameter a the right hand side always converges, whereas the left hand side converges only when a is small enough, invalidating (2.68).

We can see this problem more sharply for the $N_f = N_c$ theory. The magnetic partition function has poles at $2N_c a = \mathbb{Z}\backslash\{1\}$, as follows from the definition of the function $l(z)$. The electric partition function, however, does not show any singular behavior at these points.

This is not in contradiction with the existing results in the literature. In the analysis above we assumed that a is a real parameter, however in the literature a takes values in the complex plane, where the imaginary part of a plays the role of the real mass parameter for the $\mathrm{U}(1)_A$ flavor symmetry. The S^3 partition function is known to be a holomorphic function of this complexified parameter [26, 79], and we can then regard the both sides of (2.68) as complex functions of a, establish the identities in the regions where the real part of a is small, and then analytically continue into the whole complex plane. This is what is usually meant by the identity (2.68).

However, we do not wish to turn on imaginary parts of a for the purpose of this paper. When we turn on the real mass parameter for the $\mathrm{U}(1)_A$ symmetry, the quarks $Q, \tilde{Q}$ gets a mass and hence can be integrated out in the deep IR, thereby dramatically changing the IR behavior of the theory. We need to keep a real, for the numerical analysis of the F-maximization below.

This means that we need be careful in interpreting the equality (2.68), at least for the purpose of F-maximization—When only one of the two sides converge, we should use that convergent partition function to determine the IR conformal dimensions, whereas if the both sides converge they should give the same value of the F-function

(possibly up to an overall constant independent of the parameter a) and they both give the same IR conformal dimensions.[1]

In the case of the SU(N_c) SQCD discussed here, the result (2.64) shows that the magnetic partition function is convergent for all the values of the parameter a. This is in sharp contrast with the case of the U(N_c) SQCD discussed in the previous section, where the region for the convergent magnetic partition function was complementary to that of the electric partition function; the overlapping region exists only for fine-tuned values of N_c and N_f, and vanishes in the Veneziano limit.

2.3.3 Results

We can determine the values of a and b by maximization of the free energy F, by explicitly computing the S^3 the partition functionS (2.59) and (2.62) as in (2.2.3)

Maximizing F with respect to b straightforwardly gives $b = 0$. We can then numerically search for the maximal value of F with respect to a. Note that it is crucial for our numerical analysis that F takes a maximal value, not just an extremal value.

In table 2.2 we present values of a and F at IR for small N_c. For the values $N_f = N_c = 3, 4, 5, 6$ (in entries in red boxes in Table 2.2) we find that after performing the first F-maximization that the unitarity bound (2.58) is violated for some operators, which let us to decouple corresponding operators. The details of the decoupling varies for different values of N_f and N_c, as shown in the diagonal entries of Table 2.2.

[1] It is possible to render the expression convergent by deforming the integration contour at infinity. However, the meaning of such a deformation, and the connection with the F-theorem, is not clear.

	$N_f = 2$	$N_f = 3$	$N_f = 4$	$N_f = 5$	$N_f = 6$
$N_c = 2$	.2862 (5.3743)	.3687 (7.6517)	.4064 (9.6090)	.4277 (11.4143)	.4412 (13.1306)
$N_c = 3$	-	.2222 $[M]$ (3.9915)	.322 (14.0933)	.3632 (17.4956)	.3898 (20.5698)
$N_c = 4$	-	-	$\frac{1}{8}$ $[MY, B]$ (6.5849)	.2912 (22.4819)	.3353 (27.5200)
$N_c = 5$	-	-	-	$\frac{1}{10}[MY, B]$ (9.7041)	.2693 (16.9044)
$N_c = 6$	-	-	-	-	$\frac{1}{12}$ $[Y, M, B]$ (13.5164)

Table 2.2: The scaling dimension Δ_Q of the flavor multiplets (above) and the maximal value of F-function (below), at the conformal fixed points for a few small values of N_f and N_c in 3d $\mathcal{N} = 2$ SU(N_c) SQCD with N_f flavors. We have computed this from the electric theory, except for the diagonal entries and the blue-colored entries where we used a simpler magnetic theory for more efficient numerical evaluation. For $N_c = N_f = 3, 4, 5, 6$ either one or two operators hit the unitarity bound, and consequently we need to decouple them and repeat the F-maximization with the modified F-function (2.69), until the procedure terminates. For $N_c = N_f = 4, 5, 6$ we find a sequence of decoupling of operators, leaving to a free IR theory eventually—for example, for $N_c = N_f = 4$ operators M and Y decouple first, and the baryon B becomes free after the second F-maximization, Similarly, for $N_c = N_f = 6$ we find that first Y decouples, then M, and finally B becomes free. Such a decoupling pattern is shown inside the bracket in the red box. Note that the value of the scaling dimension Δ_Q shown here is the value after all the possible decoupling effects are taken into account, and not the value after the first F-maximization.

After decoupling an operator, we need to again do F-maximization with the modified F-function, which are for example given by

$$\begin{aligned} F_{\text{magnetic}}^{M \text{ decoupling}} &= N_c^2\, l\left(\frac{1}{2}\right) + l\,(2N_c a - 1) + 2\,l(1 - N_c a)\ , \\ F_{\text{magnetic}}^{Y \text{ decoupling}} &= N_c^2\, l(1 - 2a) + l\left(\frac{1}{2}\right) + 2\,l(1 - N_c a)\ , \\ F_{\text{magnetic}}^{MY \text{ decoupling}} &= N_c^2\, l\left(\frac{1}{2}\right) + l\left(\frac{1}{2}\right) + 2\,l(1 - N_c a)\ , \end{aligned} \tag{2.69}$$

depending on whether only M, only Y or both M and Y decouple. For the choice of $N_f = N_c = 4, 5, 6$ we find after the second (and third for $N_f = N_c = 6$) F-

maximization that we need to decouple further operators, and consequently find that all the operators M, Y, B become free, leaving to a free IR theory.

Something interesting happens for $N_f = N_c \geq 6$. After the first F-maximization, we find that the monopole operator Y decouples. After decoupling Y, we find that the modified F-function apparently has no maximum. We propose to interpret this as a signal for the decoupling of the baryon B. After yet another F-maximization we find that the meson M also becomes free, leading to the critical value $a = 1/4$ and the trivial IR fixed point. One consistency check of this proposal is that the critical value $a = 1/4$ is consistent with the analysis of the Veneziano limit shown below in Figure 2.9.

Note also that the value of the F at the critical value decreases as we decrease the value of N_f. This is consistent with the F-theorem [25, 40, 41, 80], since we can give a mass to one of the flavors, thereby reducing the number of flavors by one. It is probably worth pointing out that for a fixed flavor number N_f the value of the free energy F could decrease as we increase N_c.

In Table 2.2 the monopole operator decoupling happens only in the diagonal $N_f = N_c$. However, this is an artifact of the choice of small N_c, N_f values. The constraint from the unitarity bound (2.57) becomes stronger as we increase the value of N_c, N_f, and therefore we expect to find more and more examples of (N_c, N_f) with monopole decoupling.

Expanding F in $\frac{1}{N_f}$ gives us the scaling dimension of flavor multiplets as

$$\Delta_Q(N_c, N_f) = \frac{1}{2} - \frac{2(N_c - \frac{1}{N_c})}{\pi^2 N_f} + \frac{(24N_c^2 - 48 + \frac{24}{N_c^2}) - \pi^2(\frac{10N_c^2}{3} - \frac{16}{3} + \frac{2}{N_c^2})}{\pi^4 N_f^2} + \mathcal{O}\left(\frac{1}{N_f^3}\right). \tag{2.70}$$

In the Veneziano limit, this reduces to

$$\Delta_Q(x) = \frac{1}{2} - \frac{2}{\pi^2 x} + \frac{8(36-5\pi^2)}{12\pi^4 x^2} + \mathcal{O}\left(\frac{1}{x^3}\right) . \tag{2.71}$$

The combined plot of the numerical data points as well as the large x expansion of (2.71) is shown in Figure 2.9. We find that the crack in the conformal window for SU(N_c) case is around $x_c \approx 1.46$.

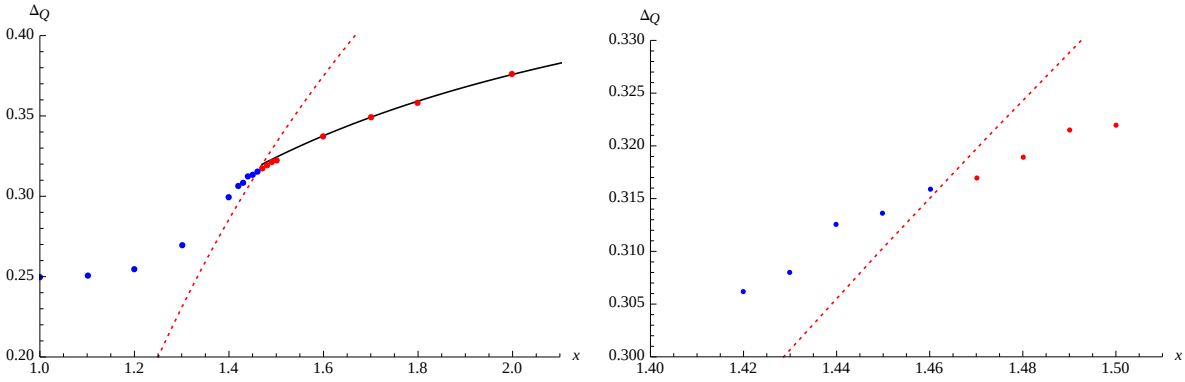

Figure 2.9: Δ_Q as a function of $x = N_f/N_c$ in the Veneziano limit. Points were computed by extrapolating small N_c numerical results. The dotted line is the unitarity bound (2.58). We find that $\Delta_Q(x)$ hits the unitarity bound at the critical value $x_c \approx 1.46$. The black curve at large values of x is the analytical approximation (2.71). In the region right to the red curve, we use electric theory, while in the left region we use magnetic theory with monopole Y decoupled when needed. The right plot is a zoomed-in version of the left one around the critical value x_c.

2.4 USp($2N_c$) SQCD

Let us next consider the USp($2N_c$) theory.[2] We find that the structure here is similar to the case of the U(N_c) theory. In particular, we find a small window where the

[2]Readers not interested in USp or SO gauge groups can proceed directly to the discussion of quiver gauge theories in section 2.7.

electric and magnetic descriptions hold simultaneously, which shrinks to a point in the Veneziano limit.

2.4.1 Dual Pairs

Electric Theory The electric theory is given by the quarks Q and the monopole operator Y. We do not have a superpotential term: $W_{\text{electric}} = 0$. The theory has $\mathrm{SU}(2N_f) \times \mathrm{U}(1)_A \times \mathrm{U}(1)_{\mathrm{R-UV}}$ flavor symmetry, under which the quark Q and the monopole operator Y transform as follows:

	$\mathrm{USp}(2N_c)$	$\mathrm{SU}(2N_f)$	$\mathrm{U}(1)_A$	$\mathrm{U}(1)_{R-UV}$
Q	$\boldsymbol{2N_c}$	$\boldsymbol{2N_f}$	1	0
Y	$\mathbf{1}$	$\mathbf{1}$	$-2N_f$	$2(N_f - N_c)$

(2.72)

Magnetic Theory For $N_f > N_c + 1$, the dual magnetic theory has $\mathrm{USp}(2N_f - 2N_c - 2)$ gauge symmetry with $2N_f$ chiral multiplets, dual quark q_i, and additional single chiral multiplets M and Y [54]. The Coulomb branch of this magnetic theory is parametrized by the monopole operator $\tilde{Y}$.

The charge assignment is given by

	$\mathrm{USp}(2N_f - 2N_c - 2)$	$\mathrm{SU}(2N_f)$	$\mathrm{U}(1)_A$	$\mathrm{U}(1)_{R-UV}$
q	$\boldsymbol{2N_c}$	$\boldsymbol{2N_f}$	-1	1
M	$\mathbf{1}$	$\boldsymbol{N_f(2N_f - 1)}$	2	0
Y	$\mathbf{1}$	$\mathbf{1}$	$-2N_f$	$2(N_f - N_c)$
$\tilde{Y}$	$\mathbf{1}$	$\mathbf{1}$	$2N_f$	$-2(N_f - N_c - 1)$

(2.73)

The theory also has a superpotential

$$W_{\text{magnetic}} = Mqq + Y\tilde{Y} \ . \tag{2.74}$$

For $N_f = N_c + 1$, we expect that the magnetic theory is trivial. We propose that the magnetic theory in this case is described by Y and M, with the superpotential

$$W = Y \,\mathrm{Pf}\,(M) \ . \tag{2.75}$$

We can verify that this theory is consistent with the charge assignment, which is given as

	$\mathrm{SU}(2N_f)$	$\mathrm{U}(1)_A$	$\mathrm{U}(1)_{R-UV}$
M	$\boldsymbol{N_f(2N_f-1)}$	2	0
Y	$\mathbf{1}$	$-2N_f$	2

(2.76)

We have a deformed moduli space $Y\,\mathrm{Pf}\,(M) = 1$ for $N_f = N_c$ [55], and the supersymmetry is broken for $N_f < N_c$. We therefore concentrate on the case $N_f > N_c$ below.

2.4.2 IR Analysis

Let us parametrize the IR R-symmetry by

$$R_{\mathrm{IR}} = R_{\mathrm{UV}} + aJ_A \ , \tag{2.77}$$

where the notation is the same as in the previous section.

Unitarity Bound The dimensions of the operators Y and M are

$$\Delta_Y = 2(N_f - N_c) - 2N_f a \ , \qquad \Delta_M = 2a \ . \tag{2.78}$$

The unitary constraint is given by

$$\begin{aligned} Y:\ a &\leq \frac{N_f - N_c - \frac{1}{4}}{N_f} \approx 1 - \frac{1}{x}\ , \\ M:\ a &\geq \frac{1}{4}\ . \end{aligned} \tag{2.79}$$

Partition Function The S^3 partition function of the electric theory is given by

$$\begin{aligned} Z_{\text{electric}} = \frac{1}{2^{N_c} N_c!} \int \prod_{i=1}^{N_c} d\sigma_i \prod_{1\leq i<j\leq N_c} [2\sinh[\pi(\sigma_i+\sigma_j)]2\sinh[\pi(\sigma_i-\sigma_j)]]^2 \\ \times \prod_{i=1}^{N_c} [2\sinh(2\pi\sigma_i)]^2 \overbrace{\exp\left[2N_f\, l(1-a\pm i\sigma_i)\right]}^{Q}\ . \end{aligned} \tag{2.80}$$

For the magnetic theory, we have

$$\begin{aligned} Z_{\text{magnetic}} = &\frac{1}{2^{N_f-N_c-1}(N_f-N_c-1)!} \\ &\times \exp\left[\overbrace{l(1-2(N_f-N_c)+2N_f a)}^{Y} + \overbrace{N_f(2N_f-1)l(1-2a)}^{M}\right] \\ &\times \int \prod_{i=1}^{N_f-N_c-1} d\sigma_i \prod_{1\leq i<j\leq N_f-N_c-1} [2\sinh[\pi(\sigma_i+\sigma_j)]2\sinh[\pi(\sigma_i-\sigma_j)]]^2 \\ &\times \prod_{i=1}^{N_f-N_c-1} [2\sinh(2\pi\sigma_i)]^2 \overbrace{\exp\left[2N_f\, l(a\pm i\sigma_i)\right]}^{q} \end{aligned} \tag{2.81}$$

for $N_f > N_c + 1$ and

$$Z_{\text{magnetic}} = \exp\left[\overbrace{l(-1+2N_f a)}^{Y} + \overbrace{N_f(2N_f-1)l(1-2a)}^{M}\right] \tag{2.82}$$

for $N_f = N_c + 1$.

Using the expansion (2.17) again, we determine the convergence bound to be

$$\begin{aligned} &\text{electric:} \quad a < \frac{N_f - N_c}{N_f} \approx 1 - \frac{1}{x} \ , \\ &\text{magnetic:} \quad a > \frac{N_f - N_c - 1}{N_f} \approx 1 - \frac{1}{x} \ . \end{aligned} \tag{2.83}$$

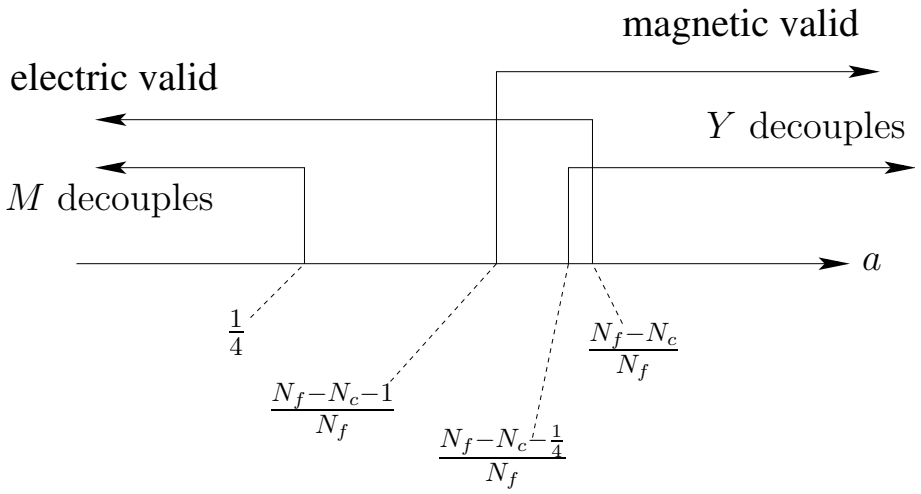

Figure 2.10: The unitarity bound and the convergence bound for 3d $\mathcal{N} = 2$ USp($2N_c$) SQCD with N_f flavors with $N_f > N_c + 1$, plotted in terms of the mixing parameter a (see (2.77)). The correct IR value of a should be determined from F-maximization. The structure here is very similar to the U(N_c) SQCD case (Figure 2.1).

2.4.3 Results

We can numerically maximize the F again for small values of N_c and N_f. The results of the numerical computation is summarized in Table 2.3.

For $N_f = N_c > 2$, we see that the monopole Y always saturates the unitarity bound, thus we set its scaling dimension at $\frac{1}{2}$. This modified magnetic theory forces $a = \frac{1}{4}$. Inside the table Y is the only operator which decouples in the IR, so the structure here is much simpler than that of the SU(N_c) SQCD discussed in previous section.

	$2N_f=4$	$2N_f=6$	$2N_f=8$	$2N_f=10$	$2N_f=12$
$2N_c=2$	.2861 (2.1502)	.3687 (4.4275)	.4064 (6.3848)	.4277 (8.1901)	.4412 (9.9064)
$2N_c=4$	-	$\frac{1}{4}$ [Y] (5.5452)	.3305 (10.8766)	.3711 (15.2865)	.3962 (19.2927)
$2N_c=6$	-	-	$\frac{1}{4}$ [Y] (10.0506)	.3038 (18.8447)	.3456 (26.1131)
$2N_c=8$	-	-	-	$\frac{1}{4}$ [Y] (15.9423)	.2822 (27.9908)
$2N_c=10$	-	-	-	-	$\frac{1}{4}$ [Y] (23.2204)

Table 2.3: The scaling dimension Δ_Q of the flavor multiplets and the maximal value of F-function (in a parenthesis), at the conformal fixed points for a few small values of N_c and N_f in 3d $\mathcal{N}=2$ USp($2N_c$) SQCD with N_f flavors. For the red boxes in the diagonal (i.e. $2N_f=2(N_c+1)$) entries, the monopole operator Y is decoupled after the first F-maximization. In most of the entries we used the electric partition functions, except in the red-colored (along the diagonal) and blue-colored (at $2N_c=8, 2N_f=12$) boxes we used magnetic partition functions, since the magnetic description is more suitable for numerical computations.

We can again check the consistency with the F-theorem by decreasing the values of N_f for a fixed N_c.

Expanding F in $\frac{1}{N_f}$ gives us the scaling dimension of flavor multiplets as

$$\Delta_Q(N_c,N_f)=\frac{1}{2}-\frac{4N_c+2}{2\pi^2N_f}+\frac{3(96N_c^2+96N_c+24)-\pi^2(40N_c^2+48N_c+14)}{12\pi^4N_f^2}+\mathcal{O}\left(\frac{1}{N_f^3}\right). \tag{2.84}$$

In the Veneziano limit, this reduces into

$$\Delta_Q(x)=\frac{1}{2}-\frac{2}{\pi^2x}+\frac{8(36-5\pi^2)}{12\pi^4x^2}+\mathcal{O}\left(\frac{1}{x^3}\right). \tag{2.85}$$

On the other hand, when x is close to 1, $(x-1)$ expansion we get $\Delta_Q(x)$:

$$\Delta_Q(x) = \frac{1}{4} + \frac{1}{4\pi}(x-1) + \frac{4-18\pi+5\pi^2}{4(2-\pi)\pi^2}(x-1)^2 + \mathcal{O}((x-1)^3) \ . \tag{2.86}$$

In Figure 2.11, we have plotted these results including the numerical data points coming from the several explicit integrations for small values of N_c and N_f. We find good agreement between numerical and analytical results, and the critical value for x is given by $x_c \approx 1.42$.

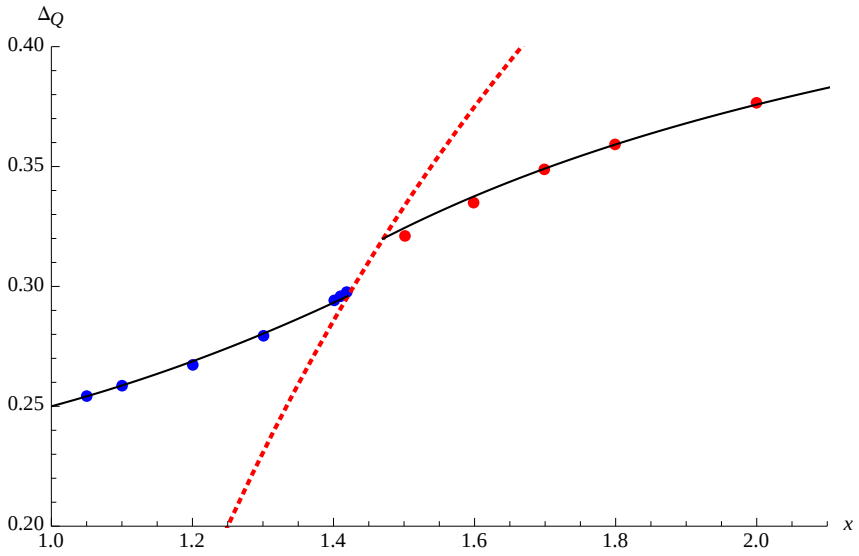

Figure 2.11: Δ_Q as a function of $x = N_f/N_c$ in the Veneziano limit. The points were computed by extrapolating small N_c numerical results. Dotted line is the convergence bound (2.83). We find that $\Delta_Q(x)$ hits the convergence bound at the critical value $x_c \approx 1.43$. The black curves at large and small values of x are the analytical approximation (2.85) and (2.86), respectively. In the region right to the red curve, we use electric theory (coloured in red), while in the left region we use magnetic theory with monopole Y decoupled (colored blue).

2.5 $\mathrm{SO}(N_c)$ SQCD

Let us now discuss the case of the $\mathrm{SO}(N_c)$ gauge group. The duality for this case is worked out in [58] (see [78, 81, 82] for a closely related discussion for $\mathrm{O}(N_c)$ theories).

We should keep in mind that the details of the duality depends on the global properties of the gauge group (e.g. $\mathrm{SO}(N_c), \mathrm{O}(N_c), \mathrm{Spin}(N_c)$ or $\mathrm{Pin}(N_c)$), as well as the set of local operators we include in the theory. For example, for the $\mathrm{O}(N_c)$ gauge group, we have two choices, denoted by $\mathrm{O}(N_c)_\pm$ [58]. In the following we first deal with the case of the $\mathrm{SO}(N_c)$ gauge group, and then come back to the cases of $\mathrm{O}(N_c)_+, \mathrm{O}(N_c)_-, \mathrm{Spin}(N_c)$ and $\mathrm{Pin}(N_c)$ gauge groups in section 2.5.4.

2.5.1 Dual Pairs

Electric Theory The electric theory has quarks Q in the fundamental representation, and as usual we have $W_{\text{electric}} = 0$. The theory also has the monopole operator Y, the baryon B, as well as a composite "baryon-monopole operator" β.

The theory has $\mathrm{SU}(N_f) \times \mathrm{U}(1)_A \times \mathrm{U}(1)_{\mathrm{R-VU}}$ continuous flavor symmetry, under which the fields $Q, \tilde{Q}, Y$ transform as follows:

	$\mathrm{SO}(N_c)$	$\mathrm{SU}(N_f)$	$\mathrm{U}(1)_A$	$\mathrm{U}(1)_{\mathrm{R-UV}}$	$\mathbb{Z}_2^{\mathcal{C}}$	$\mathbb{Z}_2^{\mathcal{M}}$	$\mathbb{Z}_2^{\tilde{\mathcal{M}}}$
Q	$\boldsymbol{N_c}$	$\boldsymbol{N_f}$	1	0			
M	$\mathbf{1}$	$\boldsymbol{N_f(N_f+1)/2}$	2	0	$+1$	$+1$	$+1$
Y	$\mathbf{1}$	$\mathbf{1}$	$-N_f$	$N_f - N_c + 2$	$+1$	-1	-1
B	$\mathbf{1}$	$(\boldsymbol{N_f})_A^{N_c}$	N_c	0	-1	$+1$	-1
β	$\mathbf{1}$	$(\boldsymbol{N_f})_A^{N_c-2}$	$-(N_f - N_c + 2)$	$N_f - N_c + 2$	-1	-1	$+1$

(2.87)

Here $(\boldsymbol{N_f})_A^{N_c-2}$ and $(\boldsymbol{N_f})_A^{N_c}$ represents totally antisymmetric representations. We have listed their discrete symmetry $\mathbb{Z}_2^{\mathcal{C}}$, $\mathbb{Z}_2^{\mathcal{M}}$ and $\mathbb{Z}_2^{\tilde{\mathcal{M}}}$ (we here list charges only for

gauge-invariant fields). We can easily check that $\mathbb{Z}_2^{\tilde{\mathcal{M}}}$ is a combination of $\mathbb{Z}_2^{\mathcal{C}}$ and $\mathbb{Z}_2^{\mathcal{M}}$, and is not independent. These discrete symmetries will play crucial roles when we change the gauge groups later in section 2.5.4.

Magnetic Theory Let us consider the case $N_f > N_c + 1$. First, the magnetic theory has dual quarks q. The meson M as well as the monopole operator Y of the electric theory, are now fundamental fields in the magnetic theory. It also has the monopole operator $\tilde{Y}$, the baryon $\tilde{B}$, and the dual baryon-monopole $\tilde{\beta}$.

Note that the baryon B and the baryon-monopole β do not appear as fundamental fields of the magnetic theory (compare this with the case of $\mathrm{SU}(N_c)$ theory). Rather they are identified with their magnetic counterparts $\tilde{B}, \tilde{\beta}$, by an identification

$$(B, \beta) \longleftrightarrow (\tilde{\beta}, \tilde{B}) \ . \tag{2.88}$$

This theory has a superpotential

$$W_{\text{magnetic}} = \frac{1}{2} M q q + \frac{i^{N_f - N_c}}{4} \tilde{Y} Y \ . \tag{2.89}$$

The theory has the same flavor symmetries as the electric theory, under which the fields transform as follows:

	$\mathrm{SO}(N_f - N_c + 2)$	$\mathrm{SU}(N_f)$	$\mathrm{U}(1)_A$	$\mathrm{U}(1)_{R-UV}$	$\mathbb{Z}_2^{\mathcal{C}}$	$\mathbb{Z}_2^{\mathcal{M}}$	$\mathbb{Z}_2^{\tilde{\mathcal{M}}}$
q	$\boldsymbol{N_f - N_c + 2}$	$\overline{\boldsymbol{N_f}}$	-1	1			
M	$\mathbf{1}$	$\frac{\mathbf{1}}{\mathbf{2}}\boldsymbol{N_f(N_f+1)}$	2	0	$+1$	$+1$	$+1$
Y	$\mathbf{1}$	$\mathbf{1}$	$-N_f$	$N_f - N_c + 2$	$+1$	-1	-1
$\tilde{Y}$	$\mathbf{1}$	$\mathbf{1}$	N_f	$N_c - N_f$	$+1$	-1	-1
$\tilde{B}$	$\mathbf{1}$	$(\boldsymbol{N_f})_A^{N_c}$	$-(N_f - N_c + 2)$	$N_f - N_c + 2$	-1	-1	$+1$
$\tilde{\beta}$	$\mathbf{1}$	$(\boldsymbol{N_f})_A^{N_c-2}$	N_c	0	-1	$+1$	-1

(2.90)

Note that the charge assignment for $\mathbb{Z}_2^{\mathcal{M}}$ and $\mathbb{Z}_2^{\tilde{\mathcal{M}}}$ symmetries here is consistent with the identification (2.88).

When $N_f = N_c - 1$, the magnetic theory has no gauge group, contains fields Y and M, with superpotential given by (see [78, 81, 82] for $\mathrm{O}(N_c)_+$ case)

$$W = Y^2 \det(M) + Mqq \,. \tag{2.91}$$

The charge assignment is given by

	$\mathrm{SU}(N_f)$	$\mathrm{U}(1)_A$	$\mathrm{U}(1)_{R-UV}$
q	$\overline{\boldsymbol{N_f}}$	-1	1
M	$\frac{\mathbf{1}}{\mathbf{2}}\boldsymbol{N_f(N_f+1)}$	2	0
Y	$\mathbf{1}$	$-N_f$	1

(2.92)

and as before this case should be treated separately from the rest.

For lower values of N_f, we have the quantum-corrected moduli space for $N_f = N_c - 2$ [82], and the supersymmetry is broken for $N_f < N_c - 2$. We will hereafter concentrate on the case $N_f \geq N_c - 1$.

2.5.2 IR Analysis

Let us parametrize the IR R-symmetry by

$$R_{\rm IR} = R_{\rm UV} + a J_A \ , \tag{2.93}$$

where $R_{\rm UV}, R_{\rm IR}, J_A$ are generators of $\mathrm{U}(1)_{\rm R-UV}, \mathrm{U}(1)_{\rm R-IR}, \mathrm{U}(1)_A$, respectively, as before.

Unitarity Bound Let us consider the electric theory. The dimensions of the operators are given by

$$\begin{aligned} &M: \ \Delta_M = 2a \ , \\ &Y: \ \Delta_Y = (N_f - N_c + 2) - N_f \, a \ , \\ &B: \ \Delta_B = N_c \, a \ , \\ &\beta: \ \Delta_\beta = (N_f - N_c + 2) - a(N_f - N_c + 2) \ . \end{aligned} \tag{2.94}$$

The unitary bound $\Delta \geq \frac{1}{2}$ gives

$$\begin{aligned} &M: \ a \geq \frac{1}{4} \ , \\ &Y: \ a \leq \frac{N_f - N_c + \frac{3}{2}}{N_f} \approx 1 - \frac{1}{x} \ , \\ &B: \ a \geq \frac{1}{2N_c} \ , \\ &\beta: \ a \leq \frac{N_f - N_c + \frac{3}{2}}{N_f - N_c + 2} \approx 1 \ . \end{aligned} \tag{2.95}$$

Notice that in the Veneziano limit, the unitarity bound for the monopole operator Y depends on the value of x, whereas that for the baryon-monopole β is independent of x.

Partition Function Let us write down the S^3 partition functions of electric and magnetic theories. The precise expression depends on whether N_c is even or odd.

For N_c even with $N_c = 2r$, the electric partition function is given by

$$\begin{aligned} Z_{\text{electric}} = \frac{1}{2^r r!} \int \prod_{i=1}^{r} d\sigma_i \prod_{1\le i<j\le r} [2\sinh[\pi(\sigma_i+\sigma_j)]2\sinh[\pi(\sigma_i-\sigma_j)]]^2 \\ \times \overbrace{\prod_{i=1}^{r} \exp\left[N_f\, l(1-a\pm i\sigma_i)\right]}^{Q} , \end{aligned} \tag{2.96}$$

while N_c odd with $N_c = 2r+1$, we have

$$\begin{aligned} Z_{\text{electric}} = \frac{1}{2^r r!} \int \prod_{i=1}^{r} d\sigma_i \prod_{1\le i<j\le r} [2\sinh[\pi(\sigma_i+\sigma_j)]2\sinh[\pi(\sigma_i-\sigma_j)]]^2 \\ \times \prod_{i=1}^{r} [2\sinh[\pi\sigma_i]]^2 \overbrace{\prod_{i=1}^{r} \exp\left[N_f\, l(1-a\pm i\sigma_i)\right]}^{Q} . \end{aligned} \tag{2.97}$$

The magnetic partition function is similar, and for $N_f - N_c + 2$ even ($N_f - N_c + 2 =: 2\tilde{r}$)

$$\begin{aligned} Z_{\text{magnetic}} = \frac{1}{2^{\tilde{r}}\tilde{r}!} \exp\left[\overbrace{l\left(1-(N_f-N_c+2)+N_f a\right)}^{Y} + \overbrace{\frac{N_f(N_f+1)}{2} l(1-2a)}^{M}\right] \\ \int \prod_{i=1}^{\tilde{r}} d\sigma_i \prod_{1\le i<j\le \tilde{r}} [2\sinh[\pi(\sigma_i+\sigma_j)]2\sinh[\pi(\sigma_i-\sigma_j)]]^2 \\ \times \overbrace{\prod_{i=1}^{r} \exp\left[N_f\, l(a\pm i\sigma_i)\right]}^{q} . \end{aligned} \tag{2.98}$$

For $N_f - N_c + 2 =: 2\tilde{r} + 1$ with $N_f > N_c + 1$ (i.e. $\tilde{r} > 0$), we have

$$
\begin{aligned}
Z_{\text{magnetic}} = \frac{1}{2^{\tilde{r}}\tilde{r}!} \exp\left[\overbrace{l\left(1 - (N_f - N_c + 2) + N_f a\right)}^{Y} + \overbrace{\frac{N_f(N_f+1)}{2} l(1-2a)}^{M} \right] \\
\int \prod_{i=1}^{\tilde{r}} d\sigma_i \prod_{1 \le i < j \le \tilde{r}} [2\sinh[\pi(\sigma_i + \sigma_j)] 2\sinh[\pi(\sigma_i - \sigma_j)]]^2 \\
\times \prod_{i=1}^{\tilde{r}} [2\sinh(\pi\sigma_i)]^2 \times \overbrace{\prod_{i=1}^{\tilde{r}} \exp\left[N_f\, l(a \pm i\sigma_i)\right]}^{q} \ .
\end{aligned}
\tag{2.99}
$$

For $N_f = N_c - 1$ (i.e. $\tilde{r} = 0$), we have

$$
Z_{\text{magnetic}} = \exp\left[\overbrace{l\left(N_f a\right)}^{Y} + \overbrace{\frac{N_f(N_f+1)}{2} l(1-2a)}^{M} + \overbrace{N_f\, l(1-a)}^{q} \right] \ . \tag{2.100}
$$

The convergence bounds of the partition functions are given in the following form, which hold irrespective of whether $N_c, N_f - N_c + 2$ are even or odd:

$$
\begin{aligned}
&\text{electric:} \quad a < \frac{N_f - N_c + 2}{N_f} \approx 1 - \frac{1}{x} \ , \\
&\text{magnetic:} \quad a > \frac{N_f - N_c}{N_f} \approx 1 - \frac{1}{x} \ .
\end{aligned}
\tag{2.101}
$$

In this case there is a small overlapping region where both electric and magnetic descriptions are valid. However the width of the overlapping region shrinks to zero in the Veneziano limit. It is therefore expected that we really should not expect both electric and magnetic descriptions to be valid, except for only for limited values of N_c and N_f.

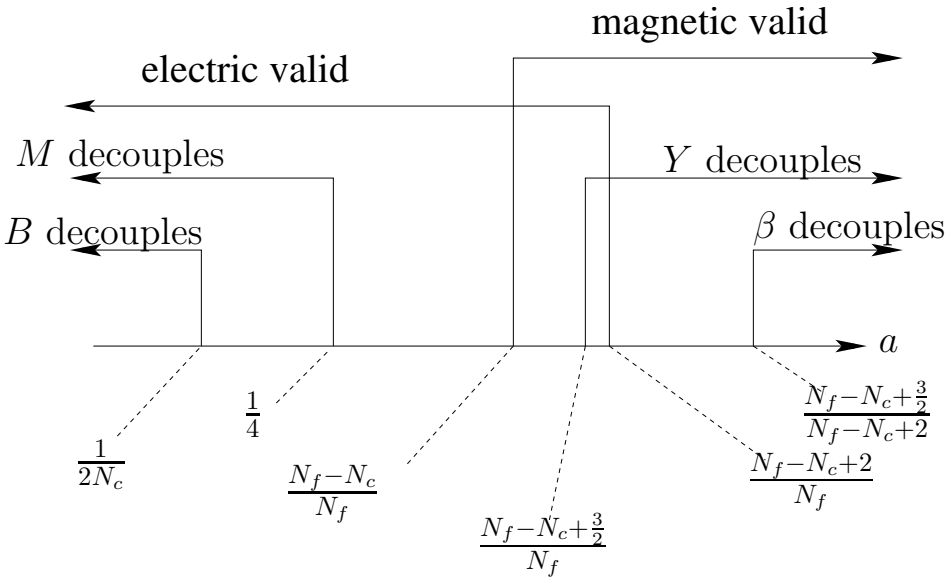

Figure 2.12: The unitarity bound and the convergence bound for 3d $\mathcal{N}=2$ SO(N_c) SQCD with N_f flavors with $N_f > N_c - 1$, plotted in terms of the mixing parameter a (see (2.93)). The correct IR value of a should be determined from F-maximization. Depending on the value of a, decoupled operators might be either none, only Y, or both Y and β. While the baryon-monopole β could in principle decouple, this does not happen in the exampled we studied, both numerically and analytically.

2.5.3 Results

We have done the F-maximization for several small values of N_c and N_f.[3] As commented before, one interesting feature of the SO(N_c) theories is the existence of the baryon-monopole operator β. This means that the baryon-monopole β, in addition to the baryon B, could decouple in the IR. In the examples we studied in Table 2.4, however, we find that β never decouples (this is also the case in the Veneziano limit, to be discussed below, see Figure 2.13).

We also compute the $\Delta_Q(N_c, N_f)$ for both odd and even N_c, in the large N_f limit. The S^3 partition functions take slightly different forms for each case, however it is natural to think that the value of $\Delta_Q(N_c, N_f)$ should coincide between the two cases

[3]Note that part of the entries have appeared in [81], which gives the critical values of a consistent with ours, in the first F-maximization. In several cases, however, the monopole operators decouple and we need to do another F-maximization, to determine the correct U(1) R-symmetry.

	$N_f=1$	$N_f=2$	$N_f=3$	$N_f=4$	$N_f=5$	$N_f=6$
$N_c=2$	1/3 (.8724)	.4085 (2.6271)	.4370 (3.5311)	.4519 (4.3723)	.4611 (5.1795)	.4674 (5.9655)
$N_c=3$	-	.2775 [Y] (1.8721)	.3532 (3.8607)	.3923 (5.4647)	.4149 (6.9098)	.4297 (8.2670)
$N_c=4$	-	-	.2324 [Y] (2.9315)	.3175 (6.7624)	.3602 (9.1754)	.3865 (11.3076)
$N_c=5$	-	-	-	.2663 [Y] (4.7671)	.2909 (8.7275)	.3358 (11.8361)
$N_c=6$	-	-	-	-	.2635 [Y] (6.7334)	.2686 (11.3107)

Table 2.4: The scaling dimension Δ_Q of the flavor multiplets (above) and the maximal value of F-function (below), at the conformal fixed points for a few small values of N_f and N_c in the 3d $\mathcal{N}=2$ SO(N_c) (or (O$_+$(N_c)) SQCD with N_f flavors. For the diagonal entries ($N_f=N_c-1$) we have used the partition function of the magnetic theory, and for entries in the red box we need to decouple the monopole operator Y. All other entries are computed in the electric theory, except in the blue boxed and diagonal entries where we used the magnetic theory for better numerical computations.

in this limit. The analytic calculation by order in $\frac{1}{N_f}$ shows that odd/even cases give the same answer, which reads

$$\Delta_Q(N_c,N_f)=\frac{1}{2}-\frac{2N_c-2}{\pi^2 N_f}+\frac{(24N_c^2-48N_c+24)-\pi^2(\frac{10}{3}N_c^2-8N_c+\frac{14}{3})}{\pi^4 N_f^2}+\mathcal{O}\left(\frac{1}{N_f^3}\right). \tag{2.102}$$

In the Veneziano limit this expansion reduces to

$$\Delta_Q(x)=\frac{1}{2}-\frac{2}{\pi^2 x}+\frac{8(36-5\pi^2)}{12\pi^4 x^2}+\mathcal{O}\left(\frac{1}{x^3}\right). \tag{2.103}$$

In the case of the magnetic theory, we can expand $\Delta(N_c,N_f)$ in order of $\frac{1}{N_c}$ which gives us

$$\Delta_Q(N_c,N_f)=\frac{1}{4}+\frac{1}{4\pi}\frac{N_f-N_c+2}{N_c}+\frac{(N_f-N_c+2)^2}{8\pi^2(\pi-2)}+O\left(\frac{1}{N_c^3}\right), \tag{2.104}$$

which reduces in the Veneziano limit into

$$\Delta_Q(x) = \frac{1}{4} + \frac{1}{4\pi}(x-1) + \frac{(26-7\pi)\pi - 8}{8\pi^2(\pi-2)}(x-1)^2 + O((x-1)^3) \ . \tag{2.105}$$

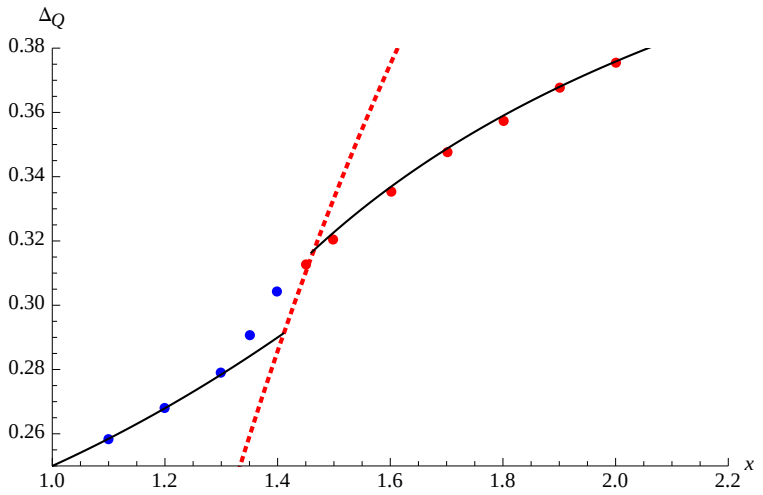

Figure 2.13: Δ_Q as a function of $x = N_f/N_c$ in the Veneziano limit. Points were computed by extrapolating small N_c numerical results. Dotted line is the unitarity bound (2.95). We find that $\Delta_Q(x)$ hits the unitarity bound at the critical value $x_c \approx 1.45$. The black curves at large and small values of x are the analytical approximation (2.103) and (2.105), respectively. In the region right to the red curve, we use electric theory, while in the left region we use magnetic theory with monopole Y decoupled.

2.5.4 $\mathrm{O}(N_c)_\pm$, $\mathrm{Spin}(N_c)$ and $\mathrm{Pin}(N_c)$ Gauge Groups

Dual Pairs Let us consider other gauge groups, $\mathrm{O}(N_c)_\pm$, $\mathrm{Spin}(N_c)$ and $\mathrm{Pin}(N_c)$. Note that all these gauge groups have the same Lie algebra as that of $\mathrm{SO}(N_c)$. These dualities can be obtained by gauging discrete $\mathbb{Z}_2$ symmetries of the $\mathrm{SO}(N_c)$ electric and magnetic theories.

When we gauge a single $\mathbb{Z}_2$ symmetry, there are three choices: $\mathbb{Z}_{\mathcal{C}}$, $\mathbb{Z}_{\mathcal{M}}$ and $\mathbb{Z}_{\tilde{\mathcal{M}}}$, leading to $\mathrm{O}(N_c)_+$, $\mathrm{O}(N_c)_-$ and $\mathrm{Spin}(N_c)$ theories, respectively, for the electric theory.

We can apply the same gauging to the magnetic theory. In fact, all terms which appear in the magnetic superpotentials (see (2.89) and (2.91)) have charge +1 under any of the three $\mathbb{Z}_2$ symmetries, and hence the gauging is consistent with the superpotential. There is one big difference from the electric case, however: the role of the $\mathbb{Z}_{\mathcal{M}}$ and $\mathbb{Z}_{\tilde{\mathcal{M}}}$ should be exchanged, following from the identification (2.88).

When we gauge two $\mathbb{Z}_2$ symmetries, there is only one choice, obtaining the $\mathrm{Pin}(N_c)_-$ theory because we are gauging all the discrete symmetries.

These gauging patterns are summarized in Figure 2.14.

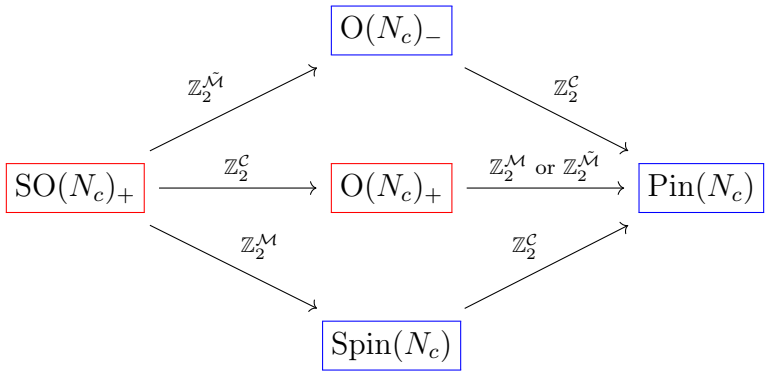

Figure 2.14: By gauging either $\mathbb{Z}_{\mathcal{C}}$, $\mathbb{Z}_{\mathcal{M}}$ and $\mathbb{Z}_{\tilde{\mathcal{M}}}$ symmetries of the $\mathrm{SO}(N_c)$ theory we obtain $\mathrm{O}(N_c)_+$, $\mathrm{O}(N_c)_-$ and $\mathrm{Spin}(N_c)$ gauge groups. By further gauging the remaining $\mathbb{Z}_2$, we obtain the $\mathrm{Pin}(N_c)$ theory. This figure represents the gauging of the electric theory, and for the magnetic theory we should exchange the role of $\mathbb{Z}_{\mathcal{M}}$ and $\mathbb{Z}_{\tilde{\mathcal{M}}}$. As we will explain later, the gauge groups boxed in red and those boxed in blue have different monopole operators, differing by a power of 2 (see (2.108)).

This immediately implies that the correct Aharony-like duality works as [58]

$$\begin{aligned}
&\mathrm{O}_+(N_c) \longleftrightarrow \mathrm{O}_+(N_f - N_c + 2) \ , \\
&\mathrm{O}_-(N_c) \longleftrightarrow \mathrm{Spin}(N_f - N_c + 2) \ , \\
&\mathrm{Spin}(N_c) \longleftrightarrow \mathrm{O}_-(N_f - N_c + 2) \ , \\
&\mathrm{Pin}(N_c) \longleftrightarrow \mathrm{Pin}(N_f - N_c + 2) \ .
\end{aligned} \tag{2.106}$$

This should be compared with the SO duality

$$\mathrm{SO}(N_c) \longleftrightarrow \mathrm{SO}(N_f - N_c + 2) \ . \tag{2.107}$$

When we gauge discrete $\mathbb{Z}_2$ symmetries, we project out the fields which has charge -1. For example, when we gauge the $\mathbb{Z}_2^{\mathcal{C}}$ symmetry (charge conjugation symmetry) we obtain the dualities for O_+ gauge groups. In this case, the baryon B and the baryon-monopole β are projected out, while their combinations such as B^2 and $B\beta$, remain in the theory.

Similarly, when we gauge either $\mathbb{Z}_{\mathcal{M}}$ or $\mathbb{Z}_{\tilde{\mathcal{M}}}$ symmetry, the monopole operator in itself is projected out, and we instead have its square:

$$Y_{\mathrm{Spin}} = Y_{\mathrm{O}_-} = Y_{\mathrm{Pin}} := Y^2 \ . \tag{2.108}$$

IR Analysis We now come to a natural question: does the gauging of the discrete symmetries discussed above have any impact on the IR behavior of the theory?

It turns out most of the preceding analysis for SO gauge groups does not require any modification. This is because we are primarily interested in F-maximization, which requires only the S^3 partition function with no operators inserted, and hence is insensitive to gauging of discrete symmetries.

There is one big change, however. While we have the same set of operators, gauging makes some of the gauge-invariant operators gauge-variant. Since the unitarity bound applies only to gauge-invariant operators, gauging the discrete symmetry will in general change the unitarity bounds.

In the analysis for the SO gauge groups we did not find any examples where the baryon B, the meson M, or the baryon-monopole β decouple. We can therefore concentrate on the monopole operator Y. As we discussed above, the change for Spin,

	$N_f=1$	$N_f=2$	$N_f=3$	$N_f=4$	$N_f=5$	$N_f=6$
$N_c=2$	1/3 (0.8724)	.4085 (2.6271)	.4370 (3.5311)	.4519 (4.3723)	.4611 (5.1795)	.4674 (5.9655)
$N_c=3$	-	.2696 (1.8664)	.3532 (3.8607)	.3923 (5.4647)	.4149 (6.9098)	.4297 (8.2670)
$N_c=4$	-	-	.2324 (2.9316)	.3175 (6.7624)	.3602 (9.1754)	.3865 (11.3076)
$N_c=5$	-	-	-	.2663 [Y] (4.7671)	.2909 (8.7275)	.3358 (11.8361)
$N_c=6$	-	-	-	-	0.2635 [Y] (6.7334)	.2686 (11.3107)

Table 2.5: The scaling dimension Δ_Q of the flavor multiplets and the maximal value of F-function (in the parenthesis), at the conformal fixed points for a few small values of N_f and N_c in the 3d $\mathcal{N}=2$ Spin(N_c) (O$_-$(N_c) or Pin(N_c)) SQCD with N_f flavors. For the diagonal entries ($N_f=N_c-1$) we have used the partition function of the magnetic theory, and for entries in red box we need to decouple the monopole operator Y. All other entries are computed in the electric theory, except in the blue boxed and diagonal entries where we used the magnetic theory for better numerical computations. Compare this with Table 2.4.

O$_-$ and Pin gauge groups is that the gauge-invariant monopole operator is not Y, but rather $Y_{\text{spin}}=Y^2$ (2.108), whose scaling dimension is twice that of Y.

This immediately means that the unitarity bound for Y in (2.95) is replaced by

$$Y_{\text{spin}}:\ a\le\frac{N_f-N_c+\frac{7}{4}}{N_f}\approx 1-\frac{1}{x}\ , \tag{2.109}$$

As expected, the difference from the SO case gauging disappears in the Veneziano limit.

We can redo the IR analysis, obtaining the new table as in Table 2.5. Clearly the difference can only happen when the monopole operator Y decouples in the SO theory. In the table this happens when $N_f=N_c-1=2,3$, when the monopole operator Y no longer decouples.

2.6 Digression on Group Theory

While the analyses in sections 2.3, 2.4 and 2.5 are treated separately, some of the structures can be understood in a more unified manner from the representation theory of the Lie algebras, as one might expect.

To give an example for this phenomenon, let us point out that the scaling dimension of the quarks and anti-quarks $\Delta_Q = \Delta_{\tilde{Q}}$, in the large N_f expansion up to the order of $\frac{1}{N_f^2}$, can be uniformly represented as

$$\Delta_Q(N_c, N_f) = \frac{1}{2} - \frac{4C_F}{\pi^2}\frac{1}{N_f} + \frac{96C_F^2 - \pi^2(8C_F^2 + \frac{8}{3}C_F C_A)}{\pi^4}\frac{1}{N_f^2} + O\left(\frac{1}{N_f^3}\right) , \quad (2.110)$$

where C_F and C_A are quadratic Casimirs in fundamental and adjoint representation, respectively. Concretely, we have

$$\begin{aligned}
\mathrm{U}(N_c): &\quad C_F = \frac{N_c}{2} , \quad C_A = N_c - \frac{1}{N_c} , \\
\mathrm{SU}(N_c): &\quad C_F = \frac{N_c^2 - 1}{2N_c} , \quad C_A = N_c , \\
\mathrm{USp}(2N_c): &\quad C_F = \frac{2N_c + 1}{4} , \quad C_A = N_c + 1 , \\
\mathrm{SO}(N_c): &\quad C_F = \frac{N_c - 1}{2} , \quad C_A = N_c - 2 ,
\end{aligned} \quad (2.111)$$

with which we can verify that (2.110) reproduce the formulas (2.43), (2.70), (2.84) and (2.102). We expect the formula (2.110) to apply to SQCD with other gauge groups, e.g. exceptional gauge groups. Quadratic Casimirs appear in the (2.110) because they can be computed via Feynman diagrams (*cf.* [47, Appendix B]). Note that in the leading Veneziano limit we always have $C_F \sim \frac{N_c}{2}, C_A \sim N_c$, washing differences among gauge groups away. This is the reason why the plots of Δ_Q (in Figures 2.9, 2.11 and 2.13), as well as the critical value x_c, are similar among different choices of gauge groups with the same ranks.

2.7 Gauging and Quiver Gauge Theories

The difference between $\mathrm{U}(N_c)$ theory and the $\mathrm{SU}(N_c)$ theory is an example where the gauging of a flavor symmetry dramatically modifies the IR dynamics. We have also seen in section 2.5.4 that gauging of discrete symmetries also changes the IR decoupling. These can be thought of as particular examples of more general phenomena where the gauging of a flavor symmetry modifies the IR dynamics of the theory.

As yet another example of this type, we study gauging of the $\mathrm{SU}(N_f)$ flavor symmetry of the SQCD, to obtain a quiver gauge theory with a product gauge group. We discuss the effect of the gauging to the IR R-symmetry, and to the decoupling of monopole operators. Such quiver gauge theories naturally arise in string theory (see e.g [83, 84] and references therein), and (as we will discuss later in the next section) for example in the compactifications of M5-branes.

2.7.1 Electric Gauging

Let us start with the $\mathrm{U}(N_c)$ SQCD with N_f flavors, discussed in section 2.2.

As shown in (2.5), this theory has $\mathrm{SU}(N_f)_L \times \mathrm{SU}(N_f)_R$ symmetry. Let us choose to gauge the diagonal $\mathrm{SU}(N_f)$ of these two $\mathrm{SU}(N_f)$ symmetries, which we denote by $\mathrm{SU}(N_f)_V$. The resulting theory then has $\mathrm{U}(N_c) \times \mathrm{SU}(N_f)$ gauge symmetry, and $\mathrm{SU}(N_f)_A \times \mathrm{U}(1)_A \times \mathrm{U}(1)_J \times \mathrm{U}(1)_{\mathrm{R-UV}}$ flavor symmetry, where $\mathrm{SU}(N_f)_A$ is the axial (anti-diagonal) combination of $\mathrm{SU}(N_f)_L \times \mathrm{SU}(N_f)_R$. As a result of this gauging, we obtain a quiver gauge theory, whose quiver diagram is shown in Figure 2.15.

One remark is that the resulting theory has a symmetry exchanging N_c and N_f. In fact, the gauge group can equivalently be taken as $(\mathrm{U}(N_c) \times \mathrm{U}(N_f))$, with matters in the bifundamental representations $Q : (\boldsymbol{N_c}, \overline{\boldsymbol{N_f}})$ and $\tilde{Q} : (\overline{\boldsymbol{N_c}}, \boldsymbol{N_f})$. This is a quiver gauge theory, and since we only have bifundamental matters, the overall U(1)

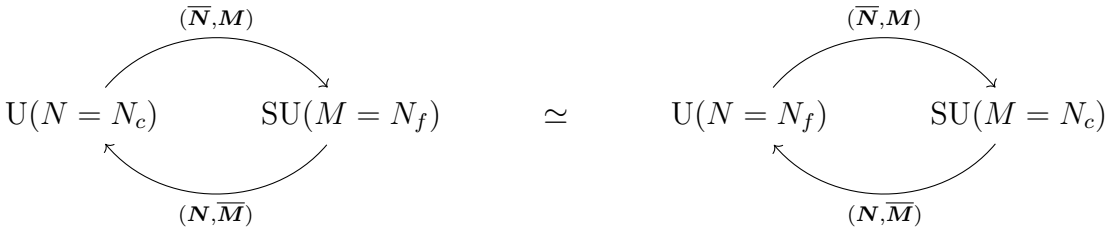

Figure 2.15: A Quiver diagram for the electric quiver gauge theory considered in this section. The quiver gauge theory can be obtained by gauging the $\mathrm{SU}(M)$ flavor symmetry of $\mathrm{U}(N)$ SQCD with M flavors, or by gauging the $\mathrm{U}(N)$ flavor symmetry of $\mathrm{SU}(M)$ SQCD with N flavors. Note that the gauge group can be thought of $\mathrm{SU}(N)\times\mathrm{U}(M), \mathrm{U}(N)\times\mathrm{SU}(M)$ or $(\mathrm{U}(N)\times\mathrm{U}(M))/\mathrm{U}(1)$, all describing the same theory. The theory therefore has symmetry exchanging N and M. The arrows represent bifundamental $\mathcal{N}=2$ chiral multiplets.

of the $(\mathrm{U}(N_c)\times\mathrm{U}(N_f))$ gauge group trivially decouples, leading to the $(\mathrm{U}(N_c)\times\mathrm{U}(N_f))/U(1)\simeq\mathrm{U}(N_c)\times\mathrm{SU}(N_f)$ gauge group as before.

In the rest of this section we use the notation $N:=N_c, M:=N_f$, to make this symmetry more manifest. In fact, now that the symmetry is manifest we can regard the same quiver gauge theory as obtained from the gauging $\mathrm{SU}(N)_V$ flavor symmetry of the $\mathrm{U}(M)$ SQCD with N flavors, with N and M reversed from above (Figure 2.15).

Now, the question we ask in this subsection is whether or not this gauging of the $\mathrm{SU}(M)$ symmetry has any effect in the discussion of the IR scaling dimension and the decoupling of monopole operators.

The best way to see this is to write down the S^3 partition function as the parameter a corresponding to the mixing of the $\mathrm{U}(1)_A$ symmetry:

$$\begin{aligned} Z_{\mathrm{U}(N)\times\mathrm{SU}(M)}(a) = \frac{1}{N!}\frac{1}{M!}\int\prod_{i=1}^{N}d\sigma_i\prod_{i=1}^{M}d\rho_j\,\delta\left(\sum_{j=1}^{M}\rho_j\right) \\ \times\overbrace{\prod_{1\le i<j\le N}\sinh^2[\pi(\sigma_i-\sigma_j)]\prod_{1\le i<j\le M}\sinh^2[\pi(\rho_i-\rho_j)]}^{\text{measure}} \\ \times\overbrace{\prod_{i=1}^{N}\prod_{i=1}^{M}\exp\left[l(1-a+i\sigma_i-i\rho_j)+l(1-a-i\sigma_i+i\rho_j)\right]}^{\text{bifundamental } Q,\tilde{Q}}\ . \end{aligned} \tag{2.112}$$

Note that the integral is kept invariant under the simultaneous shift of σ_i and ρ_j, and this represents the overall decoupled U(1) commented on before. The same partition function can also be written as

$$Z_{(\mathrm{U}(N)\times\mathrm{U}(M))/\mathrm{U}(1)}(a) = \frac{1}{N!}\frac{1}{M!}\int\prod_{i=1}^{N}d\sigma_i\prod_{i=1}^{M}d\rho_j\,\delta\left(\sum_{i=1}^{N}\sigma_i+\sum_{j=1}^{M}\rho_j\right) \times\overbrace{\prod_{1\le i<j\le N}\sinh^2[\pi(\sigma_i-\sigma_j)]\prod_{1\le i<j\le M}\sinh^2[\pi(\rho_i-\rho_j)]}^{\text{measure}} \times\overbrace{\prod_{i=1}^{N}\prod_{i=1}^{M}\exp\left[l(1-a+i\sigma_i-i\rho_j)+l(1-a-i\sigma_i+i\rho_j)\right]}^{\text{bifundamental } Q,\tilde{Q}}\ . \tag{2.113}$$

In either way, it is clear that gauging dramatically changes the partition function as a function of the parameter a, and consequently the IR R-charges/conformal dimensions of the theory. In fact, this is to be expected since we have a manifest symmetry between N and M after gauging; by contrast $N_c = N, N_f = M$ theory and $N_c = M, N_f = N$ clearly have different IR dynamics, as we have seen in the rest of this paper.

This symmetry between N and M is actually a source for trouble, when we consider the convergence bound for the electric S^3 partition function. The convergence bound before gauging was worked out in (2.64), and since now we have symmetry and N and M, we should impose the same constraint with N and M (N_c and N_f) exchanges. This gives

$$a < \min\left(\frac{M-N+1}{M}\ ,\quad \frac{N-M+1}{N}\right) \le \min\left(\frac{1}{M}\ ,\ \frac{1}{N}\right)\ , \tag{2.114}$$

and in particular a will be negative unless $N = M$.

Note that the convergence constraint is ameliorated by including flavor matters to gauge groups SU(N) and SU(M). Suppose that we include k flavors (l flavors) to

gauge groups SU(N) and SU(M). The convergence constraint then reads

$$a < \min\left(\frac{M-N+k+1}{M}\ ,\quad \frac{N-M+l+1}{N}\right)\ , \tag{2.115}$$

and in particular the constraint in practice goes away for the sufficiently large k and l. Such flavors are natural from string theory constructions, however we will set $k = l = 0$ in the discussion below, to simplify analysis.

2.7.2 Magnetic Gauging

To avoid this convergence issue, one might be tempted to switch to the magnetic description. Instead of gauging the flavor symmetry of the electric theory, we can choose to gauge the flavor symmetry of the magnetic theory.

For the case $M > N \geq 1$, we can first go to the magnetic theory of SU(N) SQCD with M flavors, and then gauge the U(M) $\simeq$ SU(M) $\times\, U(1)_B$ flavor symmetry of the theory. Note that these magnetic descriptions break the symmetry between N and M, clear from the fact that we need to take $M \geq N$ for the magnetic descriptions. The resulting partition function is given by (compare this with (2.62)):

$$\begin{aligned}
Z^{\mathrm{SU}(N)\times\mathrm{U}(M)}_{\text{magnetic}} &= \frac{1}{(M-N)!}\frac{1}{M!}\int \prod_{i=1}^{M-N} d\sigma_i \prod_{i=1}^{M} d\rho_j\, d\rho\ \delta\left(\sum_{j=1}^{M}\rho_j\right) \\
&\times \overbrace{\prod_{1\leq i<j\leq M-N}\sinh^2[\pi(\sigma_i-\sigma_j)]\prod_{1\leq i<j\leq M}\sinh^2[\pi(\rho_i-\rho_j)]}^{\text{measure}}\ e^{2\pi b\rho} \\
&\times \overbrace{\prod_{i,j=1}^{M}\exp\left[\,l(1-2a+i\rho_i-i\rho_j)\right]}^{M}\exp\left[\overbrace{l\,(1+2M\,a-2(M-N+1))}^{Y}\right] \\
&\times \overbrace{\prod_{i=1}^{M-N}\prod_{j=1}^{M}\exp\left[l\,(a\pm i\sigma_i\mp i\rho_j)\right]}^{q,\,\tilde{q}}\times\overbrace{\exp\left[l\left(1+(M-N)-M\,a\pm iN\,\rho\mp i\sum_{1\leq j\leq M-N}\sigma_j\right)\right]}^{b,\,\tilde{b}}\ .
\end{aligned} \tag{2.116}$$

Equivalently, we can start with the U(N) SQCD with M flavors, and then gauge the SU(M) flavor symmetry (compare (2.16)):

$$
\begin{aligned}
Z^{\mathrm{U}(N)\times\mathrm{SU}(M)}_{\text{magnetic}} = \frac{1}{(M-N)!}\frac{1}{M!}\overbrace{\exp\left[l\left(1-(M-N+1)\pm b+M\,a\right)\right]}^{V_\pm} \\
\times\int\prod_{i=1}^{M-N}d\sigma_i\prod_{j=1}^{M}d\rho_j\,\delta\left(\sum_{j=1}^{M}\rho_j\right) \\
\times\overbrace{\prod_{1\le i<j\le M-N}\sinh^2[\pi(\sigma_i-\sigma_j)]\prod_{1\le i<j\le M}\sinh^2[\pi(\rho_i-\rho_j)]}^{\text{measure}} \\
\times\overbrace{\prod_{i,j=1}^{M}\exp\left[\,l(1-2a+i\rho_i-i\rho_j)\right]}^{M}\times\overbrace{\prod_{i=1}^{M-N}\prod_{j=1}^{M}\exp\left[l\left(a\pm i(\sigma_i-\rho_j)\right)\right]}^{q,\tilde{q}}\ .
\end{aligned}
\tag{2.117}
$$

Using the duality between XYZ-model and $\mathcal{N}=2$ U(1) theory with single flavor, we can easily show that (2.116) and (2.117) are equivalent up to a constant phase.

Unfortunately, the convergence bound for (2.116) and (2.117) is satisfied for

$$
a>\frac{M-N-1}{M}\quad\text{and}\quad a<0\ , \tag{2.118}
$$

where the first (second) inequality comes from the convergence of the σ (ρ) integrals. In other words the partition function (2.116) and (2.117) cannot be used for any practical F-maximization.

The situation is better for the case $M=N$. We can then gauge the SU($M=N$) flavor symmetry of the magnetic U(N) theory, leading to the partition function

$$
Z^{N=M}_{\text{magnetic}}=\frac{1}{N!}\overbrace{\exp\left[l(Na\pm b)\right]}^{V_\pm}\prod_{i=1}^{N}\int d\rho_j\,\delta\left(\sum_{j=1}^{N}\rho_j\right)\overbrace{\prod_{i,j=1}^{N}\exp\left[l(1-2a+i\rho_i-i\rho_j)\right]}^{M}\ . \tag{2.119}
$$

We can instead choose to gauge the $\mathrm{U}(N) \simeq \mathrm{SU}(N)_V \times U(1)_B$ flavor symmetry of the magnetic $\mathrm{SU}(M)$ theory, leading to the expression

$$\begin{aligned} Z^{N=M}_{\text{magnetic}} = \frac{1}{N!} \overbrace{\exp\left[l(1-2+2Na)\right]}^{Y} \int d\rho\, e^{2\pi b\rho} \overbrace{\exp\left[l(1-Na \pm i\rho)\right]}^{B,\tilde{B}} \\ \times \int \prod_{j=1}^{N} d\rho_j\, \delta\left(\sum_{j=1}^{N} \rho_j\right) \overbrace{\prod_{i,j=1}^{N} \exp\left[l(1-2a+i\rho_i - i\rho_j)\right]}^{M} \ . \end{aligned} \tag{2.120}$$

We can easily show that these partition functions converges when $a < \frac{1}{2}$.

It is natural to expect that the magnetic quiver theories discussed here are dual to the electric quiver gauge theories discussed before. We have implicitly assumed that the order of two operations, gauging the flavor symmetry and going to the dual magnetic description, commute with each other. Since the duality at hand is an IR duality, gauging the flavor symmetry could change the behavior under the RG flow, and hence spoil the IR duality.

However, we expect that this does not happen when the gauge coupling for the newly-gauged flavor symmetry is much smaller than other gauge couplings. If in the UV the gauge coupling for $\mathrm{SU}(N)$ is much larger than that for the $\mathrm{SU}(M)$ gauge group, one can imagine that the strong coupling effect of $\mathrm{SU}(N)$ kicks in first, and then the dynamics of $\mathrm{SU}(M)$ does not matter until at much lower scales. We can then discuss the dynamics of $\mathrm{SU}(N)$ and $\mathrm{SU}(M)$ gauge groups separately. Since the S^3 partition function is independent of gauge couplings, the equality of the S^3 partition functions should hold for any value of the gauge coupling, giving further evidence for the duality after gauging.

Numerical Results The numerical analysis of the quiver case is computationally more challenging than the SQCD case, and as we have seen the convergence bound tends to be more strict. Therefore, let us consider the simplest case of $N = M$

$N=2$	$N=3$	$N=4$	$N=5$
.2172	.1962	.1804	.1567
(3.5322)	(7.5009)	(12.1339)	(15.2490)

Table 2.6: The critical value of the parameter a and the critical value of the F-function (in the parenthesis), for the $\mathrm{SU}(N)\times\mathrm{U}(N)\sim(\mathrm{U}(N)\times\mathrm{U}(N))/\mathrm{U}(1)$ theory, computed from the magnetic partition function (2.119). Notice that the critical value of a is different from that in Table 2.2 before gauging the $\mathrm{U}(N)$ flavor symmetry. In all these cases there is no indication that any operator decouple in the IR.

magnetic theory in here. We can then do F-maximization for the partition function (2.119) (compare with Table 2.2). The numerical results for the values $N=M=2,3,4,5$ are summarized in Table 2.6.

There are two remarks on this result. First, the value of a at the maximum is different from that before gauging, as expected. Another non-trivial result is that none of these cases exhibit operator decoupling. This is partly because the meson M of the magnetic theory, after gauging, is now an adjoint field with respect to the newly-introduced gauge symmetry, and hence is not gauge invariant. Therefore there is no need to consider the unitarity bound of the meson itself.

2.7.3 General Quivers

Having discussed quiver gauge theories with two nodes, we can discuss a more general 3d $\mathcal{N}=2$ quiver gauge theories, whose matter content is determined by a quiver diagram, i.e. an oriented graph[4]. We can then gauge the appropriate flavor symmetries, whose effect is to concatenate two quiver diagrams and to generate a more complicated quiver diagram (Figure 2.16). For example, if we glue two quivers Q_1, Q_2 at a node to obtain a new quiver Q, then partition function for the larger quiver Q can

[4]We also need to specify the superpotentials, however this choice does not really modify the qualitative features of the conclusions below.

be schematically written in the form

$$Z_Q[\sigma_1, \sigma_3](a_1, a_2) = \int d\sigma_2 \, Z_{\text{vector}}[\sigma_2] \, Z_{Q_1}[\sigma_1, \sigma_2](a_1) \, Z_{Q_2}[\sigma_2, \sigma_3](a_2) \ , \tag{2.121}$$

where $Z_{\text{vector}}[\sigma_2]$ is the contribution from the vector multiplet which is gauged under the gluing, and $a_{1,2}$ denote the parameters repressing the flavor symmetries of the theories $Q_{1,2}$.

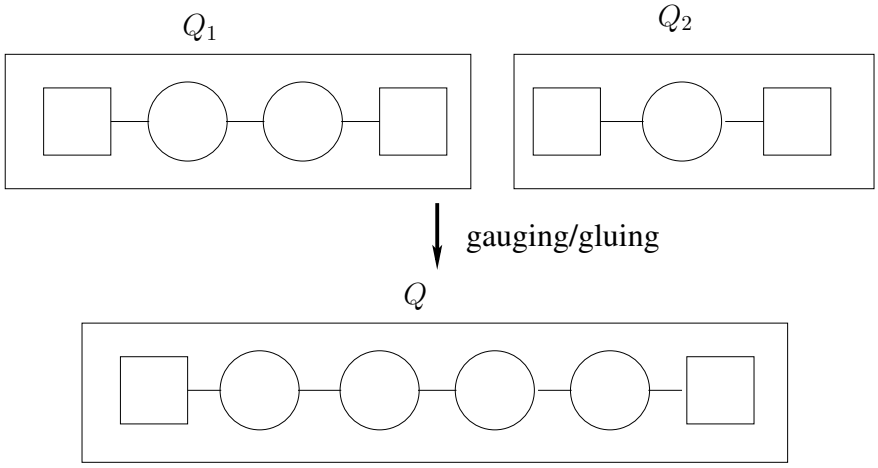

Figure 2.16: We can generate a larger quiver Q by gluing together two quivers Q_1 and Q_2. In gauge theory language the circle (the square) represents the gauge (global) symmetry, each of which can be for example $\mathrm{U}(N_c)$ or $\mathrm{SO}(N_c)$ with different values of N_c for different nodes. Gluing in this context means to take two flavor symmetries (represented by two squares in the middle, which we assume to contain the same flavor symmetry group) and gauge the diagonal subgroup of the product. The partition function behaves nicely under this gluing, however not the F-maximization nor the IR behavior.

As before, the extremum of $Z_Q[\sigma_1, \sigma_3](a_1, a_2)$ as a function of a_1 (a_2) is in general different from that of the $Z_{Q_1}[\sigma_1, \sigma_2](a_1)$ ($Z_{Q_2}[\sigma_2, \sigma_3](a_2)$). This means that to tell whether the monopole operator for the gauge group in the quiver Q_1 decouples or not, we need to know in advance the detailed data for the quiver Q_2, no matter how large the quiver Q_2 may be.[5] This is in sharp contrast with the case of 3d $\mathcal{N} = 4$

[5]In the spirit of [85] one might be tempted to say that there is a "long-range entanglement in the theory space". It would be interesting to explore this point further, and connect the discussion here to the entanglement in the dual statistical mechanical model discussed in [86, 87].

supersymmetry, where the IR decoupling of the monopole operators can be checked locally at the quiver diagram, by verifying the inequality $N_f \geq 2N_c$ (*cf.* [88, 89] for recent discussion in gravity dual).

2.8 Adding the Chern-Simons term

Let us conclude this chapter with studying U(N_c) theory with the Chern-Simons term. It is instructive to understand what happens to the monopole operators when we turn on a Chern-Simons term at level k, which explicitly violates parity. The Chern-Simons term gives a topological mass [90] $m_T \sim g^2 k$ to the monopole operators, completely lifting the Coulomb branch of the theory. Even though the monopole operators do not exist along the Coulomb branch, one may still worry that these operators exist at the origin of the moduli space. This turns out not to be the case. By looking at the Gauss law constraint, one sees that the monopole operators are not gauge invariant when $k \neq 0$. To construct gauge invariant operators out of the monopole operators, one must act with flavor modes. However, the resulting dressed monopole operators are no longer chiral [77].

When $|k| > 0$ we may use the electric theory to describe the IR fixed point for the values of N_f and N_c which satisfy the condition

$$|k| + N_f - N_c \geq 0 \tag{2.122}$$

for a supersymmetric vacuum. Now we do not have to worry about the dimensions of the monopole operators hitting the unitarity bound. The S^3 partition function nicely illustrates this observation. The partition function of the $U(N_c)_k$ gauge theory at CS

level k with N_f non-chiral flavors is given by

$$Z = \frac{1}{N_c!}\int\left(\prod_{i=1}^{N_c}\frac{d\lambda_i}{2\pi}e^{ik\frac{\lambda_i^2}{4\pi}}\right)\left(\prod_{i<j}^{N_c}4\,\sinh^2\left[\frac{\lambda_i-\lambda_j}{2}\right]\right)\prod_{i=1}^{N_c}e^{N_f[\ell(1-\Delta+i\frac{\lambda_i}{2\pi})+\ell(1-\Delta-i\frac{\lambda_i}{2\pi})]}\,. \tag{2.123}$$

When k is non-zero we may always rotate the contour of integration so that (2.123) converges exponentially.

2.8.1 The Giveon-Kutasov duality

Magnetic dual descriptions of the IR fixed points are also available when we turn on Chern-Simons terms; they are described by the Giveon-Kutasov duality [56]. The Giveon-Kutasov dual of the electric theory is similar to the Aharony dual of the $k = 0$ theory, whose matter content is given in table 2.8, except that the fields $V_\pm$ and $\tilde{V}_\pm$ are no longer present. The dual gauge group is $U(|k| + N_f - N_c)_{-k}$, and the superpotential of the dual theory is simply $W = \tilde{q}_a M_b^a q^b$ $(a, b = 1, \ldots, N_f)$. The S^3 partition function of the dual theory is

$$Z = \frac{e^{N_f^2\ell(1-2\Delta)}}{(|k|+N_f-N_c)!}\int\left(\prod_{i=1}^{|k|+N_f-N_c}\frac{d\lambda_i}{2\pi}e^{-ik\frac{\lambda_i^2}{4\pi}}\right)\left(\prod_{i<j}^{|k|+N_f-N_c}4\,\sinh^2\left[\frac{\lambda_i-\lambda_j}{2}\right]\right)$$
$$\prod_{i=1}^{|k|+N_f-N_c}e^{N_f[\ell(\Delta+i\frac{\lambda_i}{2\pi})+\ell(\Delta-i\frac{\lambda_i}{2\pi})]}\,. \tag{2.124}$$

We may use the magnetic formulation of the theory everywhere above the supersymmetry bound; on the three-sphere this gives results identical to the electric formulation [62]. The special case where $|k| + N_f - N_c = 0$ is similar to the $k = 0$, $N_f = N_c$ case; the dual theory has no gauge group, and a simple calculation using (2.124) shows that F is maximized at $\Delta = 1/4$.

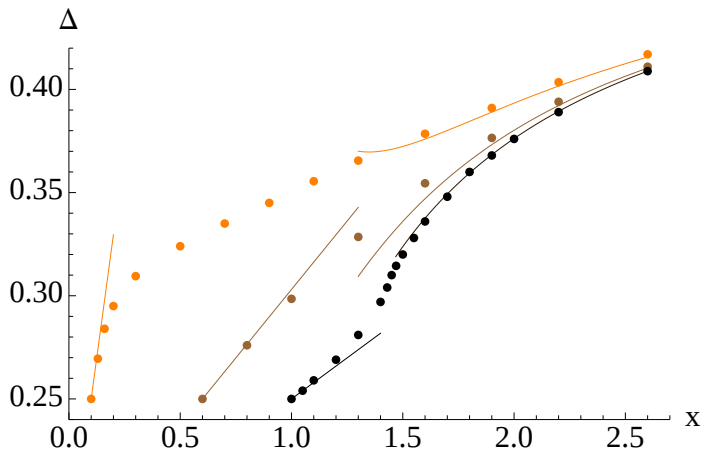

Figure 2.17: Δ as a function of $x = \frac{N_f}{N_c}$ in the Veneziano limit at various value of $\kappa = |k|/N_c$. The black, brown, and orange points correspond to $\kappa = 0.01$, 0.4, 0.9, respectively. The points were computed numerically using the saddle point method, described in section 2.2.3. The smooth curves at larger values of x come from the analytic approximation to Δ in (2.125). The linear approximations at small x were plotted using the analytic approximation (2.126).

2.8.2 Meson scaling dimensions

It is instructive to keep track of the scaling dimension 2Δ of the gauge invariant mesons M_b^a in the Veneziano limit. When we take the Veneziano limit in the theory with a CS level, we keep fixed both $\kappa = \frac{|k|}{N_c}$ and $x = \frac{N_f}{N_c}$. We separately consider the regimes $0 < \kappa < 1$, $\kappa = 1$, and $\kappa > 1$. In the first regime, when $0 < \kappa < 1$, the supersymmetry bound is given by $x = 1 - \kappa$, with $\Delta(x = 1 - \kappa) = \frac{1}{4}$. When $\kappa = 1$, the supersymmetry bound occurs when $x = 0$, and when $\kappa > 1$ we do not reach the supersymmetry bound for any value of x. The different regimes are considered separately below.

Δ when $0 < \kappa < 1$

We calculate Δ for various values of $0 < \kappa < 1$ using the methods in section 2.2.3, with the results shown in figure 2.17. We may use either the electric or magnetic formulations of the theory to calculate Δ, and we verify numerically that they indeed

give identical results. As in the theory with $\kappa = 0$, we calculate analytic approximations to Δ about $x = \infty$ and $x = 0$ using the electric and magnetic descriptions of the theory, respectively. The first few terms in the expansion about $x = \infty$ are

$$\Delta(x, \kappa) = \Delta(x, \kappa = 0) + \frac{8\,\kappa^2}{\pi^4 x^3} + \frac{16\,(3\pi^2 - 20)\kappa^2}{\pi^6 x^4} + O(1/x^5)\,, \tag{2.125}$$

where $\Delta(x, \kappa = 0)$ is the result in (2.43), while the leading behavior in the expansion about $x = 0$ is given by

$$\Delta(x, \kappa) = \frac{1}{4} + \frac{x + \kappa - 1}{4\pi(1 - \kappa)} + O\left((x + \kappa - 1)^2\right)\,. \tag{2.126}$$

An interesting observation, which may be seen in figure 2.17, is that $\partial_x \Delta$ diverges at small x as $\kappa \to 1$ from below. We will see in the following sections that Δ behaves qualitatively differently at small x when $\kappa \geq 1$; in particular, when $\kappa \geq 1$ we find that $\Delta \geq \frac{1}{3}$ for all x.

The case $\kappa = 1$

The theory with $|k| = N_c$ is special since the magnetic dual is a $U(N_f)$ gauge theory at CS level $\mp N_c$, depending on whether $k = \pm N_c$, with N_f non-chiral flavors $(q^a, \tilde{q}_a)$ and N_f^2 neutral mesons M_b^a; the rank of the dual gauge group does not grow with N_c. Recall that this theory is also subject to the superpotential $W = \tilde{q}_a M_b^a q^b$. It is interesting to analyze this theory in the limit $N_f \ll N_c$, since in this limit the large CS level makes the $U(N_f)$ gauge theory weakly coupled. At the level of the partition function (2.124) this is seen by noting that in this limit the matrix integral localizes near the origin $\lambda_i = 0$, and the free energy reduces to

$$F(\Delta) = N_f^2 \left(-\ell(1 - 2\,\Delta) - 2\,\ell(\Delta) + \frac{1}{2}\log\frac{N_c}{N_f} + \text{const}\right) + O(N_f^4/N_c^2)\,, \tag{2.127}$$

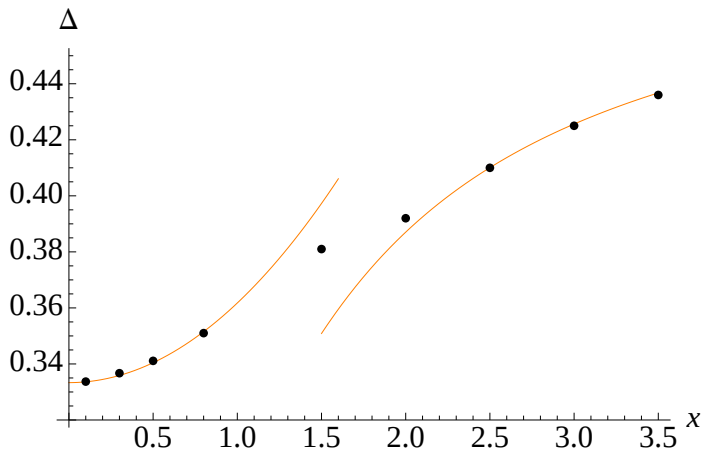

Figure 2.18: Δ as a function of $x = \frac{N_f}{N_c}$ in the Veneziano limit with $\kappa = \frac{|k|}{N_c} = 1$. The smooth orange curve at the large x was computed from the analytic approximation in (2.125), while the smooth orange curve at the small x, which approaches $1/3$ at $x = 0$, comes from the analytic approximation in (2.128). The black points were computed numerically using the saddle point method (method 1, section 2.2.3).

where the logarithmic term comes from the $U(N_f)_{N_c}$ supersymmetric Chern-Simons theory. In the limit $N_f \ll N_c$ the free energy is maximized by $\Delta = \frac{1}{3}$. As $x = \frac{N_f}{N_c}$ is increased from zero to infinity, Δ is seen to increase monotonically from $\frac{1}{3}$ to $\frac{1}{2}$. Using the methods of section 2.2.3, we may solve perturbatively for Δ at small x in the dual theory, with the result

$$\Delta(x) = \frac{1}{3} + \frac{1}{324}\left(99 - 20\sqrt{3}\pi + \frac{81(4\sqrt{3}\,\pi - 9)}{27 + 8\,\pi(2\,\pi - 3\sqrt{3})}\right) x^2 + O(x^4)\,. \qquad (2.128)$$

At large x we may use the $1/x$ expansion from the electric theory in (2.125). In figure 2.18 we plot these two analytic approximations along with the numerical results.

Theories with $\kappa > 1$

We now discuss the theory with $\kappa > 1$ in the Veneziano limit. The behavior of Δ as a function of $x = \frac{N_f}{N_c}$ is qualitatively different at small x from the behavior when $\kappa < 1$

and when $\kappa = 1$. An important observation is that when $\kappa > 1$ the scaling dimension Δ approaches $\frac{1}{2}$ at small x, i.e. when N_f is kept fixed while N_c and k are sent to infinity. This behavior is likely due to the higher spin symmetry in this limit [67–69].

The leading correction to Δ at small x can be worked out in perturbation theory. Writing

$$\Delta(x, \kappa) = \frac{1}{2} - x f(\kappa) + O(x^2) \,, \tag{2.129}$$

we can expand $f(\kappa)$ at large κ by perturbation theory in the electric theory. Using the methods in section 2.2.3 we find

$$f(\kappa) = \frac{1}{2\,\kappa^2} + \frac{\pi^2}{24\,\kappa^4} + O(1/\kappa^6) \,. \tag{2.130}$$

At values of κ near unity it is possible to approximate $f(\kappa)$ by perturbation theory in the magnetic theory, giving

$$f(\kappa) = \frac{2}{\pi^2} \frac{1}{(\kappa - 1)} + O\left((\kappa - 1)^0\right) \,, \tag{2.131}$$

which shows that $f(\kappa)$ diverges as $\kappa \to 1$ from above. In figure 2.19 we plot the analytic approximations to $f(\kappa)$ at small and large values of κ along with numeric results.

Let us stress that our results for Δ in the large N_c limit at fixed N_f and $\lambda = N_c/k$ are *not* symmetric under $\lambda \to 1 - \lambda$. For small λ we have [91]

$$\Delta_Q = \frac{1}{2} - \frac{N_f N_c}{2k^2} + \dots \,, \tag{2.132}$$

while for $\lambda \to 1$

$$\Delta_Q = \frac{1}{2} - \frac{2N_f}{\pi^2(k - N_c)} + \dots \,. \tag{2.133}$$

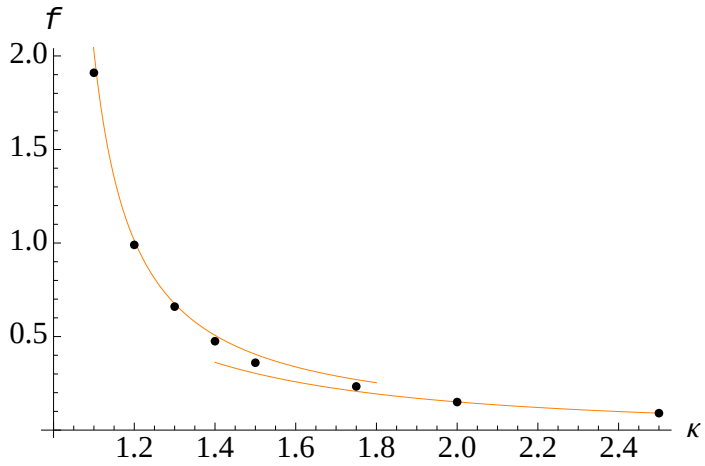

Figure 2.19: The function $f(\kappa)$, defined in (2.129), plotted over a range of $\kappa > 1$. At values of κ slightly greater than one, $f(\kappa)$ is well approximated by (2.131), which is the upper orange curve in the plot. The lower orange curve is the approximation at large κ given in (2.130). The points were computed numerically using the saddle point method described in section 2.2.3.

The lack of symmetry under $N_c \to k - N_c$ is due to the fact that the $\mathcal{N} = 2$ Giveon-Kutasov duality does not relate the isomorphic theories; the electric theory has no superpotential, but the magnetic theory has a cubic superpotential.

At large values of x we may still use the analytic approximation to Δ in (2.125). In figure 2.20 we plot Δ as a function of x for a few different $\kappa > 1$ in order to illustrate the general behavior in this regime. We also include the analytic approximations at small and large values of x in their regimes of validity.

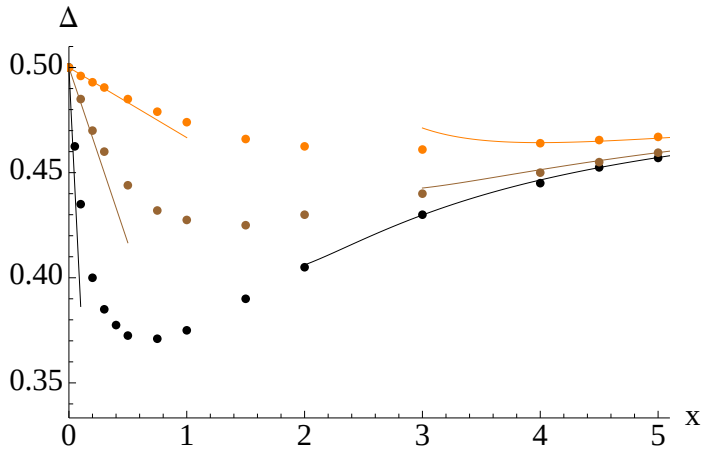

Figure 2.20: Δ as a function of $x = \frac{N_f}{N_c}$ with $\kappa = \frac{N_f}{N_c} = 1.2$ (black), $\kappa = 2$ (brown), and $\kappa = 4$ (orange). The linear approximations at small x were computed using (2.129), with $f(\kappa)$ plotted in figure 2.19. The analytic approximations at large x, which are shown as smooth curves, come from (2.125). The points were computed numerically using the saddle point method described in section 2.2.3.

Chapter 3

Rényi entanglement entropy

This chapter contains the edited version of [92], which was written in collaboration with Lauren McGough and Benjamin Safdi, and [93], which was written in collaboration with Aitor Lewkowycz, Benjamin Safdi, and Eric Perlmutter.

3.1 Introduction

Quantum entanglement is a powerful tool for characterizing the ground states of many-body quantum systems and continuum quantum field theories (QFTs). A useful way of quantifying quantum entanglement is through the Rényi entropies [43, 44]

$$S^q = \frac{\log \operatorname{tr} \rho_R^q}{1-q}\,, \qquad q > 0\,. \tag{3.1}$$

The reduced density matrix ρ_R is computed by taking the trace of the ground state density matrix $\rho = |0\rangle\langle 0|$ over the degrees of freedom living outside of the entangling region.

A particularly interesting special case is the entanglement entropy (EE) (for reviews, see [23, 94, 95]):

$$S = \lim_{q \to 1} S^q = -\operatorname{tr}(\rho_R \log \rho_R)\,. \tag{3.2}$$

At the conformal fixed points of even d-dimensional relativistic QFTs, the EE S_Σ across any smooth $(d-2)$-dimensional entangling surface Σ has a $\log \epsilon$ divergence, where ϵ is the short-distance cutoff, in addition to the power-like divergent terms $\propto \epsilon^{-2n}$, $n = 1, \ldots, (d-2)/2$. When $d = 2$, the coefficient of the $\log \epsilon$ term is proportional to the central charge of the conformal field theory (CFT) [22–24]. In $d = 4$, Solodukhin [96] has proposed that[1]

$$S_\Sigma = \alpha \frac{A_\Sigma}{\epsilon^2} + \left[\frac{a}{180}\int_\Sigma E_2 + \frac{c}{240\pi}\int_\Sigma \left(\left(\operatorname{tr} k^2 - \frac{1}{2}k^2\right) - C^{ab}{}_{ab}\right)\right] \log \epsilon + O(\epsilon^0)\,, \tag{3.3}$$

where the coefficients a and c are the two Weyl anomaly coefficients in 4-d CFT, normalized so that they both equal unity for a real scalar field.

The Rényi entropies should also possess an expansion analogous to (3.3). In $(1+1)$-dimensional CFT, it is known that the universal term scales $\propto (1 + q^{-1})$ with the Rényi parameter q [22–24]. In $(3+1)$-dimensional CFT, we do not expect the universal term in the Rényi entropy to be completely determined by a and c [97]. However, in this chapter we provide evidence for non-trivial structure in that term. As in (3.3), the universal term in the Rényi entropy has an expansion in terms of geometric invariants on the entangling surface. In Sec. 3.2, we conjecture a simple relation between the coefficient of extrinsic curvature term and that of Weyl tensor term that holds across all q and for free $(3+1)$-dimensional CFTs.

[1] A_Σ is the area of the entangling surface, and E_2 is the 2-dimensional Euler density on Σ. The extrinsic curvature is given by k^i_{ab}, where $a, b = 1, 2$ are local indices on Σ and $i = 1, 2$ label the two independent normal vectors. The quantity $C^{ab}{}_{ab}$ is the trace of the pullback of the spacetime Weyl tensor onto Σ.

In sec. 3.3, we numerically compute the CFT Rènyi entropy across an S^1 entangling surface in the $(2+1)$-dimensional free scalar theory. Since $1/(mR)$ term in this computation related to the universal term in $(3+1)$-dimension, this helps us provide solid evidence to our conjecture. Also, this Rènyi entropy itself matches with the result obtained by conformally mapping the CFT Rényi entropy to the thermal free energy on $\mathbb{H}^2$ [46]. In Sec. 3.4 we provide numerical evidence for a calculable, cutoff-independent contribution to the area-law term in $(2+1)$-dimensional massive Rényi entropy [1].

In the second half of this chapter, we focus on the different aspect of Rènyi entropy. Progress in understanding the CFT Rényi entropies across spherical entangling surfaces was made recently by expanding near $q = 1$ [98]; the corrections to the EE in d spacetime dimensions away from $q = 1$ are given by connected correlators of the Hamiltonian H of the CFT conformally mapped to $\mathbb{R} \times \mathbb{H}^{d-1}$ at temperature $T = 1/(2\pi R)$, where $\mathbb{H}^{d-1}$ is the $(d-1)$-dimensional hyperbolic space of radius R. However, for a theory of free scalar fields in various dimensions, the naive application of this expansion seems to conflict with taking derivatives of known results for S_q.

The Hamiltonian H on the hyperbolic space for computing quantum entropy is given by $H = \int_{\mathbb{H}^{d-1}} d^{d-1}x\sqrt{g}T_{\tau\tau}$, where τ is the time-like coordinate and $T_{\tau\tau}$ is the time-time component of the stress tensor. In Sec. 3.5, we review how this Hamiltonian is related to the expansion of Rènyi entropy around $q = 1$. However, we show that potential ambiguities in the definition of $T_{\tau\tau}$ familiar from ordinary QFT – the presence or absence of total derivative terms – must be properly accounted for.

We compute the Rényi entropies via CFT partition functions on two different spacetimes. One is the hyperbolic cylinder, $S^1 \times \mathbb{H}^{d-1}$, where the S^1 has circumference $2\pi Rq$. In this frame, there is an apparent choice between conformal and non-conformal stress tensors that differ by a total derivative term. This is directly related to different ways of regularizing the boundary of $\mathbb{H}^{d-1}$. The other spacetime

is a conically-singular version of flat Minkowski space, $\mathcal{C}_q \times \mathbb{R}^{d-2}$, with a deficit angle $2\pi(q-1)$ along the entangling surface; this is the spacetime generated directly by the replica trick. In this frame, there are different ways of regularizing the conical singularity that may differ by boundary terms. To compute the conventional Rényi entropies, one regulates the conical singularity by putting in a hard cut-off a distance ϵ away from the entangling surface. In here, boundary terms appear in the modular Hamiltonian localized a short distance away from the entangling surface.

We show the necessity of including these boundary terms through explicit computations. In Sec. 3.6, using the connected three-point function of H built from the *conformal* stress tensor, we derive $S''_{q=1}$ for a general CFT, where the primes denote derivatives with respect to q. We perform the calculation by utilizing a conformal mapping back to $\mathbb{R}^d$, where the stress tensor three-point function is fixed by conformal symmetry up to three calculable, theory-dependent constants. We then check our result for $S''_{q=1}$ against derivatives of previous results for S_q. Applied to CFTs with Einstein gravity duals and to free Dirac fermions across dimensions, and to free vector fields in $d = 4$, we find perfect agreement; applied to the conformal scalar, we find an apparent mismatch instead.

The resolution to this issue was laid out above: in taking derivatives of S_q with respect to q, one must take into account boundary contributions from the singular cone. In Sec. 3.7, we substantiate this statement with three different (matching) calculations of $S''_{q=1}$, performed on the spaces $\mathcal{C}_q \times \mathbb{R}^{d-2}$, S^d, and on $S^1 \times \mathbb{H}^{d-1}$. We also apply these conclusions to the computation of $S''_{q=1}$ in $\mathcal{N} = 4$ super-Yang-Mills. Due to the boundary terms in the stress tensor, this quantity depends on the 't Hooft coupling λ, consistent with known results at weak and strong coupling. If one were to neglect the boundary terms, non-renormalization of the central charges would seem to incorrectly imply non-renormalization of $S''_{q=1}$ instead.

3.2 Universal structure in Rényi entropy

In $(3+1)$-dimensional CFT, the $\log\epsilon$ term in the Rényi entropy should take the form [99]

$$S^q_\Sigma|_{\log\epsilon} = \left[\frac{f_a(q)}{180}\int_\Sigma E_2 + \frac{f_b(q)}{240\pi}\int_\Sigma \left(\operatorname{tr} k^2 - \frac{1}{2}k^2\right) - \frac{f_c(q)}{240\pi}\int_\Sigma C^{ab}{}_{ab}\right]\log\epsilon\,, \tag{3.4}$$

where the functions $f_{a,b,c}(q)$ are independent of the entangling surface. These functions must also approach the correct anomaly coefficients at $q = 1$ so as to reproduce (3.3): $f_a(1) = a$, $f_{b,c}(1) = c$.[2] In the theory consisting of n_0 free real scalars, the functions $f_a(q)$ and $f_c(q)$ have been computed explicitly, yielding the results [46, 99–102]

$$f_a(q) = n_0\frac{(1+q)(1+q^2)}{4q^3} \quad , \quad f_c(q) = n_0\frac{(1+q)(1+q^2)}{4q^3}\,. \tag{3.5}$$

Previous to this work, the function $f_b(q)$ has remained completely unknown for any theory away from $q = 1$. In Sec. 3.3 we compute the function $f_b(q)$ numerically for the free scalar theories. Within the numerical precision of our calculation, we find that $f_b(q) = f_c(q)$ in these examples. This leads us to the following conjecture,

$$\textbf{Conjecture: } f_b(q) = f_c(q) \text{ in } (3+1)\text{-dimensional CFTs.} \tag{3.6}$$

For free massless scalars, the universal term in the $(3+1)$-dimensional Rényi entropy across a cylinder of radius R is related to the $1/(mR)$ term in the large (mR) expansion of the $(2+1)$-dimensional Rényi entropy across a circle of radius R for the corresponding massive theories. A special case of this result was pointed out for the

[2] In addition, $f'_a(1) = -(9\pi^4 C_T)/2$, where C_T is the coefficient of the vacuum two-point function of stress-energy tensors, in units where $C_T = 1/(3\pi^4)$ for a real scalar field [98].

EE ($q = 1$), and Huerta [103] made use of this result to provide numerical checks of (3.3).

We generalize the calculations in [103] away from $q = 1$. As is the case with EE [103–107], it is natural to expect the Rényi entropies to have an expansion at large (mR)

$$S^q = \alpha^q \frac{R}{\epsilon} + \beta^q \, m \, (2\pi R) - \gamma^q + \sum_{n=0}^{\infty} \frac{C^q_{-1-2n}}{(mR)^{2n+1}} \, . \tag{3.7}$$

The γ^q are expected to be related to topological EE [108, 109]. We discuss the β^q in Sec. 3.4.

By dimensional reduction, the coefficient C^q_{-1-2n} in the free massive theories is related to the universal term in the Rényi entropy in the corresponding massless theory in $(2n + 4)$-dimensions. The entangling surface in the higher-dimensional theory should be thought of as $T^{2n+1} \times S^1$, where T^{2n+1} is the $(2n + 1)$-torus, whose volume is taken to be large compared to R^{2n+1}, with R the radius of the S^1. This has been noted previously for the EE [103, 105, 110], and the arguments leading to the conclusion for the Rényi entropy are the same. In particular,

$$(C^q_{-1})^{\text{scalar}} = -\frac{\pi}{240} f_b(q) \, . \tag{3.8}$$

In deriving these relations, we used the fact that when the 4-d entangling geometry is $S^1 \times S^1$, where the first S^1 has a length L much larger than the radius R of the second S^1, then (3.4) evaluates to $S^q|_{\log \epsilon} = \frac{f_b(q)}{240} \frac{L}{R} \log \epsilon$.

Note : Recently, it has been noticed that this conjecture does not hold for the holographic theories [111]. It still holds for all free theories.

3.3 Numerical Rényi entropy

By computing C^q_{-1}, we may use (3.8) to infer $f_b(q)$. We compute C^q_{-1} using the numerical method for calculating Rényi entropy proposed in [104], which is a straightforward generalization of the Srednicki procedure for numerically calculating EE [12, 103, 104, 112]. The Srednicki procedure has been used recently to numerically calculate EE with circular entangling surfaces in free massive theories [45, 103, 110, 113].

First, let us talk about how Rényi entropy can be computed across a circular entailing surface in free 3-dimensional CFT [12, 103, 104, 112]. For our purposes, the Hamiltonian is most conveniently expressed by expanding in modes of integer angular momentum n and discretizing the radial direction into N units. The method relies on the observation that the resulting Hamiltonian takes the form

$$H = \sum_n H_n \,, \qquad H_n = \frac{1}{2}\sum_i \pi_i^2 + \frac{1}{2}\sum_{ij} \phi_i K_n^{ij} \phi_j \,, \tag{3.9}$$

where π_i is the conjugate momentum to ϕ_i, and i, j run from $1, \ldots, N$. The matrix K_n^{ij} has non-zero elements [103]

$$K_n^{11} = \frac{3}{2} + n^2 + m^2 \,, \qquad K_n^{ii} = 2 + \frac{n^2}{i^2} + m^2 \,, \qquad K_n^{i,i+1} = K_n^{i+1,i} = -\frac{i+1/2}{\sqrt{i(i+1)}} \,. \tag{3.10}$$

For each n, the two-point correlators $X_{ij} = \langle \phi_i \phi_j \rangle$ and $P_{ij} = \langle \pi_i \pi_j \rangle$ are directly related to K,

$$X_n = \frac{1}{2}\left(K_n^{1/2}\right) \,, \qquad P_n = \frac{1}{2}\left(K_n^{-1/2}\right) \,, \tag{3.11}$$

and are thus easily computed. We find the q^{th} Rényi entropy across a circle of radius $R = r + \frac{1}{2}$ in lattice units by constructing the truncated matrices $X^r \equiv \left(X_{ij}\right)_{1 \le i,j \le r}$

and $P^r \equiv \left(P_{ij}\right)_{1\leq i,j\leq r}$, for each n. The Rényi entropy is then given by (3.20) with

$$S_n^q = \frac{1}{1-q}\,\mathrm{tr}\log\left[\left(\sqrt{X_n^r P_n^r}+\frac{1}{2}\right)^q - \left(\sqrt{X_n^r P_n^r}-\frac{1}{2}\right)^q\right]. \tag{3.12}$$

To compute the q^{th} Rényi entropy across a circle of radius $R = r + \frac{1}{2}$, we define a truncated $C_n^r = \left(C_{ij}\right)_n^{1\leq i,j\leq r}$ for each n. The Rényi entropy $S^q(R)$ is then given by

$$S^q(R) = \sum_n S_n^q\,, \qquad S_n^q = \frac{1}{1-q}\,\mathrm{tr}\log\left[(1-C_n^r)^q + (C_n^r)^q\right]. \tag{3.13}$$

We take our radial lattice to have $N = 200$ points. We study entangling circles of radii $30 \leq r \leq 50$ in lattice units, and mass $m = 0.01k$, $0 \leq k \leq 8$. We compute the S_n^q for $0 \leq |n| \leq 2000$

The primary sources of error in the numerical method are finite lattice size effects and finite angular momentum cutoff effects. We address the latter source of error by summing the asymptotic expansions of the S_n at large n, from the angular momentum cutoff to infinity. Finite lattice size effects are most pronounced for small angular momentum modes [114]. To adjust for this, for small n we compute the S_n^q on larger lattices and extrapolate to obtain the value as the lattice size approaches infinity. Specifically, we carry out the corrections for angular momentum modes $n = 0, 1\ldots, 5$ on lattices of size $N = 200 + 10\cdot i$ for $i = 0, \ldots, 49$. Denoting the lattice size as N, we fit the resulting data to

$$S_n = a + \frac{b_1}{N^2} + \frac{b_2\log N}{N^2} + \frac{c_1}{N^4} + \frac{c_2\log N}{N^4} + \frac{d_1}{N^6} + \frac{d_2\log N}{N^6} \tag{3.14}$$

and extrapolate to $N \to \infty$ to obtain the lattice-size-corrected value.

It was shown in [113] how, in the scalar theory, one may determine the leading, relevant eigenvalues of $\sqrt{X_n^r P_n^r}$ that go into determining $S^q(R)$ (see (3.12)) in a $1/n$ expansion at large n. A key point in the derivation is that the matrices K_n are

diagonal to leading order in $1/n$. The result is that the matrix $\sqrt{X_n^r P_n^r} + \frac{1}{2}$ has one eigenvalue equal to [113]

$$1 + \frac{r^2(r+1)^2}{16n^4} + O(1/n^6)\,, \tag{3.15}$$

with all other eigenvalues equal to unity to higher order in $1/n$. Similarly, the leading eigenvalue (away from zero) of the matrix $\sqrt{X_n^r P_n^r} - \frac{1}{2}$ is [113]

$$\frac{r^2(r+1)^2}{16n^4} + O(1/n^6)\,. \tag{3.16}$$

Notice that the leading-order terms in the eigenvalues are independent of the mass m.

We may calculate the $1/n$ expansion of the S_n^q by substituting the eigenvalues (3.15) and (3.16) into (3.12). The leading-order behavior of the expansion depends on whether or not $q > 1$. If $q > 1$, we find

$$S_n^q = \frac{q}{1-q}\frac{r^2(r+1)^2}{16n^4} + o(1/n^4)\,, \tag{3.17}$$

while if $q < 1$,

$$S_n^q = -\frac{1}{1-q}\left(\frac{r^2(r+1)^2}{16n^4}\right)^q + o(1/n^{4q})\,. \tag{3.18}$$

Note that when $q = 1$ there is $(\log n)/n^4$ term in the expansion, while this term is absent away from $q = 1$. To sum up, we have large n behavior of S_n^q as

$$S_n^q \sim \begin{cases} \frac{1}{n^{4q}} & q < 1 \\ \frac{1}{n^4} & q \geq 1 \end{cases}. \tag{3.19}$$

These expressions demonstrate that our numerical methods break down when $q \leq \frac{1}{4}$, since for lower values of q the sums over n are not convergent. We restrict our discussion to q greater than these critical values. Now we compute the contribution S_n^q of the n^{th} mode to the Rényi entropy:

$$S^q = S_0^q + 2\sum_{n=1}^{\infty} S_n^q \,. \tag{3.20}$$

This prescription works for integer and non-integer q, including $q < 1$. After calculating the Rényi entropy $S^q(mR)$ as a function of the dimensionless parameter mR, we calculate a renormalized quantity

$$\mathcal{F}^q(mR) = -S^q(mR) + R\,\partial_R S^q(mR) \,. \tag{3.21}$$

The renormalized Rényi entropy has the nice features of being cutoff independent and of approaching the renormalized EE [25,45] as $q \to 1$. We extract the coefficient C_{-1}^q from the $1/(mR)$ term in the large-mR expansion of this function. More specifically, we compute $\mathcal{F}^q(mR)$ over a range of mR values between 0.7 and 2.5 , and we fit this data to a function of the form

$$\mathcal{F}^q(mR) \sim \frac{\tilde{C}_{-1}^q}{mR} + \frac{\tilde{C}_{-3}^q}{(mR)^3} \,. \tag{3.22}$$

We take the $\tilde{C}_{-1}^q$ as our approximations to the C_{-1}^q. The results of these computations are shown in Fig. 3.1. We find that the numerical calculations of C_{-1}^q agree with the analytic predictions to within 3% across a broad range of q in the free theories.

We also extract the massless renormalized Rényi entropies, $S^q \equiv \mathcal{F}^q(0)$. These quantities are of interest because the massless, free theories are conformal, so each S^q may be computed analytically by mapping the computation of the Rényi entropy across the circle to the calculation of the thermal partition function on $\mathbb{H}^2$ [46,97,115].

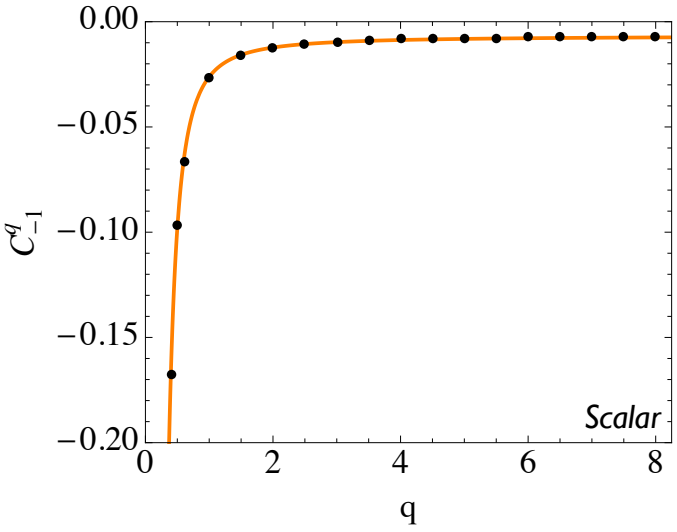

Figure 3.1: The coefficient C^q_{-1} of the $1/(mR)$ term in the large mR expansion of the Rényi entropy (see (3.91)) for the complex scalar theory. This coefficient is related to the $f_b(q)$ coefficients appearing in (3.4) in the $(3+1)$-dimensional Rényi entropy for the massless CFTs through (3.8). The orange curves show the predictions from our conjecture that $f_b(q) = f_c(q)$, with the $f_c(q)$ given in (3.5). The black points are the results of the numerical calculations. The numerical results agree with the analytic prediction to within 3% for all q.

Taking the radius of $\mathbb{H}^2$ to be R, the temperature is $1/(2\pi Rq)$. The Rényi entropy S^q is then related to the thermal free energy $F^q_{\text{therm}} = -\log|Z_q|$, where Z_q is the Euclidean partition function on $S^1 \times \mathbb{H}^2$ (the S^1 has circumference $2\pi Rq$), through the relation [97, 100]

$$S^q = \frac{qF^1_{\text{therm}} - F^q_{\text{therm}}}{1-q}\,. \tag{3.23}$$

Recently, computations [46] on $S^1 \times \mathbb{H}^2$ lead to the conjecture

$$\left(F^q_{\text{therm}}\right)^{\text{scalar}} = -\int_0^\infty d\lambda \tanh(\pi\sqrt{\lambda})\log(1-e^{-2\pi q\sqrt{\lambda}}) + q\frac{3\zeta(3)}{4\pi^2} \tag{3.24}$$

for the complex scalars . We stress that these computations involved various nontrivial elements, such as the regularization of the volume of $\mathbb{H}^2$ and the regularization of the

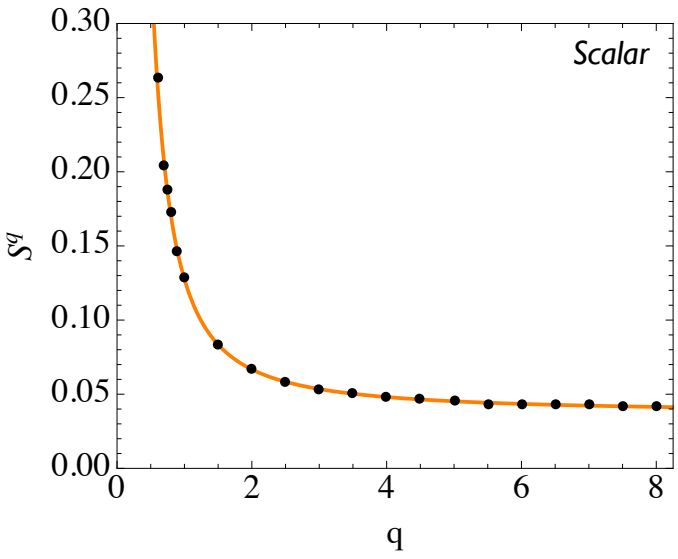

Figure 3.2: The massless Rényi entropies S^q in the free complex scalar theory as functions of the Rényi parameter q. The orange curves are the analytic predictions coming from the mapping to $S^1 \times \mathbb{H}^2$ (see (3.24)). The black points are the results of the numerical computation. We find that the numerical results agree with the analytic predictions to within 2% across all q.

sum over eigenvalues. We test these results by direct numerical computations of S^q at different values of q. In Fig. 3.2 we compare the analytic predictions (3.24) to the numerical results. Excellent agreement is seen, to within the numerical accuracy of the computation, over a wide range of q.

3.4 Calculable contributions to the perimeter law

In the previous section, we numerically calculated the renormalized Rényi entropies $\mathcal{F}^q(mR)$ across a circle of radius R in the free massive $(2+1)$-dimensional theories. We extracted the coefficients C^q_{-1} and S^q from the $\mathcal{F}^q(mR)$ and then compared the results with analytic predictions. However, there are interesting, physical aspects of the massive Rényi entropies $S^q(mR)$ that are not captured by the $\mathcal{F}^q(mR)$.

By construction, the $\mathcal{F}^q(mR)$ are not sensitive to terms in the $S^q(mR)$ that are linear in R; in particular, we cannot extract the β^q coefficients (see (3.91)) from the

renormalized Rényi entropies. In this section, we extract the β^q coefficients directly from the numerically calculated Rényi entropies.

In [116] it was conjectured, using the results in [117–119], that $\beta^1 = -1/12$ both for the massive real scalar and Dirac fermion theories. That work assumed that for a general entangling surface Σ, the β^1-term in the entanglement entropy obeys a perimeter law,

$$S_\Sigma \supset \beta^1 \, m \, \ell_\Sigma \,, \tag{3.25}$$

where ℓ_Σ is the perimeter of the entangling surface Σ. To calculate β^1, the authors chose a simple entangling geometry – the waveguide geometry – where the entanglement entropy could be calculated explicitly using the heat kernel method.

Ref. [103] checked the analytic prediction for β^1 by numerically calculating the massive entanglement entropy in the free scalar and fermion theories. Importantly, [103] used a circular entangling surface in flat spacetime. Perfect agreement was found between the numerical results and the analytic prediction. This calculation provided evidence for the perimeter-law scaling (3.25).

It is natural to ask if the β^q term in the Rényi entropy should also obey a perimeter law; if it does, then we may use the waveguide geometry to calculate the β^q explicitly. The results may then be applied to the circular geometry. The calculation in the waveguide geometry was performed in [1], and it was found that

$$\beta^q = -\frac{1+q}{24q} \tag{3.26}$$

in both the real scalar and Dirac fermion theories.

Note that $\beta^q \propto (1 + q^{-1})$ has the same q dependence as the universal term in $(1 + 1)$-dimension Rényi entropy [22–24]. This fact is not accidental, and it has a simple explanation. Using the heat kernel method, the free-field Rényi entropy in the

waveguide geometry is proportional to an appropriate integral over the heat kernel on $C_q \times S^1$, where C_q is the two-dimensional cone with deficit angle $2\pi(1-q)$ [1,116]. The heat kernel on this space factors into that on C_q and that on S^1. The two-dimensional Rényi entropy in the free theories may also be found by computing an appropriate integral over the heat kernel on C_q, and so it is not surprising that β^q inherits the same q dependence.

We check that (3.26) applies also to circular entangling surfaces in flat spacetime by generalizing the numerical calculation in [103] away from $q = 1$. For each q and each mass value m, we fit the numerically-computed Rényi entropy to the function

$$S^q = b_1^q(m)R + b_0^q(m) + b_{-1}^q(m)\frac{1}{R}\,, \tag{3.27}$$

where R is the radius of the circle. The data $b_1^q(m)$ are dominated by the UV-divergent perimeter-law term, while the β^q perimeter-law term makes a subleading contribution. To separate the two contributions, we fit the data to the function

$$b_1^q(m) = \tilde{\alpha}_2^q\, m^2 + 2\pi\tilde{\beta}^q\, m + \tilde{\alpha}_0^q\,. \tag{3.28}$$

The coefficient $\tilde{\alpha}_2^q$ accounts for finite lattice-size corrections, and $\tilde{\alpha}_0^q$ is the cutoff-dependent contribution to the perimeter law.

To further improve the numerical precision, we repeat the calculation using lattices of varying size, between $N = 200$ and $N = 350$. For each q, we fit the resulting data for $\tilde{\beta}^q$ to $\tilde{\beta}_0^q + \tilde{\beta}_1^q/N + \tilde{\beta}_2^q/N^2$. We take $\tilde{\beta}_0^q$ as our approximation to β^q. Our numerical results are compared to the prediction (3.26) in Fig. 3.3. We find that β^1 deviates from $-1/12$ by less than 0.1% in both the scalar and fermion theories. At large q the deviation from (3.26) is $\sim$2%. We emphasize that the numerical results for β^q are sensitive, at the few percent level, to the form of the fits (3.27), (3.28), and the large-N extrapolation. In particular, in Fig. 3.3 it may be seen that at large q the

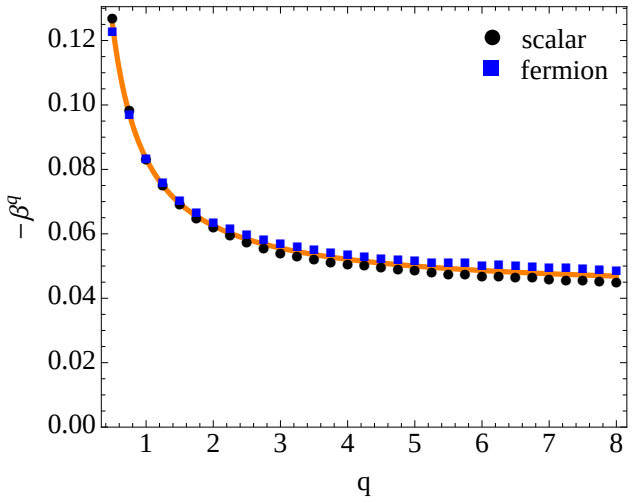

Figure 3.3: The coefficients $-\beta^q$ in the large-mR expansion of the free-field Rényi entropy (3.91). An explicit computation of the β^q in the wave-guide geometry [1] combined with the assumption that the β^q-term obeys the perimeter law, as in (3.25), leads to the analytic prediction (3.26) (solid orange) for both the real scalar and Dirac fermion theories. Our numerical results for β^1 agree with (3.26) to better than 0.1%, while the β^q at large q agree with the analytic expression to within $\sim$2%.

fermion results are systematically above the scalar ones. This gap decreases with increasing lattice size N. While the large-N extrapolation helps bring the two results into agreement, we are left with a small, residual error. Practical limitations prevent us from further increasing the lattice size.

The numerical procedures described in Sec. 3.3 were subject to less difficulty. One reason for this is that the calculations in Sec. 3.3 involved the renormalized entropies while the calculation of β^q involves the Rényi entropies directly. The process of separating the non-universal, cutoff-dominated component of the area law from the universal component is non-trivial and introduces additional lattice sensitivity. A direct, analytic calculation of the β^q for the circular entangling surface would be useful.

3.5 Rényi entropy and the modular Hamiltonian

Let us gear toward another aspect of Rènyi entropy. We begin by considering CFT Rényi entropies across spherical entangling surfaces in d flat spacetime dimensions. These quantities may be calculated from the thermal free energy on the hyperbolic space $\mathbb{H}^{d-1}$, where the temperature is $T = 1/(2\pi Rq)$, and R is the radius of $\mathbb{H}^{d-1}$, which we subsequently set to unity [21, 97]. The thermal partition function may be calculated by Wick rotating and considering the space $\mathcal{H}^d_q = S^1 \times \mathbb{H}^{d-1}$ with compactified Euclidean time:

$$ds^2_{H^d_q} = d\tau^2 + du^2 + \sinh^2 u \, d\Omega^2_{d-2} \,, \qquad \tau \sim \tau + 2\pi q \,. \tag{3.29}$$

When $q = 1$, we define $\mathcal{H}^d \equiv \mathcal{H}^d_{q=1}$. Defining $\mathcal{F}_q = -\log Z_q$, with Z_q the Euclidean partition function on $\mathcal{H}^d_q$, the Rényi entropy is given by

$$S_q = \frac{q\mathcal{F}_1 - \mathcal{F}_q}{1-q} \,. \tag{3.30}$$

The partition function on $\mathcal{H}^d_q$ is naturally written as

$$Z_q = \mathrm{tr}\left(e^{-2\pi q H_\tau}\right) \,, \tag{3.31}$$

where H_τ is the Hamiltonian that generates translations along the S^1. Using this relation, it was pointed out in [98] that derivatives of S_q with respect to q generate connected correlation functions of H_τ. In particular, expanding S_q in the vicinity of $q = 1$ leads to

$$S_q = S_1 + 2\pi \sum_{n=1}^{\infty} \frac{1}{(n+1)!} \, \partial^n_q E_q\Big|_{q=1} (q-1)^n \,, \qquad S_1 = -\mathcal{F}_1 + E_1 \,, \tag{3.32}$$

where $E_q = \langle H_\tau \rangle_q$. The subscript q is a reminder that the expectation value is to be computed at inverse temperature $2\pi q$. We may further simplify (3.32) by writing

$$\partial_q^n E_q \Big|_{q=1} = (-1)^n (2\pi)^n \langle \underbrace{H_\tau H_\tau \cdots H_\tau}_{n+1} \rangle_{q=1}^{\text{conn}} . \tag{3.33}$$

The Hamiltonian H_τ is simply related to the stress tensor, $H_\tau = \int_{\mathbb{H}^{d-1}} d^{d-1}x \sqrt{g} T_{\tau\tau}$. Because the field theory is conformally invariant, it is natural to assume that the stress tensor is the conformal one. We will show that this statement depends on the boundary conditions at infinity. One particularly important exceptional theory is that of the free conformally coupled scalar field. For the scalar to be conformal, we need to add a conformal mass term to the Lagrangian: $\mathcal{L} \supset \frac{d-2}{8(d-1)} \sqrt{g} \mathcal{R} \phi^2$. Note that on $\mathcal{H}_q^d$ the curvature scalar is given by $\mathcal{R} = -(d-2)(d-1)$. This term contributes to the stress tensor in two ways: (1) there is a contribution to $T_{\tau\tau}$ that comes from varying $\sqrt{g}$, and (2) there is a contribution that arises from varying $\mathcal{R}$. The second contribution leads to $T_{\tau\tau} \supset \nabla^2 \phi^2$, where the Laplacian is only over the coordinates on $\mathbb{H}^{d-1}$. It is important to remember that in deriving this term, one must integrate by parts on $\mathbb{H}^{d-1}$. Here, the boundary conditions on the hyperbolic space become important.

Following the normal procedure leads to the conformal stress tensor[3]

$$T_{\tau\tau}^{\text{conf}} = (\partial_\tau \phi)^2 - \frac{1}{2} \partial_\mu \phi \partial^\mu \phi + \frac{(d-2)}{8(d-1)} \mathcal{R} \phi^2 + \frac{d-2}{4(d-1)} \nabla^2 \phi^2 . \tag{3.34}$$

We will show that for the scalar theory, when we regularize the space $\mathcal{H}_q^d$ by putting a cutoff at infinity, it is in fact what we call the "non-conformal" stress tensor

$$T_{\tau\tau} = (\partial_\tau \phi)^2 - \frac{1}{2} \partial_\mu \phi \partial^\mu \phi + \frac{(d-2)}{8(d-1)} \mathcal{R} \phi^2 \tag{3.35}$$

[3]Note that since the metric is a direct product of $S^1 \times \mathbb{H}^{d-1}$, $\mathcal{R}_{\tau\tau} = 0$

that enters into H_τ.[4] This stress tensor can be thought of as arising from not integrating the variation of the curvature scalar by parts.

Because these two stress tensors differ only by a total derivative, it may appear that this difference does not affect H_τ. This is in fact not the case, since we are introducing a boundary at some large value of the u coordinate, which we call u_0 [21]. Note that u_0 is related to the UV cutoff ϵ of the theory through the relation $\epsilon \sim e^{-u_0}$. In particular, the regularized volume of the hyperbolic space is found by subtracting off the power-law divergences in ϵ from the integral

$$\mathrm{Vol}(\mathbb{H}^{d-1}) = \mathrm{Vol}(S^{d-2}) \int_0^{u_0} du \sinh^{d-2} u \,. \tag{3.36}$$

This leads to the result [21, 100, 120]

$$\mathrm{Vol}(\mathbb{H}^{d-1}) = (-1)^{\lfloor \frac{d}{2} \rfloor} \frac{\pi^{\frac{d-2}{2}}}{\Gamma(\frac{d}{2})} \begin{cases} \pi \,, & d \text{ odd} \\ -2\log(R/\epsilon) \,, & d \text{ even} \,. \end{cases} \tag{3.37}$$

Note that in even-dimensional theories, the $\log \epsilon$ dependence of the Rényi entropy arises through the regularized volume of $\mathbb{H}^{d-1}$.

3.5.1 Boundary conditions and entanglement: singular vs. regularized cone

For certain theories, there is an ambiguity in the definition of the EE. In the replica trick method [121], the EE is defined through a partition function on a conically singular manifold. There is infinite curvature concentrated at the tip that needs to be regulated. The ambiguity arises from the fact that one can do so in (at least) two different ways: we refer to these as the "singular cone" and the "regularized cone".

[4] Due to the presence of the curvature term in (3.35), this is not the same thing as the "unimproved" stress tensor.

This is similar in spirit to the ambiguities that arise when trying to separate the Hilbert spaces of gauge theories in the lattice (see [122] and references therein).

In the singular cone, one places a hard-wall at a fixed distance ϵ from the singularity [121]. Note that this space has $\mathcal{R} = 0$ and a boundary. In the regularized cone, we can instead smooth out the singularity as we get closer to the tip [119]. To do this, one changes the metric such that near the tip the space is locally flat, but far from the tip the metric is unchanged. The regularized cone has $\mathcal{R}^{reg}(q) \neq 0$ and no boundary.

The singular cone and the regularized cone have natural interpretations in terms of how we treat the boundary of the space $\mathcal{H}_q^d$ [123]. In the first case, we simply cut the space off at some large value for the u coordinate u_0. In the second case, we take $T^{-1} = 2\pi q$ at small u, but then we "regulate" the spacetime so that at large u, the inverse temperature reverts to $T^{-1} = 2\pi$. In the first case, the curvature scalar is simply $\mathcal{R} = -(d-2)(d-1)$, independent of q, while in the latter case the curvature receives q-dependent corrections $\mathcal{R}^{reg}(q)$ at large u.[5]

In many situations, the method used to regulate the cone/$\mathcal{H}_q^d$/Rindler space does not affect physical quantities. However, the choice of regularization *does* affect theories for which $\delta S/\delta\partial g \neq 0$. In these cases, one must integrate by parts to derive the stress tensor. If we are using the singular cone method, we must be careful when integrating by parts, since the spaces have boundaries.

This discussion is reminiscent of computations of quantum black hole entropy via the conical singularity method. In [124], the contribution of quantum fields to black hole entropy was considered. The usual way to compute black hole entropy [125] consists of evaluating the gravitational action as a function of the temperature and then taking derivatives with respect to the temperature. This prescription, in

[5]Note that if we were working in Rindler space, which is conformally equivalent to $\mathcal{H}_q^d$ [21], the regularized cone method maps to the regularized manifold described in [119], which does not have a boundary.

which we have a family of smooth geometries labeled by the temperature, can be thought of as being analogous to the regularized cone. When computing the quantum contribution to the black hole entropy from conformal scalars near a black hole (and trying to express it as EE), there is a "contact term" on the horizon. This can be understood as the Wald entropy due to the quantum fields, coming from their direct coupling to curvature of the regularized cone: in other words, $S_{BH} = S_{EE} + \langle S_{wald} \rangle$. This type of term also appears in the contribution of bulk quantum fields to $1/N$-corrected holographic EE [126, 127]. In this case, the prescription is to compute bulk EE across the Ryu-Takayanagi surface, supplemented by possible Wald-type terms.

Returning to Rényi entropy, the previous discussion makes clear that the definition of the Hamiltonian H_τ is sensitive to the choice of regularization. In the scalar theory, working on the singular cone gives the non-conformal stress tensor $T_{\tau\tau}$, while the regularized cone gives the conformal stress tensor $T^{\text{conf}}_{\tau\tau}$, as will be discussed. This is because if we are in the regularized cone, we can integrate by parts without problems, while additional boundary terms arise when integrating by parts in the singular cone [123].

With regard to computing EE and Rényi entropy, one might be tempted to ask, "which regularization of the cone should we use?" The singular cone is the regularization appropriate for the conventional definition of EE. For example, we will see that the singular cone method matches the results of lattice calculations of Rényi and EE as well as previous analytic calculations of these quantities, while the regularized cone method does not. Accordingly, in taking q-derivatives as in (3.32), we should be using the non-conformal stress tensor in our definition of H_τ.

3.5.2 Warmup: stationarity on $S^1 \times \mathbb{H}^2$

There is a straightforward example that illustrates the fact that it is the non-conformal stress tensor $T_{\tau\tau}$ that enters into the Hamiltonian for the scalar field. We consider

the connected two-point function

$$\int_{\mathcal{H}^3} d^3x\sqrt{g(x)}\langle H_\tau\phi^2(x)\rangle_{q=1}^{\text{conn}} = \int_{\mathcal{H}^3} d^3x\sqrt{g(x)}\int_{\mathbb{H}^2} d^2y\sqrt{g(y)}\langle T_{\tau\tau}(y)\phi^2(x)\rangle_{q=1}^{\text{conn}}\,. \quad (3.38)$$

If $T_{\tau\tau}$ were the conformal stress tensor, then this quantity would vanish, since

$$\langle T_{\tau\tau}^{\text{conf}}(y)\phi^2(x)\rangle_{q=1} = 0 = \langle\phi^2(x)\rangle_{q=1}\,. \quad (3.39)$$

This follows from the fact that $\mathcal{H}^3$ is related to flat space by a conformal transformation, and the two-point function of the conformal stress tensor with a primary operator in flat space vanishes, along with the one-point function of the primary operator. This argument is used in [128] in the general context of perturbations of EE by the addition of relevant operators, but as we see here, the situation is more subtle.

We may calculate the quantity in (3.38) by calculating the partition function of the massive scalar field on $\mathcal{H}^3_q$. The action of the theory is given by

$$I = \int_{\mathcal{H}^3_q} d^3x\sqrt{g}\left[\frac{1}{2}(\partial_\mu\phi)^2 - \frac{1}{8}\phi^2 + \frac{m^2}{2}\phi^2\right], \quad (3.40)$$

so that when $m^2 = 0$ the theory is conformal. The Euclidean free energy $\mathcal{F}_q(m^2)$ of this theory was calculated as a function of m^2 and q in [46]:

$$\mathcal{F}_q(m^2) = \int_0^\infty d\lambda\mathcal{D}(\lambda)\left[\log\left(1 - e^{-2\pi q\sqrt{\lambda+m^2}}\right) + \pi q\sqrt{\lambda+m^2}\right], \quad (3.41)$$

with the density of states given by

$$\mathcal{D}(\lambda)d\lambda = \frac{\text{Vol}(\mathbb{H}^2)}{4\pi}\tanh(\pi\sqrt{\lambda})d\lambda\,. \quad (3.42)$$

Note that λ parameterizes the eigenvalues of the $m^2 = 0$ Laplacian on $\mathbb{H}^2$.

The two-point function in (3.38) is related to $\mathcal{F}_q(m^2)$ through the equation

$$\int_{\mathcal{H}^3} d^3x\sqrt{g(x)}\langle H_\tau\phi^2(x)\rangle^{\rm conn}_{q=1} = -\frac{1}{\pi}\,\partial_q\partial_{m^2}\mathcal{F}_q(m^2)\Big|_{q=1,m^2=0}\,. \tag{3.43}$$

The resulting integral is UV divergent, but we may regularize the integral through a cut-off in $\lambda \sim 1/\tilde{\epsilon}^2$. The scaling follows from the fact that λ has mass dimension two. Then,

$$\begin{aligned}\int_{\mathcal{H}^3} d^3x\sqrt{g(x)}\langle H_\tau\phi^2(x)\rangle^{\rm conn}_{q=1} &= \frac{1}{4}\int_0^{1/\tilde{\epsilon}} d\lambda\frac{1}{\sqrt{\lambda}} - \pi\int_0^\infty d\lambda{\rm csch}(2\pi\sqrt{\lambda}) \\ &= \frac{1}{2\tilde{\epsilon}} - \frac{\pi}{16}\end{aligned} \tag{3.44}$$

The fact that the finite, $\tilde{\epsilon}$-independent term above is non-vanishing tells us that H_τ is computed from the non-conformal $T_{\tau\tau}$.

We may understand this fact is a somewhat more illuminating way by an explicit computation of $\langle H_\tau\int\phi^2\rangle^{\rm conn}_{q=1}$. Because of (3.39), we only have to compute $\langle(\nabla^2\phi^2)\int\phi^2\rangle^{\rm conn}_{q=1}$:

$$\begin{aligned}\int_{\mathcal{H}^3} d^3x\sqrt{g(x)}\langle H_\tau\phi^2(x)\rangle^{\rm conn}_{q=1} &= -\frac{1}{8}{\rm Vol}(\mathbb{H}^2)\int_0^\infty du\sinh u \\ &\qquad \int_0^{2\pi} d\phi_0\int_0^{2\pi} d\tau\langle\nabla^2\phi^2(0)\phi^2(u,\phi_0,\tau)\rangle^{\rm conn}_{q=1} \\ &= -\int_0^\infty du\sinh u\int_0^{2\pi} d\tau\frac{\cos\tau\cosh u - 1}{16(\cos\tau-\cosh u)^3} \\ &= -\frac{\pi}{16}\,.\end{aligned} \tag{3.45}$$

where ϕ_0 is the $\mathbb{H}^2$ angular coordinate. Note that we have used translation invariance to place the first ϕ^2 at the origin and factor out a regulated volume of the hyperbolic space. The regulated volume also introduces a UV divergent term, but the important observation is that the finite term above matches that in (3.44). In computing (3.45),

we explicitly used the propagator for the scalar field on $\mathcal{H}^3$:

$$\langle\phi(u_1,\phi_1,\tau_1)\phi(u_2,\phi_2,\tau_2)\rangle_{q=1} = \frac{1}{4\pi\sqrt{2\cosh(u_1)\cosh(u_2)-2\cos(\phi_1-\phi_2)\sinh(u_1)\sinh(u_2)-2\cos(\tau_1-\tau_2)}}\,. \tag{3.46}$$

An alternative way to evaluate (3.43) is to calculate $\langle\phi^2\rangle_q$ at finite q in the $m^2 = 0$ CFT. The calculation of $\langle\phi^2\rangle_q$ was performed in [129], where it was found that $4\pi\langle\phi^2\rangle_q = -(q-1)\frac{\pi}{8}$. Then, a straightforward calculation leads again to the result in (3.44):

$$-\frac{1}{\pi}\,\partial_q\partial_{m^2}\mathcal{F}_q(m^2)\Big|_{q=1,m^2=0} = -\mathrm{Vol}(\mathbb{H}^2)\partial_q\langle\phi^2\rangle_q = -\frac{\pi}{16}\,. \tag{3.47}$$

3.6 The Rényi entropy near $q = 1$

In this section we calculate the Rényi entropy perturbatively in q, near $q = 1$, using the formalism of Sec. 3.5. We begin by discussing $S'_{q=1}$ and then we discuss $S''_{q=1}$. Throughout this section, we will work in an arbitrary spacetime dimension d, unless otherwise stated.

3.6.1 $S'_{q=1}$ and the two-point function of H_τ

We may calculate $S'_{q=1}$ using (3.32) and (3.33):

$$S'_{q=1} = -2\pi^2\langle H_\tau H_\tau\rangle^{\mathrm{conn}}_{q=1}\,. \tag{3.48}$$

Then, using the relation between H_τ and $T_{\tau\tau}$ and translation invariance, we may write

$$S'_{q=1} = -2\pi^2\mathrm{Vol}(\mathbb{H}^{d-1})\int_{\mathbb{H}^{d-1}} d^{d-1}x\sqrt{g}\langle T_{\tau\tau}(0)T_{\tau\tau}(x)\rangle^{\mathrm{conn}}_{q=1}\,. \tag{3.49}$$

For now, we assume that $T_{\tau\tau}$ is simply the conformal stress tensor, with no additional boundary terms, and we use conformal invariance to evaluate the integral above. This calculation was performed in [98], where it was shown that

$$S'_{q=1} = -\mathrm{Vol}\Big(\mathbb{H}^{d-1}\Big)\frac{\pi^{d/2+1}\Gamma(d/2)(d-1)}{(d+1)!}C_T\,. \tag{3.50}$$

C_T is the coefficient of the stress-tensor two-point function, whose normalization we define shortly. We will re-derive (3.50) from a perspective that will be useful when calculating $S''_{q=1}$. Then, we will address the scalar theory, for which $T_{\tau\tau}$ has additional boundary terms.

Note that in (3.49) we are free to choose arbitrary values for the Euclidean times of the two stress tensors. We will fix the first stress tensor to be at $\tau_1 = 0$, and we let $\tau_2 = \tau$ be arbitrary for the second stress tensor. We will then see explicitly that the final result does not depend on τ.

The connected correlation functions on $\mathcal{H}^d$ may be calculated by utilizing a conformal transformation between that space and flat $\mathbb{R}^d$ [21]. Writing

$$ds^2_{\mathbb{R}^d} = dt^2 + dr^2 + r^2 d\Omega^2_{d-2}\,, \tag{3.51}$$

it may be verified that the coordinate transformation

$$t = \frac{\sin\tau}{\cosh u + \cos\tau}\,, \qquad r = \frac{\sinh u}{\cosh u + \cos\tau} \tag{3.52}$$

conformally maps $\mathbb{R}^d$ to $\mathcal{H}^d$:

$$ds^2_{\mathbb{R}^d} = \Omega^2 ds^2_{\mathcal{H}^d}\,, \qquad \Omega = \frac{1}{\cosh u + \cos\tau}\,. \tag{3.53}$$

The conformal stress tensor transforms simply under the conformal transformation;

$$T_{\alpha\beta}(x) = \tilde{T}_{\alpha\beta}(x) + S_{\alpha\beta}(x)\,, \qquad \tilde{T}_{\alpha\beta}(x) \equiv \Omega^{d-2}\frac{dX^a}{dx^\alpha}\frac{dX^b}{dx^\beta}T_{ab}(X)\,, \tag{3.54}$$

where the x^μ are coordinates on $\mathcal{H}^d$ and the X^a are coordinates on $\mathbb{R}^d$. The stress tensor $T_{ab}(X)$ is that in flat spacetime. The tensor $S_{\alpha\beta}(x)$ is an anomalous term that vanishes in odd d, while in even d, $S_{\alpha\beta}(x) = \langle T_{\alpha\beta}(x)\rangle_{\mathcal{H}^d}$.

In both even and odd dimensions d, connected correlation functions of $T_{\alpha\beta}(x)$ on $\mathcal{H}^d$ are equal to connected correlation functions of $\tilde{T}_{\alpha\beta}(x)$ in flat spacetime. This is trivial in odd d, since in that case the anomalous term vanishes, while in even d this may be verified through a direct calculation [98].

Using (3.49) and (3.54), we find that

$$\begin{aligned} S'_{q=1} = -\frac{2\pi^2}{2^d}\mathrm{Vol}\big(\mathbb{H}^{d-1}\big)\mathrm{Vol}(S^{d-2})\int_0^\infty du\,\sinh^{d-2}u\,\Bigg[\Big(\frac{1}{\cos\tau+\cosh u}\Big)^{d+2} \\ \Big((1+\cos\tau\cosh u)^2\langle T_{tt}(0)T_{tt}(t,r)\rangle_{\mathbb{R}^d} \\ +2\sin\tau\sinh u(1+\cos\tau\cosh u)\langle T_{tt}(0)T_{tr}(t,r)\rangle_{\mathbb{R}^d} \\ +\sin^2\tau\sinh^2 u\langle T_{tt}(0)T_{rr}(t,r)\rangle_{\mathbb{R}^d}\Big)\Bigg]\,, \end{aligned} \tag{3.55}$$

where t and r are related to τ and u through (3.52). The flat-space two-point functions of conformal stress tensors are given by [130]

$$\langle T_{ab}(0)T_{cd}(x)\rangle = C_T\frac{I_{ab,cd}(x)}{x^{2d}}\,, \tag{3.56}$$

where

$$I_{ab,cd}(x) = \frac{1}{2}\left(I_{ac}(x)I_{bd}(x) + I_{ad}(x)I_{bc}(x)\right) - \frac{1}{d}\delta_{ab}\delta_{cd}\,, \qquad I_{ac}(x) = \delta_{ac} - 2\frac{x_a x_c}{x^2}\,. \tag{3.57}$$

Equation (3.55) simplifies considerably if we take $\tau = \pi$, for then we only need the two-point function $\langle T_{tt}(0)T_{tt}(0,r)\rangle_{\mathbb{R}^d}$. With this specific choice of τ, it is straightforward to verify (3.50) for all dimensions d. With arbitrary τ, it is more illuminating to work in a specific dimension d, as otherwise the equations are cumbersome. The simplest example is $d = 2$. In this case, (3.55) becomes

$$S'_{q=1} = -C_T \frac{\pi^2}{2} \log(R/\epsilon) \int_0^\infty du \left(\frac{1}{\cos\tau - \cosh u}\right)^4 \Big(\cos(2\tau)\cosh(2u) - 4\cos\tau\cosh u + 3\Big)\,. \tag{3.58}$$

It is interesting to study the behavior of the integrand above near $u = 0$. The leading term is $\mathcal{O}\big(u^0\big)$, and the coefficient is proportional to $\sin(\tau/2)^{-4}$. So long as $\tau \neq 0, 2\pi$, the expansion near $u = 0$ is well behaved. If $\tau = 0$ or 2π, on the other-hand, then the integrand $\propto u^{-4}$ near $u = 0$, and the integral does not converge. Restricting $\tau \neq 0, 2\pi$, we may perform the integral in (3.58) explicitly, and we find

$$S'_{q=1} = -\frac{\pi^2}{3} C_T \log(R/\epsilon)\,, \tag{3.59}$$

independent of τ, and consistent with (3.50). We learn that we should be careful to avoid taking the different stress-energy tensors inside the correlators at coincident Euclidean times, otherwise we may find divergences. We will see explicitly that the same phenomenon is realized in the calculation of $S''_{q=1}$.

3.6.2 $S''_{q=1}$ and the three-point function of H_τ

The calculation of $S''_{q=1}$ is more complicated than that of $S'_{q=1}$, primarily because the three-point function of stress-energy tensors is less constrained than the two-point function. We make the choices $\tau_1 = 0$ and $\tau_2 = \pi$ for the first two stress tensors, but we leave $\tau_3 = \tau$ arbitrary. Our final result for $S''_{q=1}$ should be independent of τ, which

serves as a consistency check. We may then write

$$\begin{aligned} S''_{q=1} = & \frac{8\pi^3}{3\,2^d}\mathrm{Vol}\Big(\mathbb{H}^{d-1}\Big)\mathrm{Vol}(S^{d-2})\mathrm{Vol}(S^{d-3}) \\ & \int_0^\infty du \int_0^\infty dv \int_0^\pi d\theta \sin^{d-3}\theta \sinh^{d-2} u \sinh^{d-2} v \left[\left(\frac{1}{\cos\tau + \cosh u}\right)^{d+2}\right. \\ & \left(\frac{1}{\cosh v - 1}\right)^d \Big((1+\cos\tau\cosh u)^2 \langle T_{tt}(0)T_{tt}(0,r')T_{tt}(t,r)\rangle^{\mathrm{conn}}_{\mathbb{R}^d} \\ & +2\sin\tau\sinh u(1+\cos\tau\cosh u)\langle T_{tt}(0)T_{tt}(0,r')T_{tr}(t,r)\rangle^{\mathrm{conn}}_{\mathbb{R}^d} \\ & \left.+\sin^2\tau\sinh^2 u\langle T_{tt}(0)T_{tt}(0,r')T_{rr}(t,r)\rangle^{\mathrm{conn}}_{\mathbb{R}^d}\Big)\right] , \end{aligned} \tag{3.60}$$

where t and r are again given by (3.52), and $r' = \sinh v/(\cosh v - 1)$. We begin by considering the theory in $d = 2$, where the three-point function takes a simple form.

Warmup: $d = 2$

In complex coordinates $(z, \bar{z}) = (t + ir, t - ir)$, the three-point functions in $d = 2$ are given by

$$\langle T(0)T(z_1)T(z_2)\rangle^{\mathrm{conn}} = \frac{c}{z_1^2 z_2^2 (z_1 - z_2)^2}\,, \qquad \langle \bar{T}(0)\bar{T}(\bar{z}_1)\bar{T}(\bar{z}_2)\rangle^{\mathrm{conn}} = \frac{c}{\bar{z}_1^2 \bar{z}_2^2 (\bar{z}_1 - \bar{z}_2)^2}\,, \tag{3.61}$$

where c is the central charge. Here, $T(z) = 2\pi T_{zz}$ and $T(\bar{z}) = 2\pi T_{\bar{z}\bar{z}}$, while $T_{z\bar{z}} = 0$ by conformal symmetry. We may relate the specific three-point functions appearing in (3.60) to the ones above through

$$\begin{aligned} \langle T_{tt}(0)T_{tt}(0,r')T_{tt}(t,r)\rangle^{\mathrm{conn}}_{\mathbb{R}^2} &= -\langle T_{tt}(0)T_{tt}(0,r')T_{rr}(t,r)\rangle^{\mathrm{conn}}_{\mathbb{R}^2} \\ &= \frac{\langle T(0)T(w)T(z)\rangle^{\mathrm{conn}} + \langle \bar{T}(0)\bar{T}(\bar{w})\bar{T}(\bar{z})\rangle^{\mathrm{conn}}}{(2\pi)^3}\,, \\ \langle T_{tt}(0)T_{tt}(0,r')T_{tr}(t,r)\rangle^{\mathrm{conn}}_{\mathbb{R}^2} &= i\frac{\langle T(0)T(w)T(z)\rangle^{\mathrm{conn}} - \langle \bar{T}(0)\bar{T}(\bar{w})\bar{T}(\bar{z})\rangle^{\mathrm{conn}}}{(2\pi)^3}\,, \end{aligned} \tag{3.62}$$

Using (3.62), (3.61), and (3.60), we find

$$S''_{q=1} = \frac{c\log(R/\epsilon)}{6}\frac{1}{4}\int_{-\infty}^{\infty} du \int_{-\infty}^{\infty} dv \\ \frac{2\cos\tau\Big(\cosh(v-u)-\cosh(u)\Big) - \cos 2\tau\cosh(v-2u) - \cosh v + 2}{\cosh^2(v/2)\Big(\cos\tau+\cosh(v-u)\Big)^2(\cos\tau-\cosh u)^2}\,. \tag{3.63}$$

The integral is convergent so long as $\tau \neq 0, \pi, 2\pi$. That is, we are not allowed to take coincident Euclidean times for any of the stress-energy tensors. If $\tau = 0, 2\pi$, the integrand is ill-behaved at $u = 0$; if $\tau = \pi$, the integral diverges along the line $v = u$. Restricting τ to lie away from these three points, we may integrate (3.63) exactly, and we find

$$S''_{q=1} = \frac{c}{3}\log(R/\epsilon)\,. \tag{3.64}$$

This is independent of τ. It is furthermore consistent with the known $d = 2$ formula[6]

$$S_q = \frac{c}{6}\left(1+\frac{1}{q}\right)\log(R/\epsilon)\,. \tag{3.65}$$

$S''_{q=1}$ in general d

In general dimension d, we may still evaluate (3.60) explicitly because the three-point functions of stress tensors in flat space are fixed by conformal invariance up to three theory-dependent coefficients, which we label as $\mathcal{A}$, $\mathcal{B}$, and $\mathcal{C}$, following the notation of [130, 131]:

$$\langle T_{\mu\nu}(x)T_{\rho\sigma}(y)T_{\alpha\beta}(z)\rangle^{\text{conn}}_{\mathbb{R}^d} = \frac{I_{\mu\nu,\mu'\nu'}(x-z)I_{\rho\sigma,\rho'\sigma'}(y-z)}{|x-z|^{2d}\,|y-z|^{2d}} t_{\mu'\nu',\rho'\sigma',\alpha\beta}(Z)\,. \tag{3.66}$$

[6]Note that (3.65) is also consistent with (3.59) upon setting $C_T = c/(2\pi^2)$.

Here, $t_{\mu'\nu',\rho'\sigma',\alpha\beta}(Z)$ is a tensor structure depending on the coefficients $\mathcal{A}$, $\mathcal{B}$, and $\mathcal{C}$ [131], and

$$Z_\mu = \frac{(x-z)_\mu}{(x-z)^2} - \frac{(y-z)_\mu}{(y-z)^2}\,. \tag{3.67}$$

As may be seen in (3.60), we need three types of three-point functions of stress tensors, differing by the stress-tensor indices. The simplest three-point function takes the form

$$\langle T_{tt}(x)T_{tt}(y)T_{tt}(z)\rangle^{\text{conn}}_{\mathbb{R}^d} = \frac{1}{|x-z|^{2d}\,|y-z|^{2d}}\frac{8(\mathcal{A}+\mathcal{C})-(10\mathcal{A}+\mathcal{B}+10\mathcal{C})d+4\mathcal{A}d^2}{(Z^2)^{\frac{d}{2}}4d^2}\,, \tag{3.68}$$

Using (3.66) and following the definition of $t_{\mu'\nu',\rho'\sigma',\alpha\beta}(Z)$ in [131], we find another two three-point functions

$$\begin{aligned}\langle T_{tt}(x)T_{tt}(y)T_{ti}(z)\rangle^{\text{conn}}_{\mathbb{R}^d} = \frac{1}{|x-z|^{2d}\,|y-z|^{2d}}\frac{1}{4d^3}\frac{\hat{Z}_t\hat{Z}_i}{(Z^2)^{\frac{d}{2}}}\{&2\mathcal{A}(-4+d(4+d((-1+d)^2\\ &+(-2+d)^2(2+d)\hat{Z}_i\hat{Z}_t-(-2+d)^2(2+d)\hat{Z}_t^2)))\\ &+\mathcal{B}(4+d(2+d(-2-d+2(-4+d^2)\hat{Z}_i\hat{Z}_t+4(2+d-d^2)\hat{Z}_t^2\\ &+(-2+d)d(4+d)\hat{Z}_t^4)))\\ &-2\mathcal{C}(8+d(12+d(-4+3d+4(-4+d^2)\hat{Z}_i\hat{Z}_t\\ &-2(8+d(-2+3d))\hat{Z}_t^2+d(8+d(2+d))\hat{Z}_t^4)))\}\end{aligned} \tag{3.69}$$

$$\langle T_{tt}(x)T_{tt}(y)T_{ij}(z)\rangle^{\text{conn}}_{\mathbb{R}^d} = \frac{1}{4d^3\,|x-z|^{2d}\,|y-z|^{2d}\,(Z^2)^{\frac{d}{2}}}$$
$$\Big\{d\hat{Z}_i\hat{Z}_j(2\mathcal{A}(-8+d^2+(-2+d)^2d(2+d)\hat{Z}_t^2)$$
$$+\mathcal{B}d(10-2d-d^2+(-2+d)(4+d(6+d))\hat{Z}_t^2)$$
$$+2\mathcal{C}(-8+d(2+16\hat{Z}_t^2+d(4+d-(2+d)(4+d)\hat{Z}_t^2))))$$
$$+\delta_{ij}\{\mathcal{B}d(-2+(-2+d)d(1-(-2+d)\hat{Z}_t^2))$$
$$+2\mathcal{A}(8+d(12-3d-2d^2+(-2+d)(8+d(8+3d))\hat{Z}_t^2))$$
$$+2\mathcal{C}(8+d(2+4d-d^2+(-16+d(4+(-10+d)d))\hat{Z}_t^2))\}\,, \tag{3.70}$$

where $\hat{Z}_t = \frac{Z_t}{|Z|}$, $\hat{Z}_i = \frac{Z_i}{|Z|}$.

We then proceed by substituting the explicit three-point functions into (3.60) and performing the integrals over u, v, and θ. While the intermediate steps involve complicated evaluations, the final result is a simple expression in terms of $\mathcal{A}$, $\mathcal{B}$, and $\mathcal{C}$:

$$S''_{q=1} = \frac{4\pi^{d+1}}{3d^3(d+2)\Gamma(d-1)}\text{Vol}(\mathbb{H}^{d-1})\left((4d^2-10d+8)\mathcal{A} - d\,\mathcal{B} - (10d-8)\mathcal{C}\right)\,. \tag{3.71}$$

3.6.3 Explicit checks of $S''_{q=1}$

In this subsection we explicitly calculate $S''_{q=1}$ in a variety of examples where S_q is known for general q, and we compare the resulting expressions with the perturbative results of the last subsection. The same check was performed in [98] for $S'_{q=1}$, with agreement in all cases considered. We consider both free theories and theories with holographic duals in a variety of dimensions. We find agreement in all examples except those involving free scalar fields. As already mentioned, the free scalar fields are more complicated because in that case $T_{\tau\tau}$ has additional boundary contributions. We discuss the free scalar theory in the following subsection.

Theories with gravitational duals

Consider CFTs in arbitrary dimension d that admit holographic limits with Einstein gravity duals, for simplicity. The bulk action is taken to be

$$S = \frac{1}{2\ell_p^{d-1}} \int d^{d+1}x\sqrt{-g}(R + 2\Lambda)\,. \tag{3.72}$$

The 3-point function coefficients $\mathcal{A}, \mathcal{B}, \mathcal{C}$ for such theories at strong coupling were computed holographically in [132]:

$$\begin{aligned}
\mathcal{A}_{\rm Ein}(d) &= -\frac{1}{2\ell_p^{d-1}} \frac{2d^4\Gamma(d)}{\pi^d(d-1)^3} \\
\mathcal{B}_{\rm Ein}(d) &= -\frac{1}{2\ell_p^{d-1}} \frac{2d^2(d^3-d^2+1)\Gamma(d)}{\pi^d(d-1)^3} \\
\mathcal{C}_{\rm Ein}(d) &= -\frac{1}{2\ell_p^{d-1}} \frac{d^3(2d^2-2d-1)\Gamma(d)}{2\pi^d(d-1)^3}\,.
\end{aligned} \tag{3.73}$$

Substituting these expressions into (3.71), one finds

$$S''_{q=1} = \mathrm{Vol}(\mathbb{H}^{d-1}) \frac{1}{2\ell_p^{d-1}} \frac{4\pi(4d^2-8d+3)}{3(d-1)^2}\,. \tag{3.74}$$

We now compare this to the non-perturbative result for S_q, obtained holographically in [97]. Because the calculation can be mapped to a thermal free energy calculation on $\mathcal{H}^d_q$, at strong coupling one can compute the free energy of the dual black hole spacetimes. These are asymptotically AdS black hole solutions of Einstein gravity with hyperbolic spatial slices and continuously tunable temperature $T^{-1} = 2\pi q$. With the asymptotic AdS radius set to unity, one finds [97]

$$S_q = \frac{\pi q}{q-1} \mathrm{Vol}(\mathbb{H}^{d-1}) \frac{1}{\ell_p^{d-1}} \left(2 - x_q^d - x_q^{d-2}\right)\,, \tag{3.75}$$

where x_q, the radial position of the horizon as a function of q, is defined as

$$x_q = \frac{1}{qd}\left(1 + \sqrt{1 - 2dq^2 + d^2q^2}\right) . \tag{3.76}$$

Taking two derivatives of (3.75) at $q = 1$, one recovers (3.74).

Free fields

The values of $(\mathcal{A}, \mathcal{B}, \mathcal{C})$ for free fields can be found in [130, 131]. Substituting these values into (3.71), we obtain the following results. For Dirac fermions, we find

$$\partial_q^2 S^D_{q=1} = (-2)^{-\lfloor \frac{d}{2} \rfloor} \sqrt{\pi}\Gamma\left(\frac{d}{2}\right) \frac{(d - \frac{2}{3})}{d(d+2)\Gamma\left(\frac{d-1}{2}\right)} \begin{cases} \pi\,, & d \text{ odd} \\ -4\log(R/\epsilon)\,, & d \text{ even}\,, \end{cases} \tag{3.77}$$

while for complex scalars,

$$\partial_q^2 \tilde{S}^S_{q=1} = (-1)^{\lfloor \frac{d}{2} \rfloor} \Gamma^2\left(\frac{d}{2}\right) \frac{15d^3 - 48d^2 + 52d - 16}{6(d-1)^2(d+2)\Gamma(d+1)} \begin{cases} \pi\,, & d \text{ odd} \\ -2\log(R/\epsilon)\,, & d \text{ even}\,. \end{cases} \tag{3.78}$$

Note that we have given the scalar-field predictions above an extra tilde. This is to distinguish these results, which come from the general formula (3.71), from the results of the explicit calculations of S^S_q. We need to distinguish the two results because they disagree. As previously advertised, the disagreement is due to the fact that for the scalar theory, there are additional boundary contributions to the stress tensor that are important.

To make the discussion above more explicit, we now compare the results (3.77) and (3.78) to computations of S_q for all q.

- *Dirac fermions*

In $d = 3$, we may use the results of [46], where it was shown that

$$\mathcal{F}_q^D = 2\int_0^\infty dz\, z \coth(\pi z) \log\left(1 + e^{-2\pi q z}\right) + q\frac{\zeta(3)}{\pi^2}\,. \tag{3.79}$$

In even dimensions the computations are simpler. In $d = 4$, one finds [133]

$$S_q^D = -\frac{(1+q)(7+37q^2)}{720q^3}\log(R/\epsilon)\,. \tag{3.80}$$

This can be extended to $d = 6, 8$ by computing the functional determinant of the Dirac operator on $\mathcal{H}_q^d$ (see the appendix B of [93]). Taking two derivatives of all of these, we find

$$\begin{aligned}
d = 3: &\quad \partial_q^2 S_{q=1}^D = -\frac{7\pi^2}{180}\,,\\
d = 4: &\quad \partial_q^2 S_{q=1}^D = -\frac{5}{18}\log(R/\epsilon)\,,\\
d = 6: &\quad \partial_q^2 S_{q=1}^D = \frac{4}{27}\log(R/\epsilon)\,,\\
d = 8: &\quad \partial_q^2 S_{q=1}^D = -\frac{11}{150}\log(R/\epsilon)\,.
\end{aligned} \tag{3.81}$$

In each case, the results match (3.77).

- *Complex scalars*

In $d = 3$, we may again use the results of [46], where it shown that for complex conformal scalars

$$\mathcal{F}_q^S = -2\int_0^\infty dz\, z \tanh(\pi z) \log\left(1 - e^{-2\pi q z}\right) + q\frac{3\zeta(3)}{4\pi^2}\,. \tag{3.82}$$

In $d = 4$, similar computations give the well-known result [100]

$$S_q^S = -\frac{(1+q)(1+q^2)}{180q^3}\log(R/\epsilon)\,. \tag{3.83}$$

S_q^S for complex conformal scalars in $d = 6$ and 8 are also known as well (see the appendix B of [93]). Computing their second derivatives, we find

$$\begin{aligned} d=3: &\quad \partial_q^2 S^S_{q=1} = -\frac{2\pi^2}{45} \\ d=4: &\quad \partial_q^2 S^S_{q=1} = -\frac{1}{9}\log(R/\epsilon)\,, \\ d=6: &\quad \partial_q^2 S^S_{q=1} = \frac{1}{54}\log(R/\epsilon)\,, \\ d=8: &\quad \partial_q^2 S^S_{q=1} = -\frac{1}{300}\log(R/\epsilon)\,. \end{aligned} \tag{3.84}$$

This time, in each case we find a mismatch with (3.78):

$$\begin{aligned} d=3: &\quad \partial_q^2 \tilde{S}^S_{q=1} = \frac{113}{128}\cdot \partial_q^2 S^S_{q=1} \\ d=4: &\quad \partial_q^2 \tilde{S}^S_{q=1} = \frac{8}{9}\cdot \partial_q^2 S^S_{q=1} \\ d=6: &\quad \partial_q^2 \tilde{S}^S_{q=1} = \frac{113}{125}\cdot \partial_q^2 S^S_{q=1} \\ d=8: &\quad \partial_q^2 \tilde{S}^S_{q=1} = \frac{313}{343}\cdot \partial_q^2 S^S_{q=1}\,. \end{aligned} \tag{3.85}$$

- *Maxwell field in* $d = 4$

We may also consider the Maxwell field in $d = 4$, where the theory is conformal. In this case, an explicit computation of the Rényi entropy gives [99]

$$S_q^V = -\frac{1+q+31q^2+91q^3}{180q^3}\log(R/\epsilon)\,. \tag{3.86}$$

Using this result, one finds $\partial_q^2 S^V_{q=1} = -(4/9)\log(R/\epsilon)$. This matches the general formula (3.71) upon using $(\mathcal{A},\mathcal{B},\mathcal{C})$ for the Maxwell field [130, 131].

3.6.4 $S''_{q=1}$ for the free scalar field

Earlier, we explained the source of the apparent mismatch (3.85); our computations leading to (3.71) used the conformal stress tensor. But as mentioned in Sec. 3.5, this

is incompatible with the ordinary definitions used in computing Rényi entropy. It is important to correctly take the boundary contributions to $T_{\tau\tau}$ into account in order to match the known results for $S''_{q=1}$.

Before moving on to the calculation, note that $S'_{q=1}$ suffers no such ambiguity. The reason is that, as we will see below, $\langle H_\tau^{\rm conf} H_\tau\rangle - \langle H_\tau^{\rm conf} H_\tau^{\rm conf}\rangle \propto \langle H_\tau^{\rm conf}\int \nabla^2\phi^2\rangle$, which vanishes because of conformal symmetry. Here, $H_\tau^{\rm conf}$ uses the conformal stress tensor, while H_τ is the correct Hamiltonian that includes the boundary terms.

Mapping to flat space with a conical singularity

Instead of evaluating $\langle H_\tau H_\tau H_\tau\rangle_{q=1}^{\rm conn}$ directly, it turns out to be convenient to instead calculate $\langle H_\tau\rangle_q$ and then afterwards take two derivatives with respect to q and evaluate the result at $q=1$. This is convenient is because conformal symmetry constrains $\langle\phi^2\rangle_q = a(q)$, independent of the coordinates on $\mathcal{H}_q^d$. This then means that

$$\langle T_{\tau\tau}(x)\rangle_q = \langle T_{\tau\tau}^{\rm conf}(x)\rangle_q - \frac{d-2}{4(d-1)}\nabla^2\langle\phi^2(x)\rangle_q = \langle T_{\tau\tau}^{\rm conf}(x)\rangle_q \tag{3.87}$$

We now proceed by conformally mapping $\langle T_{\tau\tau}^{\rm conf}\rangle_q$ to a more convenient background, where the quantity has already been computed in $d=3$ and $d=4$. In particular, we utilize a mapping from $\mathcal{H}_q^d$ to the singular cone, $\mathcal{C}_q\times\mathbb{R}^{d-2}$. Writing the metric on $\mathcal{H}_q^d$ in Poincaré coordinates as

$$ds^2_{\mathcal{H}_q^d} = d\tau^2 + \frac{dz^2+\sum_{i=1}^{d-2}dy_i^2}{z^2}\,, \quad \tau\sim\tau+2\pi q \tag{3.88}$$

we find

$$ds^2_{\mathcal{H}_q^d} = \frac{1}{z^2}ds^2_{\mathcal{C}_q\times\mathbb{R}^{d-2}}\,, \qquad ds^2_{\mathcal{C}_q\times\mathbb{R}^{d-2}} = dz^2 + z^2d\tau^2 + \sum_{i=1}^{d-2}dy_i^2\,. \tag{3.89}$$

$\mathcal{C}_q$ is the two-dimensional flat space with a conical singularity at the origin $z = 0$, since τ has period $2\pi q$.

By symmetry and scaling arguments, we know that

$$\langle T^{\rm conf}_{\tau\tau}(\tau, z, y_i)\rangle_q^{\mathcal{C}_q\times\mathbb{R}^{d-2}} = \frac{F(q)}{z^{d-2}}\,, \tag{3.90}$$

for some function $F(q)$ that vanishes at $q = 1$. It then follows that

$$\partial_q^m S_q\Big|_{q=1} = \frac{2\pi}{m+1}{\rm Vol}(\mathbb{H}^{d-1})\;\partial_q^m F(q)\Big|_{q=1}\,, \tag{3.91}$$

where we have used the conformal mapping

$$\langle T^{\rm conf}_{\tau\tau}(\tau, z, y_i)\rangle_q^{\mathcal{H}^d_q} - \langle T^{\rm conf}_{\tau\tau}(\tau, z, y_i)\rangle_1^{\mathcal{H}^d} = F(q)\;. \tag{3.92}$$

In $d = 4$, $\langle T^{\rm conf}_{\tau\tau}\rangle_q$ was computed in the background of the cone in [132], with the result

$$F(q) = \frac{(q^2-1)\Big[(q^2-1)3(2b-c) - 2a(q^2+3)\Big]}{23040\pi^2 q^4}\,, \tag{3.93}$$

where

$$a = 24n_S + 72n_D + 144n_V\,, \qquad b = -8n_S - 44n_D - 248n_V\,, \qquad c = -240n_V\,, \tag{3.94}$$

and n_S, n_D, n_V are the numbers of complex scalars, Dirac fermions, and vector fields, respectively. Substituting (3.93) into (3.91), we may verify that this for-

mula agrees with the explicit results for the free scalar, fermion, and vector field in (3.83), (3.80), (3.86), respectively.[7]

For the $d = 3$ scalar, the expression for $F(q)$ is somewhat more complicated than the functions found in $d = 4$. The calculation was performed in [136], with the result

$$F(q) = \frac{1}{8\pi^2}\int_0^\infty du \frac{1}{\sinh u}\left(\frac{\coth u}{\sinh^2 u} - \frac{1}{q^3}\frac{\coth(u/q)}{\sinh^2(u/q)}\right). \tag{3.95}$$

Substituting (3.95) into (3.91), we may verify explicitly that the formula above is in agreement with the explicit computation of the Rényi entropy on $\mathcal{H}^3_q$ performed in [46] (see the result quoted in (3.82)).

The scalar-field result for $S''_{q=1}$ may also be understood by an explicit computation of $\langle H_\tau H_\tau H_\tau\rangle^{\text{conn}}_{q=1}$, so long as we include the correct boundary contributions to the stress tensor. In Appendix 3.7 we perform this check in two ways. The first method involves conformally mapping this correlation function from $\mathcal{H}^d$ to the sphere S^d. The second method involves directly computing $\langle H_\tau H_\tau H_\tau\rangle^{\text{conn}}_{q=1}$ on $\mathcal{H}^d$.

The mapping from the $\mathcal{H}^d$ to S^d has a subtlety that is worth some explanation. With the inclusion of the boundary terms, the stress tensors do not transform nicely under conformal transformations. To circumvent this fact, we use the observation that on $\mathcal{H}^d_q$, $\langle T_{\tau\tau}\rangle_q = \langle T^{\text{conf}}_{\tau\tau}\rangle_q$. Then, we conformally map the one-point function of $T^{\text{conf}}_{\tau\tau}$ to the one-point function of the conformal stress tensor on the multi-covered sphere, take two derivatives with respect to q, which brings down two non-conformal stress tensors, and then set $q = 1$. In the end, we see that on S^d we need to evaluate the three-point function of one conformal stress tensor with two non-conformal stress tensors. This is shown explicitly in the following section.

[7] It was recently shown in [134] that in a general $d = 4$ CFT, $F(q)$ is proportional to $f_c(q)$, a function appearing in the log term of the Rényi entropy for generic entangling surfaces [135].

3.7 Additional checks for the scalar $S''_{q=1}$

Here we explicitly calculate $\langle H_\tau H_\tau H_\tau \rangle^{\text{conn}}_{q=1}$ for the scalar field, including the correct boundary terms. We verify that once the boundary terms are included, the calculations agree with the explicit results for $S''_{q=1}$.

3.7.1 The three-point function on the sphere

The calculation on the sphere utilizes the following conformal transformation from $\mathcal{H}^d$ to S^d:

$$\begin{aligned} ds^2_{\mathcal{H}^d} &= d\tau^2 + d\rho^2 + \sinh^2\rho d\Omega^2_{d-2} \\ &= \frac{1}{\sin^2\theta}(\sin^2\theta d\tau^2 + d\theta^2 + \cos^2\theta d\Omega^2_{d-2}) = \frac{1}{\Omega^2} ds^2_{S^d}\,. \end{aligned} \tag{3.96}$$

where $\sinh\rho = \cot\theta$. Under the conformal transformation, the scalar propagator transforms by

$$\langle \phi(x)\phi(y)\rangle_{S^d} = \Omega(x)^{\frac{d-2}{2}}\Omega(y)^{\frac{d-2}{2}}\langle \phi(x)\phi(y)\rangle_{\mathcal{H}^d}\,. \tag{3.97}$$

Now, we may calculate the three-point function of modular Hamiltonians

$$\langle H_\tau H_\tau H_\tau\rangle = \int d^{d-1}x_1\sqrt{g_1}\int d^{d-1}x_2\sqrt{g_2}\int d^{d-1}x_3\sqrt{g_3}\langle T_{\tau\tau}(x_1)T_{\tau\tau}(x_2)T_{\tau\tau}(x_3)\rangle\,, \tag{3.98}$$

with the stress tensors $T_{\mu\nu}$ given by

$$T^\alpha_{\mu\nu} = \partial_\mu\phi\partial_\nu\phi - \frac{1}{2}g_{\mu\nu}(\partial\phi)^2 + \xi(\alpha\mathcal{R}_{\mu\nu} - \frac{1}{2}g_{\mu\nu}\mathcal{R})\phi^2 - \alpha\xi(\nabla_\mu\nabla_\nu - g_{\mu\nu}\nabla^2)\phi^2\,. \tag{3.99}$$

where $\xi = \frac{d-2}{4(d-1)}$, and $\alpha = 1$ (conformal) or $\alpha = 0$ (non-conformal). Let us introduce a new notation, whereby $T^{\rm conf}_{\tau\tau} \equiv T^1_{\tau\tau}$ and $T_{\tau\tau} \equiv T^0_{\tau\tau}$, and correspondingly for H^1_τ and H^0_τ.

To calculate the three-point function $\langle T^{\alpha_1}_{\tau\tau}(x_1) T^{\alpha_2}_{\tau\tau}(x_2) T^{\alpha_3}_{\tau\tau}(x_3)\rangle^{\rm conn}$, it is convenient to first compute $G(x_1 - x_4)G(x_2 - x_5)G(x_3 - x_6)$. Then one may take derivatives of this combination of Green's functions, along with taking appropriate limits for the coordinates, to recover the three-point function of stress tensors.

We are allowed to set $x_1 = 0$ in the correlation function and factor out a regulated volume of the hyperbolic space, $\mathrm{Vol}(\mathbb{H}^{d-1})$. It is then a straightforward if tedious exercise to compute the three-point function:

$$\langle H^1_\tau H^0_\tau H^0_\tau \rangle = \begin{cases} -\frac{1}{60\pi}\,, & d = 3 \\ -\frac{1}{24\pi^3}\log(R/\epsilon)\,, & d = 4\,, \end{cases} \tag{3.100}$$

$$\langle H^1_\tau H^1_\tau H^1_\tau \rangle = \begin{cases} -\frac{1}{60\pi}\frac{113}{128}\,, & d = 3 \\ -\frac{1}{24\pi^3}\frac{8}{9}\log(R/\epsilon)\,, & d = 4\,. \end{cases} \tag{3.101}$$

Here, H^1_τ denotes the modular Hamiltonian with the conformal stress tensor on the sphere, while H^0_τ denotes the non-conformal stress tensor. Using (3.33), we may obtain the second derivatives of the Rényi entropy at $q = 1$.

The three-point function of conformal stress tensors in (3.101) agrees with the results in (3.85). However, as discussed in Sec. 3.6.4, the correct three-point function to compute for reproducing the $S''_{q=1}$ is that in (3.100). This was explained in Sec. 3.6.4. Indeed, the results in (3.100) are consistent with the explicit calculations of $S''_{q=1}$ given in (3.84).

3.7.2 The three-point function on $S^1 \times \mathbb{H}^{d-1}$

Now we will calculate the three-point functions directly on $\mathcal{H}^d$. In this case, we need to consider additional boundary terms at infinity that are needed to have a well-defined variational principle. That is, we need to add the boundary action $S_{\text{bdry}} = \frac{1}{2}\int_{\rho=\infty}\sqrt{g}\delta\phi\partial_\rho\phi$ so that $\delta S + \delta S_{\text{bdry}} = 0$, when evaluated on solutions to the equations of motion. Therefore, the non-conformal stress tensor becomes

$$\begin{aligned}\int T_{\tau\tau} &= \int\left((\partial_\tau\phi)^2 - \frac{1}{2}\partial_\mu\phi\partial^\mu\phi + \frac{(d-2)}{8(d-1)}\mathcal{R}\phi^2\right) + \int_{\rho=\infty}\frac{1}{2}\phi\partial_\rho\phi \\ &= \tilde{H}^0_\tau + B\,,\end{aligned} \tag{3.102}$$

where $\tilde{H}^0_\tau$ refers to the modular Hamiltonian formed with the usual non-conformal stress tensor and B is the additional boundary term needed on $\mathcal{H}^d$.

While the three-point function $\langle H^1_\tau H^1_\tau H^1_\tau\rangle$ doesn't receive corrections from the boundary term B, the three-point function $\langle H^1_\tau H^0_\tau H^0_\tau\rangle$ does receive important corrections. The necessary calculation is

$$\langle H^1_\tau H^0_\tau H^0_\tau\rangle = \langle H^1_\tau \tilde{H}^0_\tau \tilde{H}^0_\tau\rangle + 2\langle H^1_\tau \tilde{H}^0_\tau B\rangle + \langle H^1_\tau BB\rangle\,. \tag{3.103}$$

In $d = 3$, an explicit calculation gives $\langle H^1_\tau \tilde{H}^0_\tau \tilde{H}^0_\tau\rangle = -17/(1920\pi)$, $\langle H^1_\tau \tilde{H}^0_\tau B\rangle = -1/(128\pi)$ and $\langle H^1_\tau BB\rangle = 1/(128\pi)$. In $d = 4$, we find $\langle H^1_\tau \tilde{H}^0_\tau \tilde{H}^0_\tau\rangle = 0 = \langle H^1_\tau \tilde{H}^0_\tau B\rangle$ and $\langle H^1_\tau BB\rangle = -1/(24\pi^3)\log(R/\epsilon)$. Substituting these results into (3.103), we recover the expected results given in (3.101).

To summarize, we have seen explicitly that the mismatch noted in (3.85) is explained by the boundary contributions to the Hamiltonian.

3.8 Rényi entropy in $\mathcal{N} = 4$ super-Yang-Mills

As a corollary to the previous results, we are able to resolve a puzzle raised in [98] about the behavior of $S''_{q=1}$ in $\mathcal{N} = 4$ SYM as a function of the 't Hooft coupling λ. The puzzle is as follows. Because $S''_{q=1}$ is fixed by the stress-tensor 3-point function on $\mathbb{R}^4$, one expects that this quantity is independent of the coupling λ: $\partial_\lambda S''_{q=1}(\lambda) = 0$. One may check this conjecture by comparing the explicit Rényi entropies at weak and strong coupling in the large-N limit. However, using the free field results for scalars, fermions and vectors, and comparing the known holographic result, one finds that [98]

$$\lim_{\lambda\to 0} S''_{q=1}(\lambda) \neq \lim_{\lambda\to\infty} S''_{q=1}(\lambda)\,. \tag{3.104}$$

In particular,

$$\lim_{\lambda\to 0} S''_{q=1}(\lambda) = -\frac{4}{3}N^2\log(R/\epsilon)\,, \qquad \lim_{\lambda\to\infty} S''_{q=1}(\lambda) = -\frac{35}{27}N^2\log(R/\epsilon)\,. \tag{3.105}$$

Evidently, $S''_{q=1}(\lambda)$ is given by some non-trivial function of λ. What failed about the non-renormalization argument?

The culprit is the contribution of the scalar field. As we have shown, one should really be using the non-conformal stress tensor in the three-point function on $\mathbb{R}^4$. This object is not subject to a non-renormalization theorem. In particular, the difference between stress tensors, $T^{\text{conf}}_{\tau\tau} - T_{\tau\tau} \sim \nabla^2\phi^2$, is a conformal descendant of the Konishi operator. This operator is not protected by supersymmetry and decouples at strong coupling, where it acquires an anomalous dimension $\Delta \sim \lambda^{1/4}$. Therefore, the non-renormalization conjecture is incorrect, and $S''_{q=1}(\lambda)$ is indeed a non-trivial function of λ.

This is consistent with the result of Sec. 3.6.3. The general lesson is that at strong coupling, the regularized and singular cones merge into one prescription, because the boundary terms in the stress tensor are suppressed.

As a further check on this interpretation, the λ-dependence of $S''_{q=1}(\lambda)$ should not be visible at any order in perturbation theory around $\lambda = \infty$. We can confirm this at first non-trivial order in α' corrections: in [137], the first correction to (3.74) in type IIB supergravity due to $O(\alpha'^3)$ corrections involving the metric and five-form was computed. The correction scales like $(q-1)^3$; this completes the argument.

Bibliography

[1] A. Lewkowycz, R. C. Myers, and M. Smolkin, "Observations on entanglement entropy in massive QFT's," *JHEP*, vol. 1304, p. 017, 2013. (document), 3.1, 3.4, 3.4, 3.3

[2] G. Parisi and N. Sourlas, "Random Magnetic Fields, Supersymmetry and Negative Dimensions," *Phys. Rev. Lett.*, vol. 43, p. 744, 1979. 1

[3] G. Parisi and N. Sourlas, "Supersymmetric Field Theories and Stochastic Differential Equations," *Nucl. Phys.*, vol. B206, pp. 321–332, 1982. 1

[4] N. Sourlas, "Introduction to supersymmetry in condensed matter physics," *Physica D: Nonlinear Phenomena*, vol. 15, no. 1, pp. 115–122, 1985. 1

[5] M. Tomka, M. Pletyukhov, and V. Gritsev, "Supersymmetry in quantum optics and in spin-orbit coupled systems," *Scientific reports*, vol. 5, 2015. 1

[6] N. Seiberg, "Electric-magnetic duality in supersymmetric non-Abelian gauge theories," *Nucl. Phys.*, vol. B435, pp. 129–146, 1995. 1, 2.1

[7] W. E. Caswell, "Asymptotic Behavior of Nonabelian Gauge Theories to Two Loop Order," *Phys. Rev. Lett.*, vol. 33, p. 244, 1974. 1

[8] T. Banks and A. Zaks, "On the Phase Structure of Vector-Like Gauge Theories with Massless Fermions," *Nucl.Phys.*, vol. B196, p. 189, 1982. 1, 2.1

[9] O. Aharony, A. Hanany, K. A. Intriligator, N. Seiberg, and M. Strassler, "Aspects of N=2 supersymmetric gauge theories in three-dimensions," *Nucl.Phys.*, vol. B499, pp. 67–99, 1997. 1, 1.1, 2.1, 2.2, 2.2.1, 2.3.1, 2.3.1

[10] O. Aharony and A. Hanany, "Branes, superpotentials and superconformal fixed points," *Nucl. Phys.*, vol. B504, pp. 239–271, 1997. 1

[11] L. Bombelli, R. K. Koul, J. Lee, and R. D. Sorkin, "A Quantum Source of Entropy for Black Holes," *Phys. Rev.*, vol. D34, pp. 373–383, 1986. 1

[12] M. Srednicki, "Entropy and area," *Phys. Rev. Lett.*, vol. 71, pp. 666–669, 1993. 1, 3.3

[13] M. M. Wolf, F. Verstraete, M. B. Hastings, and J. I. Cirac, "Area laws in quantum systems: mutual information and correlations," *Physical review letters*, vol. 100, no. 7, p. 070502, 2008. 1

[14] M. B. Hastings, I. González, A. B. Kallin, and R. G. Melko, "Measuring renyi entanglement entropy in quantum monte carlo simulations," *Physical review letters*, vol. 104, no. 15, p. 157201, 2010. 1

[15] J.-M. Stéphan, G. Misguich, and V. Pasquier, "Rényi entanglement entropies in quantum dimer models: from criticality to topological order," *Journal of Statistical Mechanics: Theory and Experiment*, vol. 2012, no. 02, p. P02003, 2012. 1

[16] H. Yao and X.-L. Qi, "Entanglement entropy and entanglement spectrum of the kitaev model," *Physical review letters*, vol. 105, no. 8, p. 080501, 2010. 1

[17] B. Swingle and T. Senthil, "Entanglement structure of deconfined quantum critical points," *arXiv preprint arXiv:1109.3185*, 2011. 1

[18] B. Swingle, "Rényi entropy, mutual information, and fluctuation properties of fermi liquids," *Physical Review B*, vol. 86, no. 4, p. 045109, 2012. 1

[19] S. Ryu and T. Takayanagi, "Holographic Derivation of Entanglement Entropy from AdS/CFT," *Phys. Rev. Lett.*, vol. 96, p. 181602, 2006. 1

[20] R. C. Myers and A. Sinha, "Holographic c-theorems in arbitrary dimensions," *JHEP*, vol. 01, p. 125, 2011. 1, 1.4.1, 2.2.4, 2.2.5

[21] H. Casini, M. Huerta, and R. C. Myers, "Towards a derivation of holographic entanglement entropy," *JHEP*, vol. 1105, p. 036, 2011. 1, 1.4.1, 3.5, 3.5, 3.5, 5, 3.6.1

[22] P. Calabrese and J. L. Cardy, "Entanglement Entropy and Quantum Field Theory," *J. Stat. Mech.*, vol. 0406, p. P06002, 2004. 1, 3.1, 3.1, 3.4

[23] P. Calabrese and J. L. Cardy, "Entanglement entropy and quantum field theory: A Non-technical introduction," *Int.J.Quant.Inf.*, vol. 4, p. 429, 2006. 1, 3.1, 3.1, 3.1, 3.4

[24] P. Calabrese and J. Cardy, "Entanglement entropy and conformal field theory," *J.Phys.A*, vol. A42, p. 504005, 2009. 1, 3.1, 3.1, 3.4

[25] H. Casini and M. Huerta, "On the RG running of the entanglement entropy of a circle," *Phys.Rev.*, vol. D85, p. 125016, 2012. 1, 1.4.1, 2.2.4, 2.2.5, 2.3.3, 3.3

[26] D. L. Jafferis, "The Exact Superconformal R-Symmetry Extremizes Z," *JHEP*, vol. 1205, p. 159, 2012. 1, 1.2, 1.2.1, 1.2.2, 1.2.2, 1.3.2, 2.1, 2.1, 2.2.2, 2.2.2, 2.3.2

[27] A. Kapustin, B. Willett, and I. Yaakov, "Exact Results for Wilson Loops in Superconformal Chern- Simons Theories with Matter," *JHEP*, vol. 03, p. 089, 2010. 1.2, 1.2.1, 1.2.2, 2.1, 2.2.2

[28] N. Hama, K. Hosomichi, and S. Lee, "Notes on SUSY Gauge Theories on Three-Sphere," *JHEP*, vol. 1103, p. 127, 2011. 1.2, 2.1, 2.2.2

[29] C. G. Callan, Jr., "Broken scale invariance in scalar field theory," *Phys. Rev.*, vol. D2, pp. 1541–1547, 1970. 1.3.1

[30] K. Symanzik, "Small distance behavior in field theory and power counting," *Commun. Math. Phys.*, vol. 18, pp. 227–246, 1970. 1.3.1

[31] K. G. Wilson, "Renormalization group and critical phenomena. 1. Renormalization group and the Kadanoff scaling picture," *Phys. Rev.*, vol. B4, pp. 3174–3183, 1971. 1.3.1

[32] K. G. Wilson, "Renormalization group and critical phenomena. 2. Phase space cell analysis of critical behavior," *Phys. Rev.*, vol. B4, pp. 3184–3205, 1971. 1.3.1

[33] K. G. Wilson and J. B. Kogut, "The Renormalization group and the epsilon expansion," *Phys. Rept.*, vol. 12, pp. 75–200, 1974. 1.3.1

[34] A. B. Zamolodchikov, "Irreversibility of the Flux of the Renormalization Group in a 2D Field Theory," *JETP Lett.*, vol. 43, pp. 730–732, 1986. 1.3.1

[35] J. L. Cardy, "Is there a c-theorem in four dimensions?," *Phys.Lett.*, vol. B215, pp. 749–752, 1988. 1.3.1

[36] Z. Komargodski and A. Schwimmer, "On Renormalization Group Flows in Four Dimensions," *JHEP*, vol. 1112, p. 099, 2011. 1.3.1

[37] D. Anselmi, D. Freedman, M. T. Grisaru, and A. Johansen, "Nonperturbative formulas for central functions of supersymmetric gauge theories," *Nucl.Phys.*, vol. B526, pp. 543–571, 1998. 1.3.2, 2.2.5

[38] D. Anselmi, J. Erlich, D. Z. Freedman, and A. A. Johansen, "Positivity constraints on anomalies in supersymmetric gauge theories," *Phys. Rev.*, vol. D57, pp. 7570–7588, 1998. 1.3.2

[39] K. A. Intriligator and B. Wecht, "The Exact superconformal R symmetry maximizes a," *Nucl. Phys.*, vol. B667, pp. 183–200, 2003. 1.3.2

[40] D. L. Jafferis, I. R. Klebanov, S. S. Pufu, and B. R. Safdi, "Towards the F-Theorem: $\mathcal{N} = 2$ Field theories on the three-sphere," *JHEP*, vol. 1106, p. 102, 2011. 1.3.2, 2.1, 2.2.4, 2.2.5, 2.3.3

[41] I. R. Klebanov, S. S. Pufu, and B. R. Safdi, "F-Theorem without Supersymmetry," *JHEP*, vol. 1110, p. 038, 2011. 1.3.2, 2.2.4, 2.2.5, 2.3.3

[42] A. Einstein, B. Podolsky, and N. Rosen, "Can quantum mechanical description of physical reality be considered complete?," *Phys. Rev.*, vol. 47, pp. 777–780, 1935. 1.4

[43] A. Rényi, "On measures of information and entropy," in *Proceedings of the 4th Berkeley Symposium on Mathematics, Statistics and Probability*, vol. 1, (Berkeley, CA), p. 547, U. of California Press, 1961. 1.4, 3.1

[44] A. Rényi, "On the foundations of information theory," *Rev. Int. Stat. Inst.*, vol. 33, no. 1, 1965. 1.4, 3.1

[45] H. Liu and M. Mezei, "A Refinement of entanglement entropy and the number of degrees of freedom," *JHEP*, vol. 1304, p. 162, 2013. 1.4.1, 3.3, 3.3

[46] I. R. Klebanov, S. S. Pufu, S. Sachdev, and B. R. Safdi, "Renyi Entropies for Free Field Theories," *JHEP*, vol. 1204, p. 074, 2012. 1.4.1, 3.1, 3.2, 3.3, 3.3, 3.5.2, 3.6.3, 3.6.3, 3.6.4

[47] B. R. Safdi, I. R. Klebanov, and J. Lee, "A Crack in the Conformal Window," *JHEP*, vol. 1304, p. 165, 2013. 2, 2.2.3, 2.6

[48] J. Lee and M. Yamazaki, "Gauging and Decoupling in 3d $\mathcal{N} = 2$ dualities," 2016. 2

[49] N. Seiberg, "Exact results on the space of vacua of four-dimensional SUSY gauge theories," *Phys.Rev.*, vol. D49, pp. 6857–6863, 1994. 2.1

[50] K. A. Intriligator and N. Seiberg, "Duality, monopoles, dyons, confinement and oblique confinement in supersymmetric SO(N(c)) gauge theories," *Nucl.Phys.*, vol. B444, pp. 125–160, 1995. 2.1

[51] K. A. Intriligator and P. Pouliot, "Exact superpotentials, quantum vacua and duality in supersymmetric SP(N(c)) gauge theories," *Phys.Lett.*, vol. B353, pp. 471–476, 1995. 2.1

[52] T. W. Appelquist, M. Bowick, D. Karabali, and L. C. R. Wijewardhana, "Spontaneous chiral-symmetry breaking in three-dimensional qed," *Phys. Rev. D*, vol. 33, pp. 3704–3713, 1986. 2.1

[53] T. Appelquist, D. Nash, and L. C. R. Wijewardhana, "Critical behavior in (2+1)-dimensional QED," *Physical Review Letters*, vol. 60, pp. 2575–2578, 1988. 2.1

[54] O. Aharony, "IR duality in d = 3 N=2 supersymmetric USp(2N(c)) and U(N(c)) gauge theories," *Phys.Lett.*, vol. B404, pp. 71–76, 1997. 2.1, 2.4.1

[55] A. Karch, "Seiberg duality in three-dimensions," *Phys. Lett.*, vol. B405, pp. 79–84, 1997. 2.1, 2.4.1

[56] A. Giveon and D. Kutasov, "Seiberg Duality in Chern-Simons Theory," *Nucl.Phys.*, vol. B812, pp. 1–11, 2009. 2.1, 2.8.1

[57] O. Aharony, S. S. Razamat, N. Seiberg, and B. Willett, "3d dualities from 4d dualities," *JHEP*, vol. 1307, p. 149, 2013. 2.1, 2.3, 2.3.1, 2.3.1, 2.3.2

[58] O. Aharony, S. S. Razamat, N. Seiberg, and B. Willett, "3d dualities from 4d dualities for orthogonal groups," *JHEP*, vol. 1308, p. 099, 2013. 2.1, 2.5, 2.5.4

[59] J. Park and K.-J. Park, "Seiberg-like Dualities for 3d N=2 Theories with SU(N) gauge group," *JHEP*, vol. 10, p. 198, 2013. 2.1, 2.3.1

[60] C. Closset, T. T. Dumitrescu, G. Festuccia, Z. Komargodski, and N. Seiberg, "Contact Terms, Unitarity, and F-Maximization in Three-Dimensional Superconformal Theories," *JHEP*, vol. 10, p. 053, 2012. 2.1

[61] C. P. Herzog, I. R. Klebanov, S. S. Pufu, and T. Tesileanu, "Multi-Matrix Models and Tri-Sasaki Einstein Spaces," *Phys.Rev.*, vol. D83, p. 046001, 2011. 2.1, 2.2.3, 2.2.3

[62] B. Willett and I. Yaakov, "N=2 Dualities and Z Extremization in Three Dimensions," 2011. 2.1, 2.3.2, 2.8.1

[63] G. Veneziano, "Some Aspects of a Unified Approach to Gauge, Dual and Gribov Theories," *Nucl.Phys.*, vol. B117, pp. 519–545, 1976. 2.1

[64] V. Niarchos, "Comments on F-maximization and R-symmetry in 3D SCFTs," *J. Phys.*, vol. A44, p. 305404, 2011. 2.1

[65] T. Morita and V. Niarchos, "F-theorem, duality and SUSY breaking in one-adjoint Chern-Simons-Matter theories," *Nucl.Phys.*, vol. B858, pp. 84–116, 2012. 2.1

[66] P. Agarwal, A. Amariti, and M. Siani, "Refined Checks and Exact Dualities in Three Dimensions," *JHEP*, vol. 10, p. 178, 2012. 2.1

[67] O. Aharony, G. Gur-Ari, and R. Yacoby, "d=3 Bosonic Vector Models Coupled to Chern-Simons Gauge Theories," *JHEP*, vol. 1203, p. 037, 2012. 2.1, 2.8.2

[68] S. Giombi, S. Minwalla, S. Prakash, S. P. Trivedi, S. R. Wadia, *et al.*, "Chern-Simons Theory with Vector Fermion Matter," *Eur.Phys.J.*, vol. C72, p. 2112, 2012. 2.1, 2.8.2

[69] C.-M. Chang, S. Minwalla, T. Sharma, and X. Yin, "ABJ Triality: from Higher Spin Fields to Strings," *J. Phys.*, vol. A46, p. 214009, 2013. 2.1, 2.8.2

[70] J. de Boer, K. Hori, and Y. Oz, "Dynamics of N=2 supersymmetric gauge theories in three-dimensions," *Nucl.Phys.*, vol. B500, pp. 163–191, 1997. 2.2.1, 2.3.1

[71] V. Borokhov, A. Kapustin, and X.-k. Wu, "Monopole operators and mirror symmetry in three-dimensions," *JHEP*, vol. 0212, p. 044, 2002. 2.2.1, 2.3.1

[72] D. Gaiotto and E. Witten, "S-Duality of Boundary Conditions In N=4 Super Yang-Mills Theory," *Adv.Theor.Math.Phys.*, vol. 13, pp. 721–896, 2009. 2.2.1

[73] D. L. Jafferis, "Quantum corrections to $\mathcal{N} = 2$ Chern-Simons theories with flavor and their AdS_4 duals," *JHEP*, vol. 08, p. 046, 2013. 2.2.1

[74] I. R. Klebanov, S. S. Pufu, S. Sachdev, and B. R. Safdi, "Entanglement Entropy of 3-d Conformal Gauge Theories with Many Flavors," *JHEP*, vol. 05, p. 036, 2012. 2.2.3

[75] I. Affleck, J. A. Harvey, and E. Witten, "Instantons and (Super)Symmetry Breaking in (2+1)-Dimensions," *Nucl. Phys.*, vol. B206, p. 413, 1982. 2.3.1

[76] F. A. H. Dolan, V. P. Spiridonov, and G. S. Vartanov, "From 4d superconformal indices to 3d partition functions," *Phys. Lett.*, vol. B704, pp. 234–241, 2011. 2.3.2

[77] D. Bashkirov, "Aharony duality and monopole operators in three dimensions," 2011. 2.3.2, 2.8

[78] F. Benini, C. Closset, and S. Cremonesi, "Comments on 3d Seiberg-like dualities," *JHEP*, vol. 10, p. 075, 2011. 2.3.2, 2.5, 2.5.1

[79] G. Festuccia and N. Seiberg, "Rigid Supersymmetric Theories in Curved Superspace," *JHEP*, vol. 06, p. 114, 2011. 2.3.2

[80] R. C. Myers and A. Sinha, "Seeing a c-theorem with holography," *Phys. Rev.*, vol. D82, p. 046006, 2010. 2.3.3

[81] C. Hwang, K.-J. Park, and J. Park, "Evidence for Aharony duality for orthogonal gauge groups," *JHEP*, vol. 11, p. 011, 2011. 2.5, 2.5.1, 3

[82] O. Aharony and I. Shamir, "On $O(N_c)$ $d = 3$ $N = 2$ supersymmetric QCD Theories," *JHEP*, vol. 12, p. 043, 2011. 2.5, 2.5.1, 2.5.1

[83] Y.-H. He, *On algebraic singularities, finite graphs and D-brane gauge theories: A String theoretic perspective*. PhD thesis, 2002. 2.7

[84] M. Yamazaki, "Brane Tilings and Their Applications," *Fortsch. Phys.*, vol. 56, pp. 555–686, 2008. 2.7

[85] M. Yamazaki, "Entanglement in Theory Space," *Europhys. Lett.*, vol. 103, p. 21002, 2013. 5

[86] M. Yamazaki, "Quivers, YBE and 3-manifolds," *JHEP*, vol. 05, p. 147, 2012. 5

[87] Y. Terashima and M. Yamazaki, "Emergent 3-manifolds from 4d Superconformal Indices," *Phys. Rev. Lett.*, vol. 109, p. 091602, 2012. 5

[88] W. Cottrell, J. Hanson, and A. Hashimoto, "Dynamics of $\mathcal{N} = 4$ supersymmetric field theories in 2+1 dimensions and their gravity dual," 2015. 2.7.3

[89] W. Cottrell and A. Hashimoto, "Resolved gravity duals of $\mathcal{N} = 4$ quiver field theories in 2+1 dimensions," 2016. 2.7.3

[90] S. Deser, R. Jackiw, and S. Templeton, "Topologically Massive Gauge Theories," *Annals Phys.*, vol. 140, pp. 372–411, 1982. 2.8

[91] A. Amariti and M. Siani, "Z-extremization and F-theorem in Chern-Simons matter theories," *JHEP*, vol. 1110, p. 016, 2011. 2.8.2

[92] J. Lee, L. McGough, and B. R. Safdi, "Rényi entropy and geometry," *Phys. Rev.*, vol. D89, no. 12, p. 125016, 2014. 3

[93] J. Lee, A. Lewkowycz, E. Perlmutter, and B. R. Safdi, "Rényi entropy, stationarity, and entanglement of the conformal scalar," *JHEP*, vol. 03, p. 075, 2015. 3, 3.6.3, 3.6.3

[94] J. Eisert, M. Cramer, and M. B. Plenio, "Area Laws for the Entanglement Entropy - a Review," *Rev. Mod. Phys.*, vol. 82, pp. 277–306, 2010. 3.1

[95] T. Nishioka, S. Ryu, and T. Takayanagi, "Holographic entanglement entropy: An Overview," *J.Phys.A*, vol. A42, p. 504008, 2009. 3.1

[96] S. N. Solodukhin, "Entanglement Entropy, Conformal Invariance and Extrinsic Geometry," *Phys. Lett.*, vol. B665, pp. 305–309, 2008. 3.1

[97] L.-Y. Hung, R. C. Myers, M. Smolkin, and A. Yale, "Holographic Calculations of Renyi Entropy," *JHEP*, vol. 1112, p. 047, 2011. 3.1, 3.3, 3.5, 3.6.3

[98] E. Perlmutter, "A universal feature of CFT Rényi entropy," *JHEP*, vol. 1403, p. 117, 2014. 3.1, 2, 3.5, 3.6.1, 3.6.1, 3.6.3, 3.8

[99] D. V. Fursaev, "Entanglement Renyi Entropies in Conformal Field Theories and Holography," *JHEP*, vol. 05, p. 080, 2012. 3.2, 3.2, 3.6.3

[100] H. Casini and M. Huerta, "Entanglement entropy for the n-sphere," *Phys.Lett.*, vol. B694, pp. 167–171, 2010. 3.2, 3.3, 3.5, 3.6.3

[101] D. Fursaev and G. Miele, "Finite temperature scalar field theory in static de Sitter space," *Phys.Rev.*, vol. D49, pp. 987–998, 1994. 3.2

[102] L. De Nardo, D. V. Fursaev, and G. Miele, "Heat kernel coefficients and spectra of the vector Laplacians on spherical domains with conical singularities," *Class.Quant.Grav.*, vol. 14, pp. 1059–1078, 1997. 3.2

[103] M. Huerta, "Numerical Determination of the Entanglement Entropy for Free Fields in the Cylinder," *Phys.Lett.*, vol. B710, pp. 691–696, 2012. 10 pages, 4 figures, typos corrected in equations and figures labels. 3.2, 3.2, 3.3, 3.3, 3.4, 3.4

[104] H. Casini and M. Huerta, "Entanglement entropy in free quantum field theory," *J.Phys.A*, vol. A42, p. 504007, 2009. 3.2, 3.3

[105] I. R. Klebanov, T. Nishioka, S. S. Pufu, and B. R. Safdi, "On Shape Dependence and RG Flow of Entanglement Entropy," *JHEP*, vol. 1207, p. 001, 2012. 3.2, 3.2

[106] H. Casini and M. Huerta, "Entanglement and alpha entropies for a massive scalar field in two dimensions," *J.Stat.Mech.*, vol. 0512, p. P12012, 2005. 3.2

[107] T. Grover, A. M. Turner, and A. Vishwanath, "Entanglement Entropy of Gapped Phases and Topological Order in Three dimensions," *Phys.Rev.*, vol. B84, p. 195120, 2011. 16.5 pages, 10 figures. 3.2

[108] A. Kitaev and J. Preskill, "Topological entanglement entropy," *Phys.Rev.Lett.*, vol. 96, p. 110404, 2006. 3.2

[109] M. Levin and X.-G. Wen, "Detecting topological order in a ground state wave function," *Phys.Rev.Lett.*, vol. 96, p. 110405, 2006. 3.2

[110] B. R. Safdi, "Exact and Numerical Results on Entanglement Entropy in (5+1)-Dimensional CFT," *JHEP*, vol. 1212, p. 005, 2012. 3.2, 3.3

[111] X. Dong, "Shape Dependence of Holographic Renyi Entropy in Conformal Field Theories," 2016. 3.2

[112] I. Peschel, "Letter to the editor: Calculation of reduced density matrices from correlation functions," *Journal of Physics A Mathematical General*, vol. 36, pp. L205–L208, Apr. 2003. 3.3

[113] I. R. Klebanov, T. Nishioka, S. S. Pufu, and B. R. Safdi, "Is Renormalized Entanglement Entropy Stationary at RG Fixed Points?," *JHEP*, vol. 1210, p. 058, 2012. 3.3, 3.3, 3.3

[114] R. Lohmayer, H. Neuberger, A. Schwimmer, and S. Theisen, "Numerical determination of entanglement entropy for a sphere," *Phys.Lett.*, vol. B685, pp. 222–227, 2010. 3.3

[115] M. Headrick, "Entanglement Renyi entropies in holographic theories," *Phys.Rev.*, vol. D82, p. 126010, 2010. 3.3

[116] M. P. Hertzberg and F. Wilczek, "Some Calculable Contributions to Entanglement Entropy," *Phys.Rev.Lett.*, vol. 106, p. 050404, 2011. 3.4, 3.4

[117] S. N. Solodukhin, "Entanglement Entropy of Black Holes," *Living Rev. Rel.*, vol. 14, p. 8, 2011. 3.4

[118] D. V. Fursaev, "Spectral geometry and one loop divergences on manifolds with conical singularities," *Phys.Lett.*, vol. B334, pp. 53–60, 1994. 3.4

[119] D. V. Fursaev and S. N. Solodukhin, "On the description of the Riemannian geometry in the presence of conical defects," *Phys.Rev.*, vol. D52, pp. 2133–2143, 1995. 3.4, 3.5.1, 5

[120] D. E. Diaz and H. Dorn, "Partition functions and double-trace deformations in AdS/CFT," *JHEP*, vol. 05, p. 046, 2007. 3.5

[121] C. Callan and F. Wilczek, "On geometric entropy," *Physics Letters B*, vol. 333, no. 1–2, pp. 55 – 61, 1994. 3.5.1

[122] H. Casini, M. Huerta, and J. A. Rosabal, "Remarks on entanglement entropy for gauge fields," *Phys.Rev.*, vol. D89, p. 085012, 2014. 3.5.1

[123] A. Lewkowycz and J. Maldacena, "Exact results for the entanglement entropy and the energy radiated by a quark," *JHEP*, vol. 1405, p. 025, 2014. 3.5.1

[124] D. N. Kabat, "Black hole entropy and entropy of entanglement," *Nucl.Phys.*, vol. B453, pp. 281–299, 1995. 3.5.1

[125] G. Gibbons and S. Hawking, "Action Integrals and Partition Functions in Quantum Gravity," *Phys.Rev.*, vol. D15, pp. 2752–2756, 1977. 3.5.1

[126] S. Ryu and T. Takayanagi, "Aspects of Holographic Entanglement Entropy," *JHEP*, vol. 0608, p. 045, 2006. 3.5.1

[127] T. Faulkner, A. Lewkowycz, and J. Maldacena, "Quantum corrections to holographic entanglement entropy," *JHEP*, vol. 1311, p. 074, 2013. 3.5.1

[128] V. Rosenhaus and M. Smolkin, "Entanglement Entropy: A Perturbative Calculation," *JHEP*, vol. 12, p. 179, 2014. 3.5.2

[129] J. Cardy, "Some results on the mutual information of disjoint regions in higher dimensions," *J.Phys.*, vol. A46, p. 285402, 2013. 3.5.2

[130] H. Osborn and A. Petkou, "Implications of conformal invariance in field theories for general dimensions," *Annals Phys.*, vol. 231, pp. 311–362, 1994. 3.6.1, 3.6.2, 3.6.3, 3.6.3

[131] J. Erdmenger and H. Osborn, "Conserved currents and the energy momentum tensor in conformally invariant theories for general dimensions," *Nucl.Phys.*, vol. B483, pp. 431–474, 1997. 3.6.2, 3.6.2, 3.6.2, 3.6.3, 3.6.3

[132] V. P. Frolov and E. Serebryanyi, "Vacuum Polarization in the Gravitational Field of a Cosmic String," *Phys.Rev.*, vol. D35, pp. 3779–3782, 1987. 3.6.3, 3.6.4

[133] J. Dowker, "Entanglement entropy for even spheres," 2010. 3.6.3

[134] A. Lewkowycz and E. Perlmutter, "Universality in the geometric dependence of Renyi entropy," *JHEP*, vol. 01, p. 080, 2015. 7

[135] D. V. Fursaev, A. Patrushev, and S. N. Solodukhin, "Distributional Geometry of Squashed Cones," *Phys.Rev.*, vol. D88, no. 4, p. 044054, 2013. 7

[136] T. Souradeep and V. Sahni, "Quantum effects near a point mass in (2+1)-Dimensional gravity," *Phys.Rev.*, vol. D46, pp. 1616–1633, 1992. 3.6.4

[137] D. A. Galante and R. C. Myers, "Holographic Renyi entropies at finite coupling," *JHEP*, vol. 1308, p. 063, 2013. 3.8